Cooperative Layered Wireless Video Multicast

D I S S E R T A T I O N

for the Degree of

Doctor of Philosophy (Electrical Engineering)

Özgü Alay

May 2010

Cooperative Layered Wireless Video Multicast

D I S S E R T A T I O N

Submitted in Partial Fulfillment
of the Requirement for the
Degree of

Doctor of Philosophy (Electrical Engineering)

at the

POLYTECHNIC INSTITUTE OF NEW YORK UNIVERSITY

by

Özgü Alay

May 2010

Approved:

_____
Department Head

_____ 20__

Copy No. _____

Approved by the Guidance Committee:

Major: Electrical Engineering

Yao Wang
Professor of
Electrical and Computer Engineering

Elza Erkip
Associate Professor of
Electrical and Computer Engineering

Shivendra S. Panwar
Professor of
Electrical and Computer Engineering

Minor: Computer Science

Keith Ross
Leonard J. Shustek Professor of
Computer and Information Science

VITA

Özgü Alay received the B.S. and M.S. degrees in Electrical and Electronics Engineering from Middle East Technical University, Ankara, Turkey, in 2003 and 2006 respectively. Since then, she has been working towards her PhD degree at Polytechnic Institute of New York University. In 2009, she worked as a summer intern at Samsung Electronics, Richardson, Texas.

Her research interests lie in the areas of multimedia signal processing and communication with special emphasis on video compression, wireless video communications and networking.

To my parents, who let me go my own way while providing all the support and help whenever I needed.

ACKNOWLEDGEMENT

This study was carried out under the supervision of Prof. Dr. Yao Wang. I gratefully appreciate her guidance, criticism, support, understanding and friendship throughout this study.

I would like to express my sincere appreciation to my co-advisor Prof. Dr. Elza Erkip for her insight, guidance, encouragement and friendship throughout this research.

I would like to acknowledge Prof. Dr. Shivendra Panwar and Dr. Thanasis Korakis for their invaluable suggestions that improved the quality of this dissertation.

This dissertation is supported by The Scientific and Technological Research Council of TURKEY and Wireless Internet Center for Advanced Technology (WICAT), an NSF Industry/University Cooperative Research Center at Polytechnic Institute of NYU.

Thanks go to members of Video Lab. for their technical support.

Finally, my beloved Emrah. It might have been the most difficult years of my life, but you made me enjoy every second of it with your support and encouragement. With your love and peace, I overcame all the difficulties and stressful times of this study. I wish you will be by my side to read these lines 20 years from now, with a smile in your eyes.

My deepest thanks and love go to my family who believed in me throughout my life and helped me discover my inner strength.

Nothing in life is impossible, so go for it with no regrets...

AN ABSTRACT

Cooperative Layered Wireless Video Multicast

by

Özgü Alay

Advisor: Yao Wang

Co-advisor: Elza Erkip

Submitted in Partial Fulfillment of the Requirements
for the Degree of Doctor of Philosophy (Electrical Engineering)

May 2010

Wireless video multicast enables delivery of popular events to many mobile users in a bandwidth efficient manner. However, providing good and stable video quality to a large number of users with varying channel conditions remains elusive. In this work, we propose the use of cooperative communications for video multicast in infrastructure-based wireless networks. We first consider user cooperation at MAC layer (two-hop relaying) and integrate two hop relaying with packet level Forward Error Correction (FEC) and layered coding to enable efficient and robust video multicast. We study two different antenna transmissions at relays: omni-directional and directional. For transmission with conventional omni-directional antennas, the relays have to transmit in non-overlapping time slots in order to avoid collision. To improve the system efficiency, we investigate directional relay transmission where relays transmit simultaneously by scheduling their beams. In both systems, we consider

a non-layered configuration, where the relays forward all received video packets and all users receive the same video quality, as well as a layered set-up, where the relays forward only the base-layer video. Our analysis shows that the non-layered system can provide better video quality to all users than the conventional direct transmission system, and the layered system enables some users to enjoy significantly better quality, while guaranteeing other users the same or better quality than direct transmission. The directional relay system can provide substantial improvements over the omni-directional relay system. To support our results, a prototype is implemented using open source drivers and socket programming, and the system performance is validated with real-world experiments.

Next, we consider a system that utilizes cooperation at physical and MAC layer, where multiple relays forward the video packets simultaneously using Randomized Distributed Space Time Codes (R-DSTC). This randomized cooperative transmission is further integrated with layered video coding and packet level FEC. We first consider a simple system where the parity packets are generated at the sender and transmitted in the same way as for video packets. Three different schemes are proposed to optimize the system parameters based on the availability of the channel information at the source station: R-DSTC with full channel information, R-DSTC with limited channel information and R-DSTC with node count. The performance of these three schemes are compared with rate adaptive direct transmission and conventional multicast that does not use rate adaptation. The results show that while rate-adaptive direct transmission provides better video quality than conventional multicast, all three proposed randomized cooperative schemes outperform both strategies significantly. Furthermore, the performance gap between R-DSTC with full channel information and R-DSTC with limited channel information or node count is relatively small, indicating the robustness of the proposed cooperative multicast scheme. We also propose an enhanced multicast system using R-DSTC where the sender only transmits video packets, and parity packets are generated by the nodes that receive

all the source packets correctly. For this case, we consider two different schemes based on the available channel information (enhanced R-DSTC with full channel information and enhanced R-DSTC with node count). The performance of these enhanced schemes are evaluated and compared with the previous schemes. The results show that the enhanced multicast R-DSTC schemes substantially outperform the multicast R-DSTC schemes.

Finally, we study the randomized cooperation from information theoretical perspective where we consider the propagation of lossy source signal. Using end-to-end distortion as a performance metric and assuming a delay constraint, we investigate the relation among the decoding SNR threshold, number of hops, diversity level of underlying Space Time Code (STC), coverage range and the distribution of end-to-end quality over users in the coverage range. In order to provide differentiated quality to users with different channel strengths, we further employ layered cooperation. We study two different layering approaches: sequential layered transmission and superimposed layered transmission. For the sequential layered transmission, we investigate the effect of the time division among different layers. For the superimposed layered transmission we investigate the effect of power allocation of different layers on the distribution of end-to-end quality of users under a real-time delivery requirement. We then compare these two schemes and show the benefits of superimposed layered transmission over sequential layered transmission.

Contents

List of Figures **xii**

List of Tables **xiv**

1 Introduction **1**
1.1 Motivation 1
1.2 Dissertation Outline 6

2 Background and Preliminaries **8**
2.1 Packet Level FEC 8
2.1.1 FEC Rate 8
2.1.2 Received Video Rate 9
2.2 Layered Video 10

3 Layered Wireless Video Multicast using Relays **13**
3.1 Introduction 13
3.2 Overview of Proposed System Architecture 16
3.2.1 Multicast Using Relays: System Model 16
3.2.2 Multicast Optimization Criteria: Single layer versus Layered Cooperation 19
3.3 Optimum Node Partition and Time Scheduling using Omni-directional Relays 22
3.4 Optimum Node Partition and Time Scheduling using Directional Relays 25
3.5 Numerical Studies based on PER Measurements 30
3.5.1 PER Measurement and Typical β Values for IEEE802.11b . . 31
3.5.2 Results for Numerical Analysis 33
3.6 Implementation Efforts and Experimental Results 37
3.6.1 Driver Implementation and Socket Programming 37
3.6.2 Layered Video Architecture 40
3.6.3 Results 41
3.7 Chapter Summary 45

4 Cooperative Layered Video Multicast using RDSTC **50**
4.1 Introduction 50
4.2 System model 52
4.3 Computation of Bit and Packet Error Rates 57
4.3.1 BER of Single Link 58
4.3.2 BER for RDSTC 58
4.3.3 Computation of PER 60
4.4 Multicast using R-DSTC 61
4.4.1 Problem Formulation and Optimization under Full Channel Information 61
4.4.2 Optimization under Partial Channel Information 66
4.5 Enhanced Multicast using R-DSTC 69
4.6 Results 71
4.7 Chapter Summary 79

5 Layered Randomized Cooperative Multicast for Lossy Data in Dense Networks **83**
5.1 Introduction 83
5.2 System Model 85
5.3 Single Layer Transmission 87
5.4 Layered Transmission 91
5.4.1 Sequential Layered Transmission 92
5.4.2 Superimposed Transmission of Multiple Layers 95
5.5 Chapter Summary 105

6 Conclusion **107**
6.1 Comparison of different systems 107
6.2 Key Contributions 109

Bibliography **113**

List of Figures

2.1 Scalable video coding. 11

3.1 Division of all the nodes into two groups 14
3.2 System set up with omni-directional relays 18
3.3 System set up with directional relays 20
3.4 Geometric model for the omni-directional relay transmission 24
3.5 Geometric model for the directional relays 27
3.6 Boundary condition to avoid overlap among relay beams 28
3.7 PER vs coverage distance at a packet size of 1470B 31
3.8 Visual Quality Comparison of Two-hop Layered Multicast with Omni-directional Relays, Directional Relays and Direct Transmission. In the layered case, Group 2 nodes experience the same quality with direct transmission. 47
3.9 The H.264 temporal scalability coding structure. 48
3.10 Experimental setup. 48
3.11 Experimental Results (omni-directional):Comparison of Single Layer Two-hop Multicast with Direct Transmission with and without FEC (averaged over 10 experiments). 49
3.12 Experimental Results (omni-directional): Comparison of Layered Two-hop Multicast with Single Layer Two-hop Multicast and Direct Transmission with FEC (averaged over 10 experiments). 49

4.1 Transmitter and receiver architecture at the relay nodes 54
4.2 Snapshot of the network. 55
4.3 Time scheduling and transmission rates for base and enhancement layers at first and second hop. 62
4.4 Transmission rates and time scheduling for RDSTC schemes 69
4.5 N_{avg}/N_T vs R_1 73
4.6 Average video rates vs number of nodes for single layer systems ($\beta = 1$). . 75
4.7 Average optimum transmission rates for single layer systems. 76
4.8 Average optimum FEC rates for single layer systems. 77
4.9 Percentage of nodes to receive all packets at all node placements versus number of nodes, N_T 78

4.10 Video rates vs number of nodes for $\mu = 30\%$. 79
4.11 Average video rates for layered cooperation for different N_T and μ. 80
4.12 Comparison of video rates for *enhanced-multicast-RDSTC* with different systems ($\beta = 1$). 81
4.13 Comparison of average optimum transmission rates for *enhanced-multicast-RDSTC* with *multicast-RDSTC*. 81
4.14 Comparison of average optimum FEC rates for *enhanced-multicast-RDSTC* with *multicast-RDSTC*. 82

5.1 Comparison of end-to-end distortion for nonorthogonal relay transmission for different decoding thresholds (τ) ($P_s = 10, \tilde{P}_r = 1, d_0 = 1, N = 5, b = 8$) 89
5.2 Comparison of end-to-end distortion for orthogonal relay transmission for different decoding thresholds (τ) ($P_s = 10, \tilde{P}_r = 1, d_0 = 1, N = 5, b = 8$) . . 90
5.3 Effect of the number of hops on the end-to-end distortion at different coverage ranges with $P_s = 10, \tilde{P}_r = 1, d_0 = 1, b = 8$ (L=∞) 91
5.4 Sequential Layered Cooperative Multicast: Comparison of end-to-end distortion for nonorthogonal relay transmissions($P_s = 10, \tilde{P}_r = 1, d_0 = 1, N_b = 5, N_e = 5, b = 8$) 94
5.5 Sequential Layered Cooperative Multicast: Comparison of end-to-end distortion for orthogonal relay transmissions($P_s = 10, \tilde{P}_r = 1, d_0 = 1, N_b = 5, N_e = 5, b = 8$) 95
5.6 Comparison of distortion for layered cooperation with different number of hops at base and enhancement layer for nonorthogonal relay transmissions ($P_s = 10, \tilde{P}_r = 1, d_0 = 1, N_b = 5, N_e = 4, b = 8$) 96
5.7 Comparison of distortion for layered cooperation with different number of hops at base and enhancement layer for orthogonal relay transmissions ($P_s = 10, \tilde{P}_r = 1, d_0 = 1, N_b = 5, N_e = 4, b = 8$) 97
5.8 The effect of β on the expected distortion for nonorthogonal relay transmissions as a function of distance for $P_s = 10$, $\tilde{P}_r = 2$, $N = 2$, $b = 4$. The 'layered' plot illustrates simultaneous transmission of layers by superposition. 102
5.9 The effect of β on the expected distortion for orthogonal relay transmissions as a function of distance for $P_s = 10$, $\tilde{P}_r = 2$, $N = 2$, $b = 4$. The 'layered' plot illustrates simultaneous transmission of layers by superposition. . . . 103
5.10 Quality improvement at closer receivers: Comparison of expected distortion for single layer randomized cooperation, sequential layered randomized cooperation and superimposed layered randomized cooperation with $P_s = 10$, $\tilde{P}_r = 2$, $N = 2$, $b = 4$ (L=∞) 104
5.11 Coverage range extension: Comparison of expected distortion for single layer randomized cooperation, sequential layered randomized cooperation and superimposed layered randomized cooperation with $P_s = 10$, $\tilde{P}_r = 2$, $N = 2$, $b = 4$ (L=∞) 105

List of Tables

3.1 Notation 17
3.2 β values with $\beta_t = 0.2$ for packet size of 1470B. 31
3.3 Number of parity packets needed for $s = 64$ source packets (packet size is 1470B) 33
3.4 Received video rate in Kbps (packet size is 1470B) 33
3.5 Optimal system configuration with omni-directional and directional relays. 34
3.6 Achievable PSNRs (dB) with omni-directional and directional relays for three different video sequences. 36
3.7 Comparison of maximum sustainable video rates based on numerical analysis and implementation results 44

4.1 Notation 53
4.2 Transmission rates for IEEE 802.11g and their corresponding modulation schemes and channel codes 72

Chapter 1

Introduction

1.1 Motivation

In recent years, the demand for video applications over wireless networks has been on the rise due to the significant increase in both the bandwidth of wireless channels and the computational power of mobile devices. To provide efficient delivery among a group of nodes at the same time, multicast has been used as an effective solution as it saves network resources by sharing a data stream across multiple nodes. However, wireless channels suffer from path loss and fading, resulting in disparate channel qualities between the sender and each receiver node, making wireless video multicast a challenging problem.

Wireless channels are characterized by their bursty and location dependent errors. Each node in a multicast system will experience packet losses with different loss pattern than its neighbors. Hence, a simple ARQ (Automatic Repeat reQuest) based scheme is not appropriate for video multicast since it can generate a large number of retransmissions. To cope with this problem, packet level Forward Error Correction (FEC) has been proposed for error control in video multicast over wireless networks [1]-[2]. To address the heterogeneity of nodes, scalable (layered) video coding can be utilized. Layered video multicast has been studied in infrastructure-based wireless networks [3]-[5]. Video multicast has also been investigated in multi-hop

networks such as ad-hoc networks [6], and mesh networks [7]-[8]. Although these studies consider layered video multicast in a multi-hop network, none of those papers have considered the use of user cooperation combined with layered video and packet level FEC in order to provide robust video multicast.

User cooperation is an effective technique to combat path loss and fading where terminals process and forward signals overheard from the senders to their intended destinations [9]-[10]. Physical layer cooperative techniques have been extensively studied as a means to provide spatial diversity [11]. A cooperative MAC layer and a cross layer design between the physical and the MAC layer have been explored in [12]-[13]. In [14]-[15], the authors consider point-to-point video communications and show that cooperation of nodes can improve video quality by providing unequal error protection. User cooperation is especially attractive for multicast, since the relays are among the intended recipients and hence, are free from the incentive and security concerns that impact the deployment of cooperation for point-to-point communications, where the relay is not the recipient of the data sent.

In this dissertation, we propose the use of cooperative communications for video multicast in infrastructure-based wireless networks. In conventional multicast design, the sender adjusts its transmission rate according to the worst channel quality among all nodes, therefore the nodes with a good channel unnecessarily suffer and experience a lower quality video than they would have if the system was targeted for them. The basic idea behind cooperative communications is that the sender targets close-by nodes by transmitting at a high transmission rate. Then, these nodes relay the received information to far away nodes. Such a scheme improves the multicast performance by providing better quality links (both sender-to-relay and relay-to-node) and hence higher sustainable transmission rates.

First, we consider cooperative communication at MAC layer without considering physical layer combining for ease of exposure. Hence, any simultaneous transmission in the system will be perceived as a collision. While extensions to a

larger number of hops is possible, we study the two-hop case to illustrate the fundamental performance gains of the proposed idea. This can be interpreted as a two-hop relaying system, since there is no physical combining. We divide all the nodes into two groups in a way that nodes in Group 1 have better average channel quality than those of Group 2. In such a system, we let the sender choose its transmission rate based on the worst channel quality of Group 1. Then, the relays (either selected among Group 1 nodes or placed at fixed locations) forward the received information to Group 2 nodes. Such a scheme not only allows nodes in Group 1 to have a higher quality signal, but also provides quality gains for the nodes in Group 2. We study two different relay transmissions: omni-directional and directional. For omni-directional relay transmission, each relay targets a subgroup of Group 2 nodes and transmits in a different time slot sequentially to avoid collision. A deficiency of this system is that the relays cannot send simultaneously, which limits the supportable video rates. To circumvent this problem, we also investigate the use of directional antennas for relay transmission. In this case, we assume the relay stations are equipped with directional antennas, and directionally transmit the relayed data to their targeted subgroups using non-overlapping beams. Although the current cost of directional antennas may be high, the significant potential performance gain motivates their use. Along with numerical evaluation, in order to validate our research in a practical environment, we further implement a prototype of the proposed system using omni-directional relays and conduct extensive experiments. The implementation is carried out in the MAC layer as well as in the application layer, using open source drivers and socket programming, along with a packet level FEC. We show that the implementation results are close to our numerical analysis.

Although directional antennas improve the multicast performance by providing simultaneous relay transmission, the system still needs to schedule and transmit the beams sequentially. A more efficient way of transmission can be achieved at physical layer where the multiple relays transmit simultaneously using a distributed

space-time code (DSTC) [16]. The basic idea behind DSTC is to coordinate and synchronize the relays such that each relay acts as one antenna of a regular Space Time Codes (STC) [17],[18]. However, in order to realize such a system, each relay participating in a DSTC needs to know exactly which antenna it will mimic in the underlying STC. Furthermore, based on the dimension of the underlying STC used, a fixed number of relays is chosen. Even though there may be other nodes who decode the source information correctly, they are not allowed to transmit, thus forfeiting the potential diversity and coding gains. Finally, a DSTC requires tight synchronization of the relay nodes, putting a heavy burden on the MAC and physical layers. In order to circumvent these problems, Randomized DSTC (R-DSTC) [19] can be used where each relay transmits a random linear combination of antenna waveforms. Randomized coding for unicast transmission in a wireless network is described in [20], where the impact on the MAC layer performance is also discussed. A joint physical and MAC design for unicast transmission using a randomized cooperative scheme is described in [21], [22].

In the second part of this dissertation, a joint physical and MAC layer cooperative video multicast scheme is considered where the relays transmit the packets simultaneously using R-DSTC. R-DSTC is especially attractive for multicast since the nodes that receive the packets can act as relays and transmit simultaneously, without the need for relay selection and scheduling. We further integrate randomized cooperation with source layering and packet level FEC. We first consider a simple system where the parity packets are generated only at the sender. We assume that the source and parity packets are not differentiated at the relays and they both go through two-hop transmission. For this case, we propose three different schemes which differ in the available network state information. The first one (R-DSTC with full channel information), assumes that the source station knows the average received SNRs between itself and each receiver node as well as between all pairs of nodes. The second scheme (R-DSTC with limited channel information), assumes that the

sender only knows the channel information between the nodes and itself. Finally, the third scheme (R-DSTC with node count) considers that the sender only knows the number of nodes in its coverage range. For each of these schemes, we optimize the system operating parameters (transmission rates of both hops and consequently the STC dimension and the FEC rate) based on the channel information, and evaluate the achievable video rate. We also consider a layered cooperative multicast system, which provides better video quality to the nodes with better channel conditions.

Note that the above schemes only consider parity packet generation at the sender. However, if we let the relays generate parity packets, we can improve the performance of the system by foregoing the first hop transmission of parity packets. Thereby, we propose an enhanced multicast system using R-DSTC where parity packets are generated by the nodes that receive all the source packets correctly. For this case, we only consider two different schemes based on the available channel information (enhanced R-DSTC with full channel information and enhanced R-DSTC with node count). For each of these schemes, we determine the optimum transmission rates for source and parity packets as well as the number of parity packets required such that the video quality at all nodes is maximized. We compare the results of the above schemes with rate adaptive direct transmission [23] and conventional multicast.

For the above mentioned randomized cooperative multicast systems, we follow a more practical approach and evaluate the performance of the system based on a IEEE 802.11g network. In [24], the authors consider a more theoretical framework where asymptotic behavior of randomized cooperative multicast system in a dense network has been studied for the propagation of lossless information. In the final part of this dissertation, we investigate the randomized cooperative multicast system from information theoretic perspective where we consider multi-stage cooperation for delivering lossy data such as multimedia signals (audio, image, and video). As the performance measure, we consider the distortion of the reconstructed signal at the receiver compared with the original source. Multimedia signals also typically have

delay constraints, for example, media data has to be delivered and rendered before its scheduled playback time. Therefore, for multimedia multicast, our goal is to minimize the end-to-end distortion of the multicast nodes in a certain coverage range under a delay constraint. We investigate the effect of decoding SNR threshold, number of hops and the diversity level of the underlying space time code (STC) on the end-to-end distortion of the multicast nodes at a fixed coverage range. We carry out our analysis using i.i.d. Gaussian source and make use of the well-known rate distortion function and the successive refinability [25] to determine the encoding-induced distortion at different source rates. Furthermore, we consider two different layered transmission: sequential and superimposed. For the sequential layered transmission, we transmit different layers sequentially by applying unequal error protection (UEP) to different layers. Alternatively, the transmission of layers can also be done simultaneously by superposition coding. We compare these layering schemes and discuss the benefits of layered transmission over single layer transmission.

1.2 Dissertation Outline

The dissertation is organized as follows. In Chapter 2, we review packet level FEC and Scalable Video Coding. In Chapter 3, we study layered video multicast using relays. We formulate the optimum user partition and time scheduling for both omni-directional and directional relay transmission. The performance of the system is demonstrated both numerically and experimentally. In Chapter 4, we consider layered multicast using R-DSTC. We formulate the video rate of cooperative multicast, and discuss the optimization of the parameters under full channel information as well as partial channel information. In Chapter 5, we explore cooperative multicast using R-DSTC from information theoretic perspective where asymptotic behavior of the system is considered in a dense network. Along with a single layer configuration, we study two different layering approaches: sequential layered transmission and

superimposed layered transmission. In Chapter 6, we conclude the dissertation.

Chapter 2

Background and Preliminaries

In this section, we discuss the packet level FEC and formulate the received video rate for direct transmission. Finally, we review Scalable Video Coding.

2.1 Packet Level FEC

Forward error correction (FEC) at the application layer is used to handle packet losses in multicast services. The basic idea of FEC is that redundant information is sent a priori by the source station, in order to be used by the receivers to correct errors/losses without contacting the source. However, such a scheme introduces overhead since extra parity packets are now transmitted by the source station. Despite additional overhead, considering the benefits for error recovery, such a scheme is widely used in a multicast environment.

In this section, we will discuss the overhead and the received video rate which is used to deliver video, considering the overhead due to FEC and other factors in the network.

2.1.1 FEC Rate

We assume that by using CRC at the link layer, each receiver is able to decide whether a packet is correctly received or not. The packets that are lost can

be viewed as *erasures* and an erasure code at the packet level can be used to recover the lost packets. In particular, for every s source packets, if we add p parity packets, we can recover all the source packets as long as the number of erasures is at most p using *perfect* codes. Reed-Solomon (RS) code provides a good example of a perfect code [26].

The *rate* of a perfect code, γ is the ratio of the number of source packets to the total number of packets, that is $\gamma = s/(s+p)$. The FEC decoding failure probability is the probability that at least $p+1$ packets are in error. While evaluating the performance of the system, for given s and average PER, we numerically determine γ so that FEC decoding failure probability is below $\varsigma = 0.5\%$. We observe that when using an error-resilient video decoder, typically there is no noticeable quality degradation when FEC decoding failure probability is below this threshold.

2.1.2 Received Video Rate

Suppose that at a direct transmission rate of R_d bits/sec, the maximum PER among all nodes in the desired coverage radius r_d is ϵ_{max}. Note that given the node placement ϖ, $\epsilon_{max}(R_d|\varpi)$ depends on the transmission rate. Hence, given ϖ, the packet level FEC rate $\gamma_d(R_d|\varpi)$ also depends on R_d. In a wireless network, multicast service usually uses a portion of the total available bandwidth. We define the effective data ratio, β, as the ratio of the bit rate used to transmit multicast payload data (e.g. video data including FEC parity packets) to the total transmission rate. Then, with direct transmission for a given β and node placement ϖ, all the nodes receive video at the same rate of:

$$R_{v_d}(R_d|\varpi,\beta) = \beta\gamma_d(R_d|\varpi)R_d \tag{2.1}$$

Note that the received video rate depends on the transmission rate for a given node placement. Here we assume a fixed bandwidth 802.11 system with different transmission rates by changing the corresponding modulation schemes. Hence, for

this system, the higher the transmission rate, the higher the PER value. In this case, since the PER is higher, we need more parity packets to correct the errors, hence γ decreases. On the other hand, as the transmission rate increases, the number of bits we can transmit increases, allowing more room for extra FEC parity packets. Therefore, in the system design, for a fixed distance, there is an optimum transmission rate that maximizes R_{v_d}. In [23], we show that a higher transmission rate together with stronger FEC is more efficient than using a lower transmission rate with weaker FEC. Motivated by this observation, to improve the video quality, we consider joint transmission rate and FEC rate adaptation for both direct transmission and cooperative multicast.

The above formulation considers single link transmission. We will derive the formulation for the received video rates of cooperative multicast systems in Chapter 3 and Chapter 4.

2.2 Layered Video

A video can be coded into multiple layers such that reception of more layers leads to better quality. A layered bitstream consists of base layer and enhancement layer(s). The base layer can be independently decoded and it provides coarse visual quality. The enhancement layers can only be decoded together with the base layer and they provide better visual quality. Scalable video coding standard, ITU H.264/SVC, defines three video scalability dimensions as illustrated in Figure 2.1:

- Temporal (frame rate) scalability: Temporal scalability is defined as representing the same video in different temporal resolutions or frame rates. Here, the motion compensation dependencies are structured so that frames can be dropped from the video bitstream. Temporal scalability can also be achieved in H.264/AVC [38].

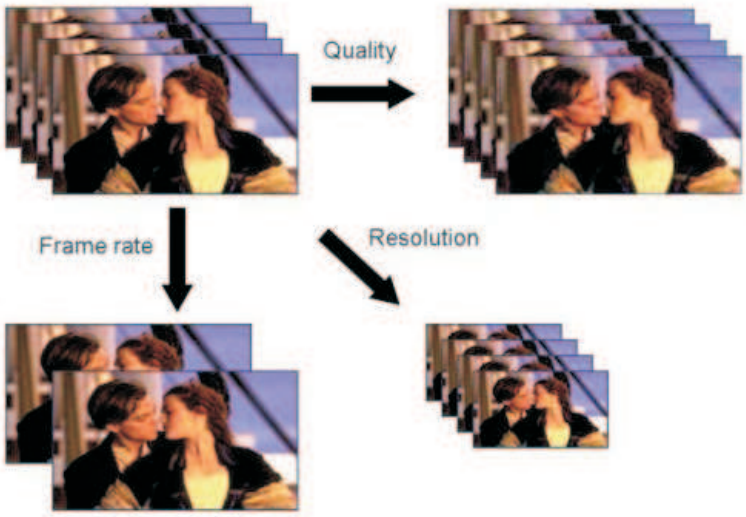

Figure 2.1: Scalable video coding.

- Spatial (resolution) scalability: Spatial scalability is defined as representing the same video in different spatial resolutions or sizes. The decoded samples of lower resolutions can be used to predict samples of higher resolutions in order to reduce the bit rate to code the higher resolutions.

- SNR (Quality) scalability: SNR scalability is defined as representing the same video in different SNR or perceptual quality. To be specific, SNR-scalable coding quantizes the DCT coefficients to different levels of accuracy by using different quantization parameters. The resulting streams have different SNR levels or quality levels. In other words, the smaller the quantization parameter is, the better quality the video stream can achieve.

Scalable video coding is a very desirable feature for many multimedia applications. For multicast applications, scalable coding can provide a range of picture quality suited to heterogeneous requirements of nodes. For cooperative multicast, we use SVC to provide differentiated quality to different nodes based on their channel conditions. Specifically, we adjust the system parameters such that close by nodes get

much better quality than that experienced in direct transmission, whereas far away nodes get video quality better than or similar to the direct transmission.

Chapter 3

Layered Wireless Video Multicast using Relays

3.1 Introduction

In this chapter, we integrate layered video coding, two-hop relaying (cooperation at MAC layer) and packet level FEC to enable efficient and robust video multicast. The basic idea behind multicast using relays is the division of all the nodes into two groups in a way that nodes in Group 1 have better average channel quality than those of Group 2 as illustrated in Figure 3.1. In such a system, we let the sender choose its transmission rate based on the worst channel quality of Group 1. Then, the relays (either selected among Group 1 nodes or placed at fixed locations) forward the received information to Group 2 nodes. Our work defines a medium access control mechanism from the sender and the relays. By scheduling the relay transmissions at the MAC layer, the relays cooperatively access the channel instead of contending for the channel by following the regular CSMA/CA protocol. Such a scheme not only allows nodes in Group 1 to have a higher quality signal, but also provides quality gains for the nodes in Group 2. Although the same principle can be extended to use more than two hops, our results show that two hop transmission is sufficient for providing good quality video multicast within the same coverage area of a sender.

We formulate and compute the optimum system parameters, including relay placement, node partition, transmission rates and FEC rates of each hop and

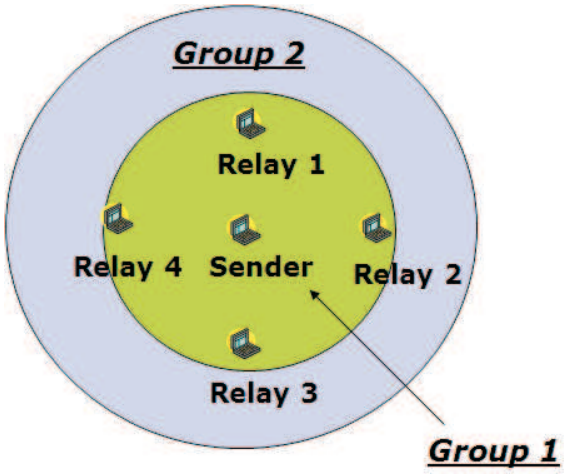

Figure 3.1: Division of all the nodes into two groups

transmission time scheduling based on the multicast optimization criteria. Our optimization in this chapter considers all possible node locations in the target coverage region, rather than a particular node placement ϖ. Therefore, the optimization depends on the coverage range r_d rather than a specific node placement. Note that optimum relay placement can be accomplished in two ways. First, if the network is dense, the relays can be selected among the intended nodes. Here, dense network ensures that there exist nodes at optimum relay locations. An example for a dense network is an urban environment, where a large number of devices access the channel at the same time. Alternatively, optimized relay positions can be used for optimal relay placement in an infrastructure based network where fixed relay nodes are introduced to the system. With fixed relays, the system will work regardless of the distribution of the nodes. The literature on optimum relay placement is mostly for unicast communication. For example, in [27], optimum placement for a single relay is discussed to maximize the capacity in IEEE.802.16j networks. [27] is extended in [29] to study the optimum relay station placement and the corresponding bandwidth and power allocation for cooperative relaying. A more theoretical work on relay selection

in sensor networks is [28] where the minimization of the average probability of error is studied. The relay placement algorithm described in this chapter on the other hand considers a multicast scenario.

We first consider omni-directional relay transmission, where each relay targets a subgroup of Group 2 nodes and transmits in a different time slot sequentially to avoid collision. A deficiency of this system is that the relays cannot send simultaneously, which limits the supportable video rates. To circumvent this problem, we also investigate using directional antennas for relay transmission. In this case, we assume the relay stations are equipped with directional antennas, and directionally transmit the relayed data to their targeted subgroups using non-overlapping beams. Although the current cost of directional antennas may be high, the significant potential performance gain motivates their use. In order to handle packet losses at each hop, we further employ packet level FEC to both schemes.

Along with numerical evaluation, in order to validate our research in a practical environment, we implement a prototype of the proposed system using omni-directional relays and conduct extensive experiments. The implementation is carried out in the MAC layer as well as in the application layer, using open source drivers and socket programming, along with a packet level FEC. We show that the implementation results are close to our numerical analysis.

This chapter is organized as follows. In Section 3.2, we introduce the system model and discuss the multicast optimization criteria. In Section 3.3 and Section 3.4, we formulate the optimum node partition and time scheduling for omni-directional and directional relay transmission, respectively. Section 3.5 analyzes the obtained numerical results. Section 3.6 summarizes our implementation efforts. We summarize the chapter in Section 3.7.

3.2 Overview of Proposed System Architecture

3.2.1 Multicast Using Relays: System Model

We study an infrastructure-based wireless network (such as WLAN, 3G or WiMAX), and assume that a sender (Base Station (BS) or Access Point (AP)) multicasts video to the nodes within a coverage area of a certain radius. Our system is based on a path loss model with a path loss exponent of PLE, which solely depends on the distance between a sender and its receiver node. In other words, the nodes closer to the transmitter have better channel qualities and hence can experience lower packet loss rates than the far away nodes. Relaying can also be used to overcome the shadowing effects in wireless networks; however in this chapter, in order to have a fair comparison with direct transmission, we assume all the nodes are in line-of-sight.

We consider optimized system parameters within a target coverage area. We divide the entire coverage area into two groups, so that nodes in Group 1 have better channel quality than nodes in Group 2. We let the sender choose its transmission rate and packet level FEC rate based on the worst channel quality in Group 1. For a chosen transmission rate and corresponding packet loss rate in a given coverage area, we apply sufficient amount of packet level FEC so that the FEC decoding failure rate is less than ς as discussed in Chapter 2. Then, the relays (either selected among Group 1 nodes or placed at fixed locations) will forward all or selected received packets from the sender to Group 2 nodes with the transmission rate and FEC rate chosen based on the worst channel quality of relays to Group 2 nodes.

The two-hop relaying strategy enables both the sender-to-Group 1 nodes' links and relay-to-Group 2 nodes' links to have better quality and hence lower packet loss rates than the sender to the worst node in the entire coverage area. By improving the channel quality we boost the transmission rates for both transmission hops. In general, Group 2 nodes can combine the received information from the sender and the relays, but in this chapter, we consider the simple case where Group 2 nodes

R_d	Direct transmission rate (Mbps)
R_1, R_2	First and second hop transmission rates (Mbps)
r_d	Direct transmission coverage range (m)
r_1, r_2	First and second hop coverage ranges (m)
r_2'	Second hop coverage range (directional)(m)
$r_{s,r}$	Distance between source and relay (m)
r_{omni}	Coverage range with omni-directional antennas (m)
r_{dir}	Coverage range with directional antennas (m)
t_1, t_2	First and second hop transmission time fractions
R_{vd}	Received video rate for direct transmission (Kbps)
R_{v1}, R_{v2}	Received video rates for Group-1 and Group-2 nodes (Kbps)
Q_d	Video quality for direct transmission (PSNR)
Q_1, Q_2	Video quality of Group-1 and Group-2 nodes (PSNR)
β	Effective data ratio
α	Separation angle of the relays
γ, γ'	FEC rate with omni-directional and directional antennas
γ_d	FEC rate for direct transmission
γ_1, γ_2	FEC rates for first and second hop transmission
θ	Directional antenna angle
ϵ	Packet Error Rate
N	Number of relays
M	Number of beams for directional antennas

Table 3.1: Notation

only listen to their designated relay. We show that even with such a two-hop relay strategy, substantial improvement in performance is possible.

Before describing the details of the proposed system, we summarize the notation used in this chapter in Table 4.1. For the baseline direct transmission system, we assume that the sender uses a transmission rate of R_d Mbps and a FEC rate of γ_d to cover nodes in a radius of r_d meters (m). Here, γ is the FEC rate with omni-directional antennas and is chosen so that after FEC decoding, the FEC decoding failure rate at all nodes is below ς. This implies that the FEC rate is chosen based on the Packet Error Rate (PER) of the node at the edge of the coverage region. Therefore, FEC rate derived in Chapter 2 for a given node placement $\gamma_d(R_d|\varpi)$ is

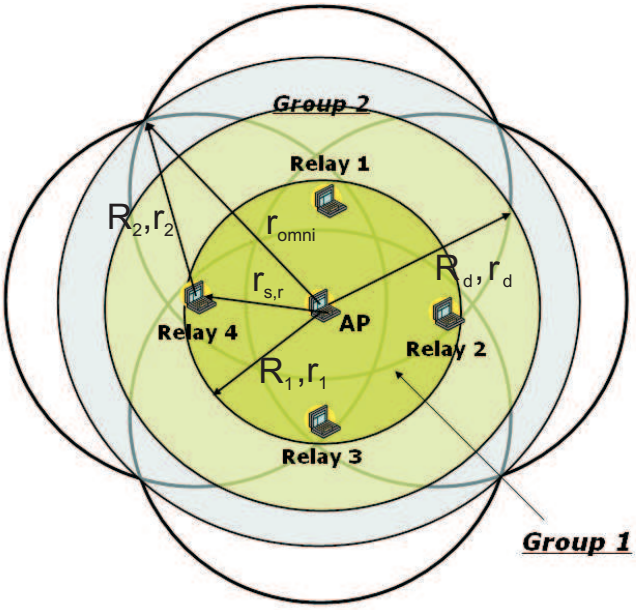

Figure 3.2: System set up with omni-directional relays

equivalent to $\gamma(R_d, r_d)$. Therefore, for the remainder of this chapter, we will follow the latter notation for the FEC rate.

For the proposed multicast system using omni-directional relays, each relay transmits to a subset of Group 2 nodes in a separate time slot. A Group 2 node only listens to its designated relay as illustrated in Figure 3.2. In Group 1, we assume a transmission rate of R_1 Mbps and a FEC rate of $\gamma_1 = \gamma(R_1, r_1)$ that can cover nodes within a radius of r_1 meters with a FEC decoding failure rate less than ς, after loss recovery with FEC. γ_1 is chosen based on the PER of the first hop. Similarly, in the second hop transmission, upon reception of the packets, the relays decode the FEC block and regenerate parity packets based on the PER of the second hop. The relays transmit the parity packets along with the source packets at a rate R_2 Mbps, and a FEC rate of $\gamma_2 = \gamma(R_2, r_2)$ is chosen to cover nodes at a distance r_2 meters from the relay.

We assume that the video data is sent in intervals of T seconds, and the

sender and the relays use T_1 and T_2 seconds for their transmissions, respectively, such that $T = T_1 + NT_2$ where N stands for the number of relays. In other words, the sender transmits during a fraction $t_1 = T_1/T$ of each transmission interval, and each relay transmits during a fraction $t_2 = T_2/T$. With this setup, we cover an area of a radius r_{omni} meters such that $r_{omni} \geq r_d$.

For the proposed system with directional relays, we assume each relay directionally transmits the data in the second hop to its targeted subgroup as depicted in Figure 3.3. In this figure, as an example, four relays are responsible for transmitting in the second hop. Each relay station uses three beams and transmits the relayed packet three times, one after the other, scanning the area around it. By scheduling simultaneous transmissions clockwise for each relay (e.g., all relays transmit simultaneously using beam 1, then beam 2, etc...), we achieve efficient spatial reuse. With directional antennas, the first hop parameters are the same as in the omni-directional case. In the second hop, the relays transmit at a rate R_2, and a FEC rate $\gamma_2 = \gamma'(R_2, r'_2, \theta)$, where each beam has an angle θ with a coverage range of r'_2 from the relay. Here, γ' is the FEC rate with directional antennas and is chosen so that after FEC decoding, the FEC decoding failure at all nodes is below a threshold. The sender uses T_1 seconds for its transmission and the relays use T_2 seconds for each beam, such that $T = T_1 + MT_2$, where M is the number of beams. Here, we cover an area of radius r_{dir} meters such that $r_{dir} \geq r_d$. The criteria to optimize the parameters both in the omni-directional and the directional case will be described next.

3.2.2 Multicast Optimization Criteria: Single layer versus Layered Cooperation

The optimum node partition and relay scheduling depends on the chosen optimization metric. In order to have a fair comparison with direct transmission, we only consider the nodes within the coverage range of direct transmission r_d. For

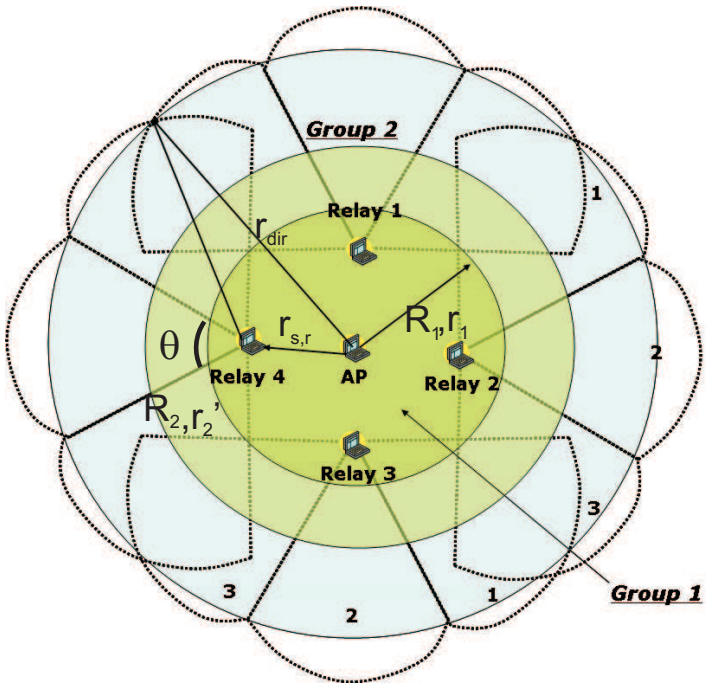

Figure 3.3: System set up with directional relays

a fixed energy consumption by the sender and coverage range, our main focus is to improve the video quality for all possible node locations in the coverage area. In general, coverage range and energy consumption of the system can also be considered as a design parameter as discussed in [30].

We define $Q_d(R_d, r_d)$ as the average quality among all nodes with direct transmission, $Q_1(R_1, r_1, t_1)$ as the average quality of Group 1 nodes and $Q_2(R_2, r_2, t_2)$ as the average quality for Group 2 nodes. Recall that, for a given transmission rate R_i (i=1,2) and coverage distance r_i, we assume that the FEC rate $\gamma(R_i, r_i)$ is chosen such that all nodes in Group i have FEC decoding failure rate less than ς. We define the video rate $R_{v_i}(R_i, r_i, t_i)$ as the rate at which video bits are delivered, which depends on the transmission rate, the FEC rate and the transmission time scheduling. Since the FEC rate is chosen so that video can be received with negligible packet

losses in all nodes in the same group, we assume the video quality in Group i only depends on the video rate of Group i, i.e. $Q_i(R_i, r_i, t_i) = Q(R_{v_i}(R_i, r_i, t_i))$, where $Q(R_v)$ indicates the quality-rate function for a given video. Note that, for a given r_i and r_d, there is a corresponding N and M for omni-directional and directional relay transmission respectively, which along with R_i and R_d, determines the dependency of t_i's. Therefore, Q_i's also depend on N and M.

We consider two different multicast optimization criteria based on the distribution of the video quality at the nodes.

Single Layer Cooperation

Single layer cooperation guarantees that all the nodes in a multicast session see the same video quality. This can be accomplished by choosing the system parameters so that $Q_1(R_1, r_1, t_1) = Q_2(R_2, r_2, t_2) = Q_c(R1, R2, r1, r2, t1, t2)$, and let the relays forward all the received video packets to Group 2. In this set up, we want to choose the system parameters to maximize Q_c. In other words, we determine the optimum parameters that maximize $Q_c = Q_1(R_1, r_1, t_1) = Q_2(R_2, r_2, t_2)$. Note that this is equivalent to maximizing the rate $R_{v_c} = R_{v_1} = R_{v_2}$.

Layered Cooperation

We also investigate layered relay transmission where the system favors Group 1 nodes. We choose the system parameters such that all Group 1 nodes (all the nodes within the area of radius r_1) receive the enhancement layer. Then, we maximize $Q_1(R_1, r_1, t_1)$ while providing Group 2 nodes with the same or better quality as in direct transmission. In this case, we find the optimum parameters that maximize $Q_1(R_1, r_1, t_1)$ while guaranteeing $Q_2(R_2, r_2, t_2) = Q_{min} \geq Q_d(R_d, r_d)$. Note that this is equivalent to maximizing R_{v_1} while having $R_{v_2} \geq R_{v_d}$.

For the two-hop multicast system, along with the transmission rates, relay selection and relay scheduling also affect the received video rate, hence the video qual-

ity. In Section 3.3 and Section 3.4, we will discuss the selection of optimum parameters in detail for omni-directional and directional relay transmission, respectively.

3.3 Optimum Node Partition and Time Scheduling using Omni-directional Relays

In this section we will first describe the time scheduling of the relays and formulate the corresponding video rates at both hops. Note that scheduling, and hence the received video rates, depend on the number of relays, N. We will derive the optimal solutions for the number of relays and their locations (i.e. node partition) using omni-directional relays following a geometric approach, so that all possible node locations with the target circular region can be covered.

For omni-directional relays, recall that the sender and the relays transmit over fractions t_1 and t_2 of the time, where $t_1 + Nt_2 = 1$. We can express the received video rates for Group 1 and Group 2, R_{v_1} and R_{v_2}, as:

$$R_{v_1} = t_1\gamma(r_1, R_1)\beta(R_1)R_1, \tag{3.1}$$

$$R_{v_2} = t_2\gamma(r_2, R_2)\beta(R_2)R_2, \tag{3.2}$$

where R_1 and R_2 stand for the transmission rates for Group 1 and Group 2, and r_1 and r_2 are the coverage ranges for Group 1 and Group 2, respectively. We apply a sufficient amount of FEC such that the FEC decoding failure rate is below ς. Therefore the video qualities in Group 1, $Q_1(R_{v_1})$, and Group 2, $Q_2(R_{v_2})$, depend entirely on the video rates R_{v_1} and R_{v_2}, respectively.

In the above formulation, note that for a fixed t_1, since the relays cannot transmit simultaneously due to collisions, the time interval that each relay can transmit t_2 decreases as N increases. On the other hand, for a fixed r_1, as N increases, each relay only needs to cover a smaller subgroup to have the same coverage as in

direct transmission and hence, a smaller r_2 will be sufficient. For a fixed transmission rate, as the coverage range for the relay r_2 decreases, the PER also decreases due to a better average channel, hence less error protection is needed leading to a higher FEC rate $\gamma(r_2, R_2)$. Therefore, while optimizing the system for a given multicast optimization criteria, we need to consider node partition and time scheduling, jointly.

We determine the optimum system parameters using a two step approach. For fixed r_1 and r_2, there may be different node partitions with different number of relays which satisfy $r_{omni} \geq r_d$ where r_{omni} is the radius of the coverage area of the omni-directional relay system. Note that, for fixed r_1 and r_2, the time each relay can transmit decreases as the number of relays increases. Therefore, for a given r_1, r_2, there is a corresponding optimum N determined by the node partition. Among the node partitions, we choose the one with minimum number of relays. Then, for this node partition, we find the optimum R_1, R_2 and t_1 based on the multicast optimization criteria. Recall that $t_1 + Nt_2 = 1$, therefore t_1 and t_2 are related through N. By repeating the above procedure for all possible (r_1, r_2), we find the optimum node partition and time scheduling. In summary, we determine the optimum values of (R_1, R_2, r_1, r_2, t_1) and the corresponding (t_2, N) for one of the multicast performance metric in Section 3.2.2.

For fixed r_1 and r_2, we find the minimum number of relays that cover all the nodes within the coverage range of direct transmission, r_d, following a geometric approach. We define $r_{s,r}$ as the distance between the base station and the relays (equal for all the relays), and r_{omni} as the radius of the coverage area of the omni-directional relay system, as illustrated in Figure 3.4.

Node partition is defined by r_1, r_2 and the separation angle α (cf. Figure 3.4). The total angle between two relays is defined to be 2α and is related to the number of relays by the equation: $N = \frac{2\pi}{2\alpha}$. We define α_{max} as the maximum angle

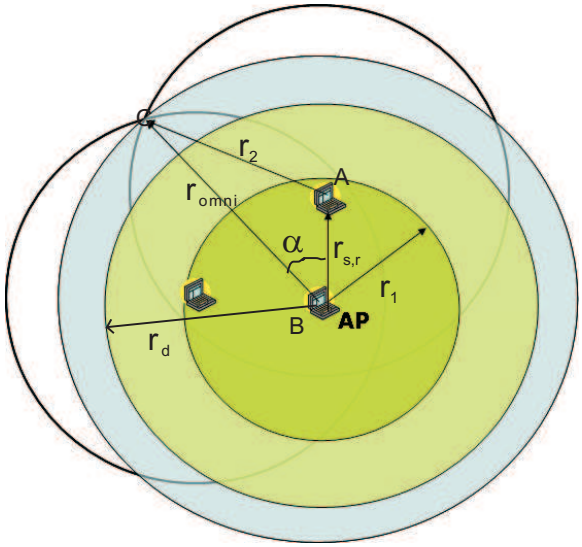

Figure 3.4: Geometric model for the omni-directional relay transmission

which satisfies the constraints below:

$$r_{s,r} \leq r_1 \tag{3.3}$$

$$r_{omni} \geq r_d \tag{3.4}$$

More specifically, Equation (3.3) states that the relay is selected from the Group 1 nodes and Equation (3.4) guarantees that all the nodes in Group 2 are covered. The separation angle will be maximum (hence the number of relays will be minimum) when $r_{s,r} = r_1$ and $r_{omni} = r_d$. Note that, the triangle, ABC, in Figure 3.4 has sides r_1, r_d and r_2. Applying the cosine theorem, we can compute α_{max} as:

$$\alpha_{max} \quad = \quad \arccos \frac{r_1^2 + r_d^2 - r_2^2}{2 r_1 r_d}, \tag{3.5}$$

Then the minimum number of relays can be calculated as:

$$N \quad = \quad \lceil \frac{2\pi}{2\alpha_{max}} \rceil. \tag{3.6}$$

After calculating the minimum number of relays, we consider that the relays are equally spaced at an angle $2\alpha = \frac{2\pi}{N}$, and $r_{s,r} = r_1$. Note that since the number of

relays needs to be an integer, the actual separation angle α is generally smaller than α_{max}, hence, the coverage area, r_{omni}, is generally greater than the coverage area of direct transmission, r_d. We calculate r_{omni} using the cosine theorem on the triangle ABC by solving for the roots of the following second order equation,

$$r_{omni}^2 - 2r_1 \cos\alpha \; r_{omni} + r_1^2 - r_2^2 = 0. \tag{3.7}$$

After computing the node partition (i.e. r_1, r_2, N), we use an exhaustive search over a discretized space of feasible R_1, R_2, t_1 and $t_2 = (1 - t_1)/N$, and find the optimum solution based on one of the multicast optimization criteria in Section 3.2.2. Note that for a chosen practical network such as IEEE802.11b, there are only a few possible transmission rates R_1 and R_2 and the corresponding r_1 and r_2. Numerical results for optimum parameters and achievable performances will be provided in Section 4.6.

3.4 Optimum Node Partition and Time Scheduling using Directional Relays

Directional antennas can significantly increase the performance of a wireless network due to their ability to point the transmission (or the reception) of an electromagnetic signal towards a specific direction. The targeted nature of the transmission results in spatial reuse, as there can be multiple transmissions in the same neighborhood without any collision. Additionally, directional transmission increases the signal energy towards the direction of the node. Directional antennas are becoming practical both in terms of size and usage, for example, there are directional antenna systems for laptops. Furthermore, for the dedicated relay model, it is quite reasonable for the relays to use directional antennas. One of the challenges of using directional antennas is adjusting the direction of the antennas to the target nodes, especially for relay networks. However, there are several MAC layer protocols for unicast in

the literature discussing the location awareness and directionality in ad-hoc networks [31],[32]. Similar approaches can be used for our MAC protocol for multicast.

When directional antennas are used, we can achieve a higher transmission rate for the same coverage range with a certain PER and the same transmission power. Alternatively, for the same transmission rate R and the same transmission power, we can achieve a larger coverage range r', compared to omni-directional antennas, which can be computed as:

$$r' = \sqrt[PLE]{\frac{2\pi}{\theta}}r, \tag{3.8}$$

where r is the coverage range with omni-directional antennas, PLE is the path loss exponent and θ is the beam angle. Note that as θ increases, r' decreases.

Using directional relays, we can have all the relays transmit simultaneously by scheduling each relay to transmit sequentially using different beams at different time slots. For example, in Figure 3.3 four relays transmit simultaneously, each with 3 beams. In the first time slot, the relays transmit using their first beams, then in the second time slot their second beams are used for the transmission, etc. Recall that the sender and each beam of the relays transmit over t_1 and t_2 fraction of the time where $t_1 + Mt_2 = 1$.

For the directional relay system, the received video rates for Group 1 is the same as in the omni-directional relay system, given in Equation (3.1). On the other hand, the received video rate for Group 2, R_{v_2}, is different from the omni-directional relay system and can be expressed as:

$$R_{v2} = t_2\gamma'(r_2', \theta, R_2)\beta(R_2)R_2, \tag{3.9}$$

where γ' is the FEC rate and $r_2{}'$ is the coverage range for directional relay transmission. While computing γ', we assume that the PER at r_2' with directional transmission is the same as the one at r_2 with omni-directional, where r_2' and r_2 are

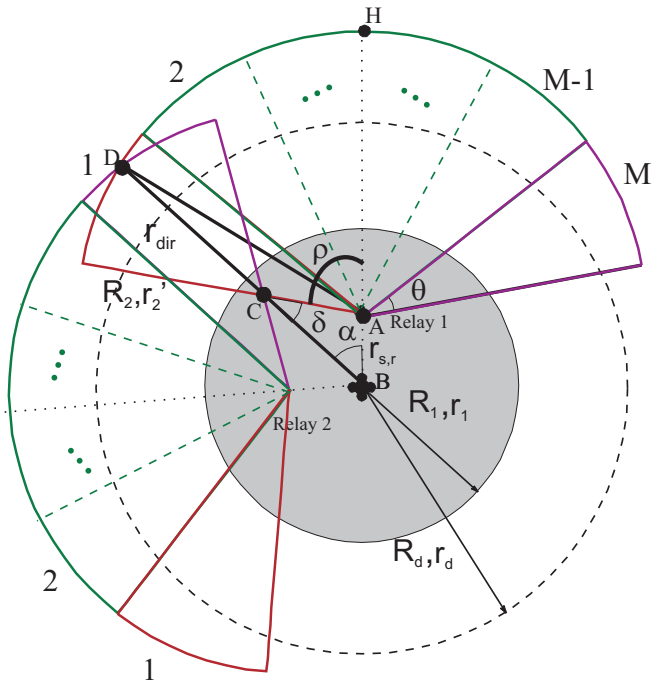

Figure 3.5: Geometric model for the directional relays

related via (3.8). Therefore, for the directional relay system, the PER is a function of r' and R, by $\epsilon'(r', R) = \epsilon(r'/\sqrt[PLE]{\frac{2\pi}{\theta}}, R)$, and the FEC rate for the directional relay transmission is related to that of the omni-directional relay transmission by $\gamma'(r_2', \theta, R_2) = \gamma(r_2'/\sqrt[PLE]{\frac{2\pi}{\theta}}, R_2)$.

Note that for a fixed t_1, the number of relays does not affect the time interval that each beam can transmit, t_2, and hence R_{v_2}. However, we do not want to consume the system resources by using more relays than necessary, so we restrict the system to use the minimum number of relays required to cover all the nodes. Note that the area covered by each relay is determined by θ and M. For a fixed θ, as we increase M, each relay can cover a larger area, hence, we need less relays to cover all the nodes. On the other hand, for a fixed t_1, as we increase M, the time interval that each beam can transmit, t_2, decreases and so does R_{v_2}. Also, note that for a fixed M, as we decrease θ, we need more relays in order to cover all nodes. However, small θ results

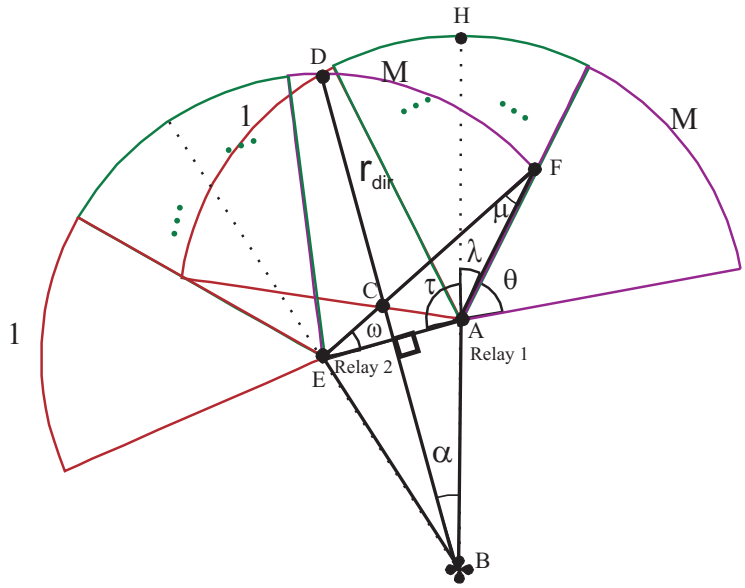

Figure 3.6: Boundary condition to avoid overlap among relay beams

in larger r_2', hence, the coverage area increases.

For directional relay transmission, we determine the optimum system parameters in two steps. For fixed r_1, r_2, θ and M, we first determine the node partition with a minimum number of relays. Therefore, for a given r_1, r_2, θ, M, there is a corresponding N determined by the node partition. Then, for this node partition, we find the optimum R_1, R_2 and t_1 based on the multicast optimization criteria. Note that t_1 and t_2 are not independent design parameters and for a particular M and t_1, the corresponding t_2 is $t_2 = (1-t_1)/M$. By repeating the above procedure for all possible r_1, r_2, θ and M, we find the optimum parameters. In summary, we determine the optimum values of (R_1, R_2, r_1, r_2, $r_{s,r}$, t_1, θ, M) and the corresponding (t_2, N) for one of the multicast performance metric in Section 3.2.2

To find the minimum number of relays, N, for a fixed r_1, r_2, θ and M, we first compute $r_2^{'}$ using r_2 and θ as in (3.8). Then using a geometric approach, we find $r_{s,r}$ and N such that relays not only cover all the nodes within the coverage range of

direct transmission, r_d, but also overlap among simultaneously transmitted beams of different relays are avoided. As illustrated in Figure 3.5, r_{dir} denotes the radius of the coverage area with directional relay transmission.

Similar to the omni-directional case, the relays are equally spaced at an angle $2\alpha = \frac{2\pi}{N}$. We want to find the maximum α, hence, the minimum number of relays satisfying the constraints below,

$$r_{s,r} \leq r_1 \tag{3.10}$$

$$r_{dir} \geq r_d \tag{3.11}$$

$$|BC| \leq r_1 \tag{3.12}$$

More specifically, (3.10) states that the relay is selected among the Group 1 nodes. In order to cover all the nodes, (3.11) states that the coverage area of directional transmission should be greater than the direct transmission coverage range. We define the point C in Figure 3.5 as the intersection of one relay's first beam and the neighbor relay's last beam. $|BC|$ is the distance between this intersection and the access point. Note that if $|BC|$ is greater than the coverage range of Group 1, there will be some nodes in Group 2 that are not covered. This is why we need to have the constraint given in (3.12). We can calculate $|BC|$ by applying the sine theorem on the triangle ABC as:

$$|BC| = \frac{r_{s,r}\sin(\pi - \rho)}{\sin\delta}, \tag{3.13}$$

where $\delta = \rho - \alpha$. Here, due to symmetric structure we use, the line BH passes through the center of Relay-1's beams, hence, on each side of this line Relay-1 spans an angle of $\rho = \frac{M}{2}\theta$. Inserting the angle values in (3.13), for a fixed $r_{s,r}$, θ, M and N, the constraint given in (3.12) can be expressed as:

$$|BC| = \frac{r_{s,r}\sin(\pi - \frac{M}{2}\theta)}{\sin(\frac{M}{2}\theta - \frac{\pi}{N})} \leq r_1. \tag{3.14}$$

Along with covering all the nodes within the coverage range of direct transmission, we also want to avoid overlap among simultaneously transmitted beams of

different relays. In Figure 3.6, we illustrate the minimum distance between the relays and the access point that avoid this. Note that if we place relays closer to the access point, relay-2's M^{th} beam will overlap with relay-1's M^{th} beam. Using the sine theorem on the AEF triangle in the figure, we have,

$$\frac{|AE|}{\sin(\mu)} = \frac{r_2'}{\sin(\widehat{EAF})}, \tag{3.15}$$

where $|AE| = 2r_{s,r}\sin(\alpha)$. Then, we can express the constraint on $r_{s,r}$ as:

$$r_{s,r} \geq \frac{r_2'\sin(\mu)}{2\sin(\alpha)\sin(\widehat{EAF})}, \tag{3.16}$$

where $\mu = \theta - 2\alpha$, $\widehat{EAF} = \tau + \lambda$, $\tau = \pi/2 + \alpha$ and $\rho = \lambda + \theta$. μ can be computed using the triangle AEF. Note that the sum of all inner angles of triangle AEF is equivalent to, $\omega + \tau + \lambda + \mu = \pi$ where $\omega = \tau - \lambda - \theta$. Inserting the angle values and $|AE|$ in (3.16), for a fixed r_2', θ, M and N, the constraint on $r_{s,r}$ can be expressed as:

$$r_{s,r} \geq \frac{r_2'\sin(\theta - 2\frac{\pi}{N})}{2\sin(\frac{\pi}{N})\sin(\pi/2 + \frac{\pi}{N} + \frac{M}{2}\theta - \theta)}. \tag{3.17}$$

We check various N values for a fixed r_2', r_1, θ and M, and find the minimum N that satisfies the above constraints. Then we calculate r_{dir} using the cosine theorem on the triangle ABD and we solve for the roots of the following second order equation,

$$r_{dir}^2 - 2\cos\alpha r_{s,r} r_{dir} + r_{s,r}^2 - r_2'^2 = 0 \tag{3.18}$$

After computing the node partition, we use an exhaustive search over a discretized space of feasible R_1, R_2, t_1 and t_2, and find the optimum solution based on the multicast optimization criteria.

3.5 Numerical Studies based on PER Measurements

In order to study the behavior of the proposed multicast strategies in a real environment, we first conducted outdoor experiments for an IEEE802.11b based

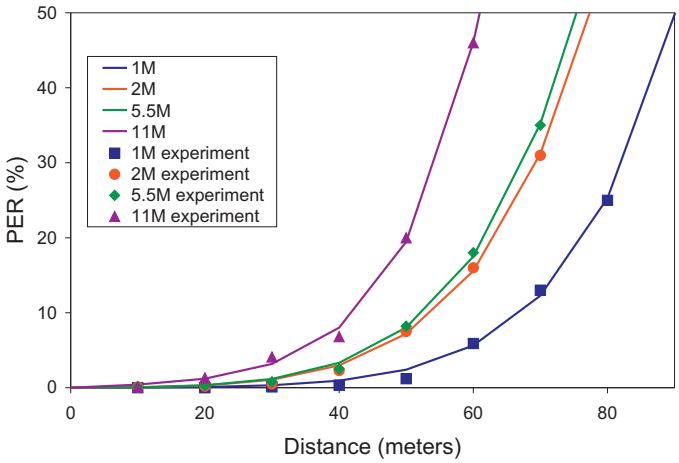

Figure 3.7: PER vs coverage distance at a packet size of 1470B

Transmission Rate(Mbps)	11	5.5	2	1
β	0.172	0.182	0.188	0.190

Table 3.2: β values with $\beta_t = 0.2$ for packet size of 1470B.

WLAN and obtained PER values for different transmission rates and various locations. Then, based on these PER measurements, we computed the amount of FEC as described in Chapter 2. Finally, as outlined in Section 3.3 and 3.4, we numerically calculated the optimum node partition and time scheduling, and determined the achievable system performances. In this section, we first describe the PER measurement study, and then report the achievable system performances of different systems.

3.5.1 PER Measurement and Typical β Values for IEEE802.11b

We measured PER using Iperf [33], which is a powerful tool for traffic generation and measurement. In our measurement setup, one of the stations runs an Iperf

client to generate UDP traffic streams, while the other runs an Iperf server which receives the traffic and collects the statistics (e.g. PER). To remove any random effects and short-term fluctuations, we ran each experiment 10 times with each run lasting 1 minute. We then averaged the results. The experiments were conducted in Columbus Park, Brooklyn, NY.

During the PER measurements, we are mainly interested in the packet losses due to channel conditions rather than the traffic contention in the channel. Recall that the effective data ratio, β, is the ratio of the time spent in transmitting the actual payload data (including the parity packets) to the total transmission time. Specifically, β has two components $\beta = \beta_t \beta_{header}$ where β_t is the proportion of the time used to transmit a given stream and β_{header} is the ratio of the time used to transmit the payload data to the time spent to transmit the payload data and the headers. For IEEE802.11, MAC and IP headers are sent at the selected transmission rate, whereas the physical layer header is always sent at the base transmission rate. Hence, β_{header} depends on the transmission rate, and as the transmission rate increases, β_{header} decreases.

In our experiments, we only use $\beta_t = 20\%$ of the total air time in order to keep the traffic level low. We ran several experiments for different distances between the access point and the node. Figure 3.7 illustrates the PER results for different distances and data rates in the broadcast mode. In this figure, the data points are the average error rates derived from the experimental results, whereas the curves show the exponentials fitted to these results. We reported a more detailed description of the experiments in [34].

We also consider the overhead introduced by MAC, IP and physical layer headers, β_{header}, (see [34] for details). We performed preliminary experiments to investigate the effect of the packet size on the received video rate and observe that for higher packet sizes, even though we have a higher PER, the received video rate is also higher. Hence, in order to minimize the header overheads, all the results reported

	10m	**20m**	**30m**	**40m**	**50m**	**60m**	**70m**	**80m**
1Mbps	1	1	1	2	4	10	15	31
2Mbps	1	1	3	7	16	24	48	-
5.5Mbps	1	1	3	7	18	28	57	-
11Mbps	1	3	7	18	31	89	-	-

Table 3.3: Number of parity packets needed for $s = 64$ source packets (packet size is 1470B)

	10m	**20m**	**30m**	**40m**	**50m**	**60m**	**70m**	**80m**
1Mbps	187	187	187	184	179	164	154	128
2Mbps	370	370	359	339	301	273	215	-
5.5Mbps	986	986	956	902	781	696	529	-
11Mbps	1863	1807	1705	1477	1275	791	-	-

Table 3.4: Received video rate in Kbps (packet size is 1470B)

in the remainder of this chapter are obtained for a packet size of 1470 Bytes. We summarize the practical β values in Table 3.2 for different transmission rates for this packet size.

3.5.2 Results for Numerical Analysis

Based on the PER's obtained, we compute the number of parity packets for $s = 64$ source packets that gives FEC decoding failure rate of $\varsigma \leq 0.5\%$. Note that, as we increase s, the delay introduced into the system also increases. On the other hand, we can not use very small s since the measured average ϵ will vary a lot from block to block. In that case, there may be many instances when the number of lost packets exceeds the correction capability of the FEC code designed based on ϵ. In Table 3.3, we specify the required number of parity packets for different distances. As seen in the table, for a fixed target distance, as we increase the transmission rate, we need to send more parity packets due to higher PER. However, the overall received

	Optimal System Configuration		*Single Layer*	*Layered*
DIRECT	$R_d = 1Mbps$ $r_d = 80m$	t	1	–
		R_{v_d} $(kbps)$	128	–
OMNI	$R_1 = R_2 = 11Mbps$ $r_1 = r_2 = 50m$ $N = 5$ $r_{omni} = 80.9m$	*Optimum* t_1	1/6	6/11
		Optimum t_2	1/6	1/11
		R_{v_1} $(kbps)$	213	635
		R_{v_2} $(kbps)$	213	128
DIRECTIONAL	$R_1 = R_2 = 11Mbps$ $r_1 = r_2 = 40m$ $r_2' = 62.6, \theta = \pi/3$ $N = 6, M = 2$ $r_{dir} = 81.45m$ $r_{s,r} = 23m$	*Optimum* t_1	1/3	0.82
		Optimum t_2	1/3	0.09
		R_{v_1} $(kbps)$	492	1221
		R_{v_2} $(kbps)$	492	128

Table 3.5: Optimal system configuration with omni-directional and directional relays.

video rate increases with transmission rate as tabulated in Table 3.4.

The packet video streams in our analysis are created by encoding three different video clips (Soccer, Foreman, Bus) with an H.264/SVC encoder using the JSVM software [39]. These videos are chosen since they possess a good variety of motion and texture characteristics. The videos are coded at fixed spatial (352x288) and temporal resolution (30fps) with quality scalability (MGS) where the base rate is set to 110kbps. We use the average of Peak Signal to Noise Ratio (PSNR) over all frames in the decoded video as the quality measure, $Q(R)$.

In order to cover a radius of 80 m with direct transmission, we need $R_d = 1Mbps$ and the optimal FEC rate is 0.674 (31 parity packets for 64 source packets).

The resulting received video rate from Table 3.4, is 128kbps. In the rest of this chapter, we numerically calculate and describe the optimal configurations using omni-directional and directional relay transmission under different multicast optimization criteria and their respective gains over direct transmission.

In Table 3.5, we compare the optimum configurations for omni-directional and directional transmission. The optimal parameters are the same for both multicast optimization criteria and given in Table 3.5 for omni-directional and directional relay transmission.

We present the average PSNR values under these optimal configurations for different videos for both omni-directional and directional relays in Table 3.6. For example, with omni-directional relays, for Foreman sequence, when we have equal quality at all nodes, we achieve a quality improvement of 1.57 dB at all nodes. When we favor Group 1 nodes, we achieve a quality improvement of 6.98 dB for Group 1 nodes compared to direct transmission, while keeping the quality of Group 2 nodes the same as in direct transmission.

Similarly, with directional relays, for Foreman sequence, when we have the same quality at all nodes, the improvement is 5.55 dB at all nodes, compared to direct transmission. Furthermore, compared to omni-directional relay transmission, the quality improvement is 3.98 dB. When we favor Group 1 nodes, while keeping the quality of Group 2 nodes the same as in direct transmission, we achieve a quality improvement of 10.15 dB for Group 1 nodes compared to direct transmission, and an improvement of 3.17 dB compared to omni-directional relay transmission.

In Figure 3.8, we compare the visual quality at the nodes using different multicast metrics for Soccer video sequence. Two-hop multicast with omni-directional relays improves the visual quality of all nodes (see Figure 3.8(b)) compared to direct transmission (see Figure 3.8(a)). Furthermore, when we favor Group 1 nodes, we significantly improve the quality of Group 1 nodes (see Figure 3.8(c)) compared to direct transmission while Group 2 nodes experience the same quality with direct

	DIRECT	OMNI		DIRECTIONAL	
Sequence	*Single Layer*	*Single Layer*	*Layered*	*Single Layer*	*Layered*
SOCCER	28.42	29.68	34.61, 28.42	33.18	38.51, 28.42
FOREMAN	29.97	31.54	36.95, 29.97	35.52	40.13, 29.97
BUS	23.28	24.57	29.71, 23.28	28.21	33.78, 23.28

Table 3.6: Achievable PSNRs (dB) with omni-directional and directional relays for three different video sequences.

transmission. Two-hop multicast with directional relays can either significantly improve the quality of all nodes (see Figure 3.8(d)) compared to direct transmission (see Figure 3.8(a)) or substantially improve the quality of Group 1 nodes (see Figure 3.8(e)) compared to direct transmission while Group 2 nodes experience the same quality with direct transmission. Furthermore, compared to omni-directional relay transmission, we achieve a higher quality for both equal quality at all nodes and best quality at Group 1 nodes.

Finally, we discuss the delay introduced by FEC into the direct transmission and two-hop multicast system. In a system that adds p parity packets to each block of s source packets, the node must wait for $n = s + p$ packet transmission times before FEC decoding. Therefore the delay due to FEC decoding is the time needed to transmit n packets, i.e. $D = Ln/R$, where L is the packet size and R is the transmission rate. In our case, we use $s = 64$ packets and $L = 1470$ Bytes. For direct transmission, $n = 95$, the delay due to the block transmission can be computed using $D_d = Ln/R_d$ which is around 0.139 seconds per FEC block. For single layer two-hop multicast using omni-directional relays, delay after first hop and the second hop can be computed using $D_1 = Ln/R_1$ and $D_2 = Ln/R_2$, respectively. The total delay after two

hop transmission is $D_{omni} = D_1 + ND_2$. With $n = 95$, $N = 5$ and $R_1 = R_2 = 11Mbps$, $D_{omni} = 0.077$ seconds. Note that for the two-hop multicast, even though the relays introduce additional delay for the FEC block, since the throughput is also higher, the total delay is still smaller compared to the direct transmission. Also note that this delay only causes initial play-out delay, which is acceptable for multicast applications. The previous discussion is for single layer two-hop multicast using omni-directional antennas. Similar computations can be carried out for the other cases.

3.6 Implementation Efforts and Experimental Results

In Section 4.6, we discussed the performance of proposed two-hop multicast strategies obtained by numerical analysis that is based on experimental PER measurements. In order to gain more insights into the system performance in a real environment, we implemented two-hop multicast with omni-directional relays in our experimental testbed [35].

Before going into the details of our implementation, we discuss the assumptions we made during our experiments. We assume that the number of relays and their MAC addresses are already known at the sender. Due to our inability to access the MAC layer firmware in a real system (the higher MAC layer functionality is implemented in the driver while the lower level time sensitive functions are implemented in the wireless card), the forwarding of data at the relay node was done as an independent transmission [36].

3.6.1 Driver Implementation and Socket Programming

We implemented the MAC layer using the open source driver Madwifi 0.9.2 [37]. The implementation details of each module are summarized as follows:

- In each packet, we added a new header between the 802.11 header and the payload that we call CoopHeader. The CoopHeader consists of the following fields: *Destination Address*, *Source Address*, *Relays Addresses* and *number of relays*. Since we are broadcasting the data, the broadcast MAC address is the destination address. The sender defines the relays for a particular broadcast, and adds their MAC addresses in the *Relays Addresses* field.

- Each station that receives a packet checks whether it is selected by the sender as a potential relay. In order to do so, it checks the *Relays Addresses* field in the CoopHeader. If one of the MAC addresses indicated in this field is equal to its address, it realizes that it is a relay and forwards the packet to the FEC module in the application layer.

- A Group 1 node only receives packets from the sender.

- A Group 2 node only receives packets from its dedicated relay and discards all other packets.

In order to implement video streaming, we built a video client/server application using UDP/IP socket programming along with FEC encoding/decoding.

In the transmitter, we run a server program that reads a FEC encoded, RTP packetized video file, and transmits the packets accordingly. At the relays, we run a program which receives packets and stores them in a file. Furthermore, we implemented a FEC module which buffers all the packets of the same block. For the second-hop transmission, we generate new parity packets and transmit them along with the source packets. At the nodes, we run a client program which receives packets and stores them in a file.

As mentioned in the beginning of this chapter, the forwarding of the block of packets by the relays is done sequentially. Specifically, we implement the scheduling among the relays by adding different delays before the transmission of each relay.

The sender sends guard packets after the transmission of each block in order to inform the relays that the transmission of one block is completed. Upon reception of the guard packets the first relay, Relay 1, starts to transmit the block of packets immediately. On the other hand, Relay 2 waits for a fixed period of time which is equal to the time needed to transmit 64 source packets and p parity packets for a particular transmission rate. After this period, Relay 2 transmits its block of packets. Rest of the relays continue the transmission in the same manner.

The relays have the ability to forward all the received packets or to filter the transmission in the second hop by transmitting only a particular video layer. This can be defined before the experiment based on a GUI designed for this purpose. Using this GUI, we are able to choose packet transmission in one of the two modes:

Single Layer Two-hop Multicast: The relays forward all the received packets.

Layered Two-hop Multicast: The relays check the header of the video packet to see whether it belongs to the base layer or the enhancement layer. A packet is forwarded only if it belongs to the base layer. This mode results in differentiated video qualities among Group 1 and Group 2 nodes.

The stored files at the relays and nodes are first FEC decoded to recover the video file. Then, we decode these files using a video decoder. Recall that for our theoretical analysis and numerical results, we assume that the chosen FEC rate based on the PER is sufficient to recover all but a few packet losses so that the video quality is completely determined by the video rate. However, in our experimental study, the applied parity packets are sometimes insufficient to correct all packet losses. In that case, only the correctly received video packets are fed into the video decoder. The decoder uses *frame copy* as the error concealment method to recover areas affected by lost packets. The video quality at each node for a particular experiment is determined by the average PSNRs of all the decoded frames of the video.

Note that the estimation of PER is important while determining the FEC rate. In the implementation part, we placed the nodes at particular distances, and

use the PER values in Figure 3.7 to determine the FEC rate. In a real system, the PER's at the farthest distance of the Group 1 and Group 2, for the optimal node partition for the expected deployment environment can be pre-measured.

3.6.2 Layered Video Architecture

Our two-hop multicast framework can in principle work with other layered coding methods as discussed in Section 2.2, but we choose to employ H.264/AVC [38] with temporal scalability for our testbed implementation since H.264/SVC currently has no slice structure support which makes error handling difficult. In our experiments, we generate temporal scalable video bit streams with slice mode to create slices which are packetized into a packet. Specifically, we use H.264 Main Profile to encode a video sequence with the coding structure shown in Figure 3.9. The base layer (BL) consists of the slices of IDR (Instantaneous Decoder Refresh) type, P type and reference B type (Bs), and the enhancement layer (EL) consists of the slices of non-reference B types (B). The arrows in the figure indicate the reference dependencies during encoding, which forms a hierarchial motion prediction structure. Note that a lost I or P picture from BL can affect all the following pictures in both BL and EL until the next IDR picture. A lost Bs picture in BL, although not affecting other pictures in the BL, affects decoding of the EL. On the other hand, the loss of any picture in the EL does not affect decoding of any other picture. For the encoding of the videos, we use the H.264 reference software JM11 and, for the decoding of the received streams, we modified the JM11 decoder so that it can support slice level errors.

The packet video streams in our experiments are created by encoding a video clip (Soccer, 352x288, 30fps, 240 frames) at a variety of bit rates. We create slices of size 1470 Bytes or less and packetized each slice into an RTP packet.

3.6.3 Results

In our experiments, we use one transmitter, three relays that are also Group 1 nodes, one Group 1 node that is not a relay and three Group 2 nodes. Although our theoretical analysis shows that to cover the 80 meter radius we need five relays, we only used three relays in the testbed to illustrate the basic idea. The experimental setup is depicted in Figure 3.10. All stations share channel 11 (2.462GHz) under IEEE802.11b ad-hoc mode. In our numerical analysis, we showed that the optimum solution is achieved when we use the maximum transmission rate of the IEEE 802.11b system in each hop. Hence, in the experiments, we compare a two-hop system (with a transmission rate of 11Mbps at each hop) with the conventional multicast system (direct transmission at 1 Mbps). Based on our numerical analysis, we place a Group 1 non-relay node and all three relays at a distance of 50m from the access point, and the Group 2 nodes are 50m apart from the relays. We arrange the 3 relays at the same distance of r_1 from the sender as the numerical analysis and have them positioned to cover more than half a circle (216 degrees) of radius 80 meter. Note that increasing the number of relays (to cover the entire circle) will lower the video quality at each node as the transmission time available for the sender and each relay will be reduced.

We first ran experiments and analyzed the conventional multicast system. Then, we conducted two sets of experiments: single layer two-hop multicast and layered two-hop multicast. In order to remove any random effect and short-term fluctuations, we ran each experiment with the same setting 10 times and averaged the results. The Group 2 results of two-hop multicast presented below are obtained by averaging the quality of all Group 2 nodes. Similarly, the Group 1 results are obtained by averaging all Group 1 nodes (including the three relays). For the direct transmission case, we averaged the results of Group 2 nodes. Note that with this set up, the reported quality for each group in the two-hop system indicates the achievable average quality at farthest node in each group, and like wise, the reported quality for the direct transmission system represents the achievable quality at the farthest node

in its coverage area.

Instead of using the theoretically derived received video rate as the video rate, we vary the video rates over a large range and see at what rate we get the best video quality. In our experiments, for each block of 64 source packets, we compute the number of parity packets using $p = \lambda k\epsilon/(1-\epsilon)$, with $\lambda = 1.2$, and ϵ determined from our measurement study. For direct transmission, this leads to a FEC rate of 0.703. For the two-hop system, the FEC rate is 0.762 in both hops. In the decoder, missing regions of a frame due to unrecoverable packet losses are recovered by using frame copy. With H.264/AVC slice structure, we found that this setting provides negligible visual degradation. Note that, in our numerical results, we only used $\beta_t = 20\%$ of the total air time in order to avoid congestion-caused losses. This leads to a low effective data ratio, $\beta \leq 20\%$. In the implementation, we not only observe the channel effect but also the congestion that is generated as we increase the video rate. Note that as we increase the video rate, β also increases. Figure 3.11 compares the results obtained for direct transmission and single layer two-hop multicast, both with and without FEC. At a low video rate, most nodes can recover all lost packets. Therefore, the video quality initially increases as the video rate increases. However, as we increase the rate beyond a certain point, due to the contention in the channel, there is not enough time for the transmission of all the packets, hence, the decoded video quality starts to drop. The results show that, the use of FEC significantly improves the video quality for both direct transmission and two-hop multicast. Note that, even at 1Mbps, there are significant packet losses at Group 2 nodes, so that direct transmission without FEC yields poor average quality. Non-layered two-hop multicast with FEC can sustain up to 1.2Mbps video rate. Above this rate, due to congestion, the video quality drops sharply. Compared to the direct transmission with FEC, where we can only sustain a video rate of 0.5Mbps, we observe that two-hop multicast significantly improves the performance. Two-hop multicast system improves the maximum achievable average PSNR to 38.89dB and 37.31dB

for Group1 and Group2 nodes, respectively, compared to 33.76 dB for all nodes with direct transmission. We observe that these PSNR numbers are very close to the encoding PSNRs at the respective video rates, suggesting that the applied FEC parity packets are able to correct almost all the lost packets at these video rates. In theory, for single layer two-hop multicast, Group 1 and Group 2 nodes should see the same quality. However, in our experiments, we observe that Group 1 nodes have slightly better quality than Group 2 nodes. This is due to the fact that if a relay does not receive all the video packets in a block in the first hop, it cannot relay all the packets to its Group 2 nodes. Moreover, there may be some additional losses in the second hop transmission.

For the layered two-hop multicast experiment, the sender transmits the base and the enhancement layer, and the relays only forward the base layer. Therefore, while Group 1 nodes experience a full frame rate of 30fps, Group 2 nodes experience a frame rate of 15fps. In Figure 3.12, we present the layered two-hop multicast results and compare with direct transmission and single layer two-hop multicast, all with FEC. The reported video rate for the layered two-hop multicast is the sum of base layer and enhancement layer rates and as the video rate increases, both the base and enhancement layer rate also increase. In our videos, the BL rate to EL rate ratio is approximately 4 (i.e. 80% of the overall video rate is BL and 20% of the overall rate is EL). Group 1 receives both BL and EL, whereas Group 2 only receives BL. Hence, $R_{v_2} = 4R_{v_1}/5$. Since sender transmits both BL and EL, and since we have 3 relays transmitting only the BL sequentially, $t_1 = 0.294, t_2 = 0.235$. When we use layered video, since the relays do not need to forward all the packets, the sender has more time to transmit ($t_1 = 0.294$ in the layered case versus $t_1 = 0.25$ in the single layer case). Therefore, the video rate at the sender can be increased to yield a higher video quality for Group 1 nodes. Note that, even though the PSNR of Group 2 nodes is slightly lower than the PSNR of Group 1 nodes, Group 2 nodes experience a frame rate of 15fps rather than 30fps. Compared to single layer two-hop multicast, layered

system was able to increase the sustainable video rate from 1.2Mbps to 1.5Mbps with a corresponding gain of PSNR from 38.89 dB to 40.21 dB at Group1, while keeping the PSNR at Group 2 about the same, but at half of the frame rate (from 37.31dB at 30 fps to 36.80dB at 15 fps).

	Direct Transmission	*Single Layer Relaying*	*Layered Relaying*
Numerical Analysis	$0.60Mbps$	$1.36Mbps$	$1.60Mbps$
Experimental Results	$0.5Mbps$	$1.2Mbps$	$1.5Mbps$

Table 3.7: Comparison of maximum sustainable video rates based on numerical analysis and implementation results

Note that the results for direct transmission, single layer and layered two-hop multicast are not directly comparable in terms of video quality (i.e. PSNR) in numerical and implementation sections due to the use of different number of relays and different video codecs. To facilitate a fair comparison, we compute the maximum supportable video rates by the experimental system with 3 relays using the same numerical analysis method of Section 3.3. Since we did not try to limit the air time to 20%, we cannot use the β assumed in our numerical analysis. In [40], the authors show that for different transmission rates, due to collisions and idle times as well as the headers, the effective throughput hence the β value for 1Mbps and 11Mbps is approximately 85% and 65% respectively. Using these β's and the actual FEC rates used in the experiments, we derive the maximum video rates supportable by different systems. In Table 3.7, we compare the numerical analysis with the experimental results. We show that the experimental results are very close to the numerical analysis.

3.7 Chapter Summary

In this chapter, we propose the integration of layered video coding, packet level FEC and two-hop relaying to enable efficient and robust video multicast in infrastructure-based wireless networks. We determine the node partition, transmission time scheduling and FEC based on the optimization criterion. We show that the use of omni-directional relays can substantially improve multicast system performance by providing better quality links (both for sender and relay) and hence, higher sustainable transmission rates. Using directional relays further improves the multicast system performance as compared to omni-directional relays. To supplement our numerical results, we further implemented a prototype using open source drivers and socket programming and validated the system performance with real-world experiments. Experimental results confirm the efficiency of our schemes and show that such an integrated system infrastructure presents a promising design for future realistic wireless multimedia multicasting networks.

There are many possible avenues for further research. The proposed system is designed so that we optimize the video quality while guaranteeing $r_{omni} \geq r_d$ and $r_{dir} \geq r_d$ for omni-directional relays and directional relays, respectively. However, coverage range or the total energy consumption can be also used as an multicast optimization criteria. In the numerical analysis of this chapter, assuming only path loss, we perform optimum relay selection and compute the maximum achievable performances with both omni-directional and directional relay transmissions. Our results are either applicable to dense networks or non-dense networks with fixed, dedicated relays. In the implementation, the relays are located at pre-computed optimum positions. In a realistic environment, node placement may not be dense and is likely to change over time. Furthermore, channel conditions are affected by both path loss and fading. Protocols that give a good estimate of the channel conditions for all nodes through an efficient feedback mechanism for multicast such as RTCP exist, however,

how to dynamically adapt node partition and relays selection based on such estimate is a challenging problem. In this work, we find the optimum parameters that maximize the video quality of multicast nodes in a single cell. More generally, one should optimize the system parameters while considering the interference to the neighboring cells. These are challenging issues and subjects of our ongoing research.

(a) Direct Transmission

(b) Single Layer (OMNI)

(c) Layered (OMNI)

(d) Single Layer (DIRECTIONAL)

(e) Layered (DIRECTIONAL)

Figure 3.8: Visual Quality Comparison of Two-hop Layered Multicast with Omni-directional Relays, Directional Relays and Direct Transmission. In the layered case, Group 2 nodes experience the same quality with direct transmission.

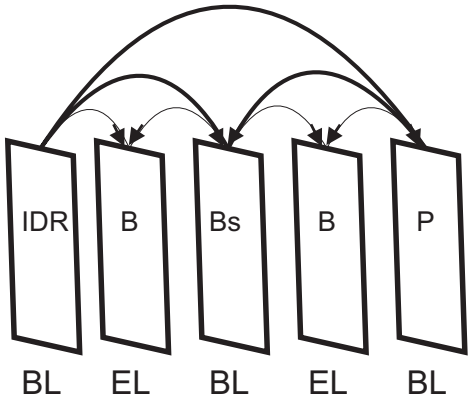

Figure 3.9: The H.264 temporal scalability coding structure.

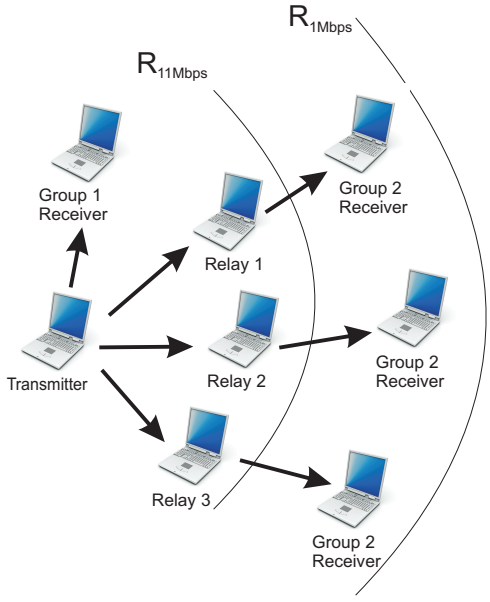

Figure 3.10: Experimental setup.

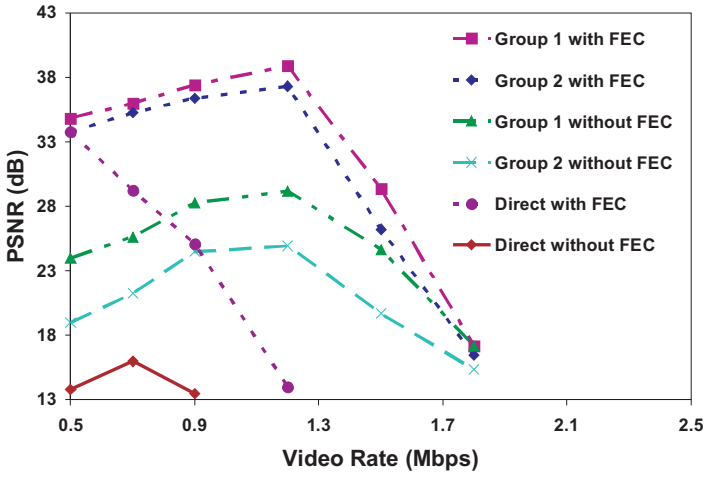

Figure 3.11: Experimental Results (omni-directional):Comparison of Single Layer Two-hop Multicast with Direct Transmission with and without FEC (averaged over 10 experiments).

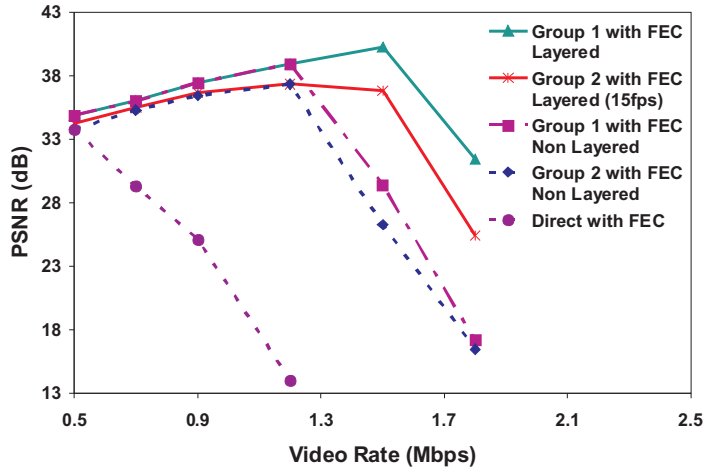

Figure 3.12: Experimental Results (omni-directional): Comparison of Layered Two-hop Multicast with Single Layer Two-hop Multicast and Direct Transmission with FEC (averaged over 10 experiments).

Chapter 4

Cooperative Layered Video Multicast using RDSTC

4.1 Introduction

In the previous chapter, we showed the benefits of cooperative multicast using relays (two-hop relaying). We first considered omni-directional relay transmission and we showed that significant gains are achievable with sequential relay transmission. We then studied the directional relay transmission to improve the multicast performance by providing simultaneous relay transmission. With this setup, the relays can transmit simultaneously, however, the beam transmission needs to be scheduled. A more spectral efficient way of transmission can be achieved at physical layer where the multiple relays transmit simultaneously using DSTC. Due to the constraints on DSTC (i.e. synchronization of the relay nodes, using a fixed number of relays each mimicing an antenna), in this chapter, we consider multicast using R-DSTC where each relay transmits a random linear combination of antenna waveforms. While two-hop relaying only considers a path loss model for simplicity on the selection of the optimum parameters, cooperative multicast using R-DSTC not only considers fading along with path loss model, but also benefits from the fading. For two-hop relaying, due to path loss model, the nodes that receive the packets in the first and second

hop transmission are clearly defined, hence named as Group 1 and Group 2 nodes, respectively. On the other hand, for cooperative multicast using RDSTC, due to different fading levels for each packet, we named the nodes that receive the packets in the first and second hop transmission as Hop-1 and Hop-2 nodes, respectively. Two-hop relaying can be implemented on the current wireless devices without any hardware modifications, as discussed in Section 3.6, since it utilizes the cooperation at MAC layer. On the other hand, cooperative multicast using R-DSTC requires some modification at the transmitter and the receiver of the relay nodes. However, due to simultaneous transmission, the performance gains are significant.

We study randomized cooperative video multicast in conjunction with packet level FEC. We first consider a simple model where the parity packets are only generated at the sender. For this case, we propose three different schemes which differ in the available network state information. The first one (R-DSTC with full channel information), assumes that the sender knows the average received SNRs between itself and each receiver node as well as between all pairs of nodes. The second scheme (R-DSTC with limited channel information), assumes that the sender only knows the channel information between the nodes and itself. Finally, the third scheme (R-DSTC with node count) considers that the sender only knows the number of nodes in its coverage range. For each of these schemes, we optimize the system operating parameters (transmission rates of both hops and consequently the STC dimension and the FEC rate) based on the channel information, and evaluate the achievable video rate.

Note that the above schemes consider that the parity packets are generated only at the sender, and even when the nodes receive all s source packets, they do not generate parity packets. However, if we let the relays generate parity packets, we can improve the performance of the system by foregoing the first hop transmission of parity packets. Therefore, we also consider an enhanced multicast model where parity packets are generated by the relays that receive all the source packets correctly. For this case, we consider two different schemes based on the available channel information

(enhanced R-DSTC with full channel information and enhanced R-DSTC with node count). For each of these schemes, we determine the optimum transmission rates for source and parity packets as well as the number of parity packets required such that the video quality at all nodes is maximized. We compare the results of the above schemes with rate adaptive direct transmission [23] and conventional multicast. We also consider a layered cooperative multicast system, which provides better video quality to the nodes with better channel conditions.

This chapter is organized as follows. We introduce the system model in Section 4.2. Section 4.3 formulates the computation of bit error rates for both direct transmission and R-DSTC. We describe the different modes of transmission and discuss the selection of the optimum parameters for multicast using R-DSTC in Section 4.4. In Section 4.5, we consider the optimization of the parameters for enhanced multicast R-DSTC. Section 4.6 analyzes the obtained results. We provide the chapter summary in Section 4.7.

4.2 System model

We study an infrastructure-based wireless network (such as Wireless LAN or cellular), and assume a sender (a base station or access point) is multicasting a compressed video stream to nodes within its coverage range of radius, r_d. We assume the nodes are randomly uniformly distributed and we define the *node placement*, ϖ, as one realization of the node locations. All nodes in the network are equipped with one antenna and can transmit at different transmission rates supported by the underlying physical layer. Note that each physical layer transmission rate, R, corresponds to a modulation level, and channel code rate. In accordance with IEEE 802.11g [41], we consider only square constellations. We assume that the channel between the source station and each node, and that between each pair of nodes, experience independent slow Rayleigh fading that is constant over the transmission time of a single packet,

R_d	Direct transmission rate for single layer (bits/sec)
$R_{d,b}, R_{d,e}$	Direct transmission rates for base and enhancement layers (bits/sec)
R_1, R_2	First and second hop transmission rates for single layer R-DSTC (bits/sec)
$R_{1,b}, R_{2,b}$	First and second hop transmission rates for the base layer (bits/sec)
$R_{1,e}, R_{2,e}$	First and second hop transmission rates for the enhancement layer (bits/sec)
γ_d, γ_c	FEC rates for single layer direct transmission and R-DSTC
$\gamma_{d,b}, \gamma_{d,e}$	Base and enhancement layer FEC rates with direct transmission
γ_b, γ_e	Base and enhancement layer FEC rates with R-DSTC
t_b, t_e	Base and enhancement layer transmission time fractions
R_{v_d}, R_{v_c}	Received video rates for direct transmission and R-DSTC (bits/sec)
R_{v_b}, R_{v_e}	Received video rates for base and enhancement layers (bits/sec)
ϖ	Node placement
L, L_b, L_e	Space time code dimension (single layer, base and enhancement layers)
R_p, L_p	Transmission rate and Space time code dimension for parity packets
γ_p	FEC rate for enhanced R-DSTC
N_T	Total number of nodes
ϵ_{max}	Maximum packet error rate among all nodes
N	Number of relays

Table 4.1: Notation

but changes independently from packet to packet. This is reasonable for video communication as a typical video packet corresponds to a video frame and lasts for 33 - 100 ms, whereas the coherence time for the channel in mobile video stream applications is typically around 100 ms. We also assume each channel experiences path loss such that the received power decays with a path loss exponent.

Before describing the details of the proposed system, we summarize the notation used in this chapter in Table 4.1. For the baseline direct transmission system, the sender transmits the packets at a physical layer transmission rate of R_d bits/sec. In order to correct the remaining packet errors after physical layer channel coding, we employ packet level FEC across video packets. We apply a packet level FEC rate of γ_d such that all the nodes in the coverage area receive the video with a FEC decoding failure probability below a certain threshold as discussed in Chapter 2.

The proposed cooperative system employs R-DSTC [19] as illustrated in

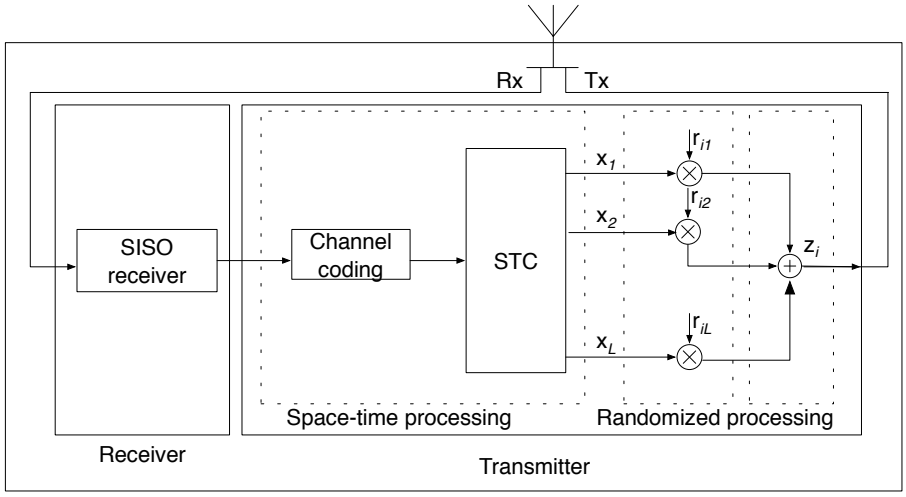

Figure 4.1: Transmitter and receiver architecture at the relay nodes

Figure 4.1, wherein a single-antenna relay employs a regular single-input and single output (SISO) decoder to decode the information sent by the source station in the first hop. Each potential relay detects bit errors in each received packet using cyclic redundancy check (CRC) and forwards the packet only when the packet is correctly received. To forward, the relay re-encodes the information and then passes the coded bits through a space-time code (STC) encoder. The output from the STC encoder is in the form of L parallel streams with each stream corresponding to an antenna in a system with L transmit antennas. However, in contrast to a multi-antenna transmitter, in a R-DSTC system, the relay transmits a random linear weighted combination of all L streams, where the weights are denoted by $\mathbf{r_n} = [\mathbf{r_{n1}}\ \mathbf{r_{n2}}\ \cdots\ \mathbf{r_{nL}}]$, with n denoting the index of each node, $n = 1, 2, \cdots, N$. The effect of different randomization vectors $\mathbf{r_i}$ is discussed in [19]. The diversity of R-DSTC based cooperation is the minimum of the STC dimension L and the number of relays. At the receiver, the equivalent channel gain (which includes the channel gain and the randomization matrix) is estimated using pilot signals [19]. Therefore, decoders already designed for space-time code reception can be directly used for R-DSTC decoding.

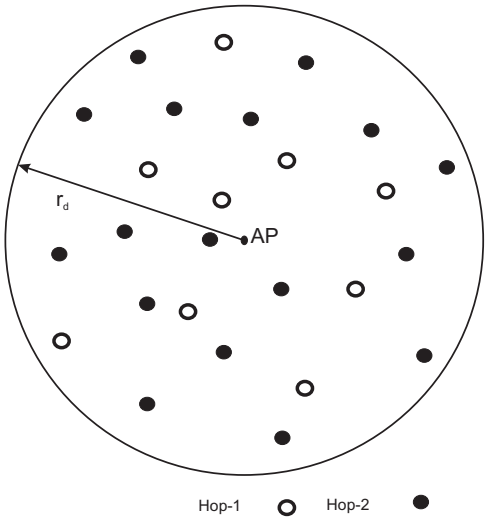

Figure 4.2: Snapshot of the network.

We integrate packet level FEC with randomized cooperation. We consider two different ways for the parity packet transmission. First one, *multicast-RDSTC*, assumes that the parity packets are only generated at the sender and forwarded by the relays. For *multicast-RDSTC*, the sender transmits a packet (source or parity packet) at a physical layer transmission rate of R_1 bits/sec. The nodes that receive the packet correctly form the relay set, and are called the Hop-1 nodes, as depicted in Figure 4.2 where a snapshot of the network for some fixed fading state is illustrated. All nodes that can correctly receive a packet from the sender re-encode and transmit the packet simultaneously at a physical layer transmission rate of R_2 bits/sec using R-DSTC with dimension L. The nodes which fail to receive the sender transmission correctly are called Hop-2 nodes, and they listen to relay transmissions to decode the original source packet. We assume that the sender does not transmit with the relays in the second hop, and Hop-2 nodes do not use the noisy signal received from the sender in Hop-1 in decoding. Combining sender and relay signals would increase the performance at Hop-2 nodes at the expense of a more complex receiver. Note that

as we increase R_1, the number of Hop-1 nodes reduces. Therefore, the sustainable data rate for the second hop, R_2, is expected to be lower in order to cover all the nodes. On the other hand, if the first hop rate, R_1 is lower, more nodes participate in the second hop transmission, and hence the second hop transmission rate, R_2 can be higher. In order to handle packet losses, the sender employs packet level FEC at a rate γ_c. Here, we assume the Hop-1 nodes do not differentiate between the source and FEC (parity) packets. The sender chooses γ_c such that after two hop transmission, the FEC decoding failure probability at each node is below ς. Successful reception of a packet does not necessarily depend on the distance to the sender due to fading. Therefore, some of the nodes that are closer to the sender may experience a bad fading level and may not be able to receive the packet. On the other hand, there are some nodes that observe a good fading level and receive the packet even though they are far away from the sender. Also, due to different fading levels for each packet, whether a node belongs to Hop-1 or Hop-2 can change from packet to packet.

In order to improve the performance of the *multicast-RDSTC*, we also consider an *enhanced-multicast-RDSTC* model, where the parity packets are generated at the relays. For *enhanced-multicast-RDSTC*, the sender transmits the source packets at a transmission rate of R_1 bits/sec and the relays forward these packets using R-DSTC with STC dimension of L at a rate R_2 bits/sec. After the completion of s source packet transmission, the nodes that receive all s source packets become *parity relays*. The parity relays generate parity packets and transmit using R-DSTC at a rate R_p bits/sec with STC of dimension L_p. Note that after each parity packet transmission, any node that receives a total of s packets out of all packets transmitted so far, can decode to obtain the s source packets become a parity relay and join the parity packet transmission. Therefore, the number of parity relays increases in time. In general, the source packets can be transmitted only in the first hop. However, due to the low diversity of the first hop transmission, the number of nodes receiving all s packets after source transmission would be very small, hence number of parity

relays would be insufficient. Therefore, the proposed scheme always uses two-hop transmission for the source packets.

In addition to the aforementioned single layer system, we also examined a layered system where the sender and relays transmit packets from different layers in separate time slots. For direct transmission, we assume the sender transmits the base layer packets at a rate $R_{d,b}$ bits/sec with a FEC rate of $\gamma_{d,b}$ and the enhancement layer packets at a rate $R_{d,e}$ bits/sec with a FEC rate of $\gamma_{d,e}$. For cooperative multicast, we only consider source layering for *multicast-RDSTC*, however extensions to *enhanced-multicast-RDSTC* can be done similarly. For *multicast-RDSTC-layered*, the sender transmits the base layer packets at a rate $R_{1,b}$ bits/sec and the relays transmit the base layer packets at a rate $R_{2,b}$ bits/sec and STC dimension L_b, both with a FEC rate of γ_b. Similarly, the transmission rates for enhancement layer packets for the first and second hop are $R_{1,e}$ and $R_{2,e}$, respectively, with a STC dimension of L_e and FEC rate of γ_e. We denote the percentage of nodes that receive both base and enhancement layers by μ. We configure the transmission rates and FEC rates so that $(100 - \mu)$ percent of the nodes get quality better than or similar to direct transmission, whereas the remaining μ percent observe significantly better quality than direct transmission.

4.3 Computation of Bit and Packet Error Rates

In the following subsections, we first discuss the computation of the instantaneous Bit Error Rate (BER) (for each channel realization), both for direct transmission and R-DSTC. Then, using this BER and the underlying channel code, we will describe the computation of average Packet Error Rate (PER). The PER in return will be used to determine the required packet level FEC rate.

4.3.1 BER of Single Link

We assume that at time k the sender transmits a symbol $\mathbf{x}(\mathbf{k})$ with energy $E_{s,s}$ and m^{th} node experiences an instantaneous channel gain of h_m from the sender. Then the received signal at the m^{th} node at time k can be written as:

$$y_m(k) = \sqrt{E_{s,s}} h_m x(k) + w_m(k) \tag{4.1}$$

where w_m is additive complex white Gaussian noise with variance N_0, and h_m is the Rayleigh random variable representing the channel gain. We can express the instantaneous received SNR at the m^{th} node, ζ_m, as

$$\zeta_m(\bar{\zeta}, h_m) = \frac{E_{s,s}\|h_m\|^2}{N_0} = \bar{\zeta}\|h_m\|^2 \tag{4.2}$$

where $\bar{\zeta}$ is the average transmit SNR.

For a M-QAM square constellation, the symbol error rate can be computed as [43]:

$$P_s(M, \zeta_m) = 1 - [1 - P_{\sqrt{M}}(M, \zeta_m)]^2 \tag{4.3}$$

with

$$P_{\sqrt{M}}(M, \zeta_m) = 2(1 - \frac{1}{\sqrt{M}})\ erf(\sqrt{\frac{3\zeta_m}{(M-1)}}) \tag{4.4}$$

where the *erf* function is defined as:

$$erf(x) = \int_x^\infty \frac{1}{\sqrt{2\pi}} e^{-y^2/2} dy \tag{4.5}$$

With Gray coding, the bit error rate for the M-QAM can be approximated by,

$$P_b(M, \zeta_m) \approx \frac{1}{\log_2 M} P_s(M, \zeta_m) \tag{4.6}$$

4.3.2 BER for RDSTC

Note that the instantaneous BER computation for the first hop of R-DSTC is the same as for the direct transmission. For the second hop, we assume N nodes

receive the packet correctly and participate as relays. Each relay transmits its data with a symbol energy of $E_{s,r}$.

We consider an underlying STC of size $L \times K$ for R-DSTC, where L is the number of antennas and K is the block length. We assume the STC is based on real orthogonal designs [42]. For $L = 2, 4, 8$, the orthogonal design provides full rate for square QAM constellation [43],[42]. For R-DSTC weights represented by a vector $\mathbf{r_n}$ for relay n, we can express the transmitted signal from the n^{th} relay at time k, as

$$z_n(k) = \sqrt{E_{s,r}}\mathbf{r_n}\mathbf{X}(\mathbf{k}), \tag{4.7}$$

where $n = 1, 2, \cdots, N$ and $k = 1, 2, \cdots, K$. Here, $\mathbf{X}(\mathbf{k})$ is the k^{th} column of the STC. We assume that each element of $\mathbf{r_n}$ is an independent complex Gaussian random variable with zero mean and variance $\frac{1}{L}$ [19]. Note that $\mathbf{X}(\mathbf{k})$ is a function of the source symbols, with the mapping determined by the underlying STC.

The receiver architecture in Hop-2 is similar to a regular STC receiver with one antenna. The received signal at node m at the k^{th} symbol interval can be expressed as

$$y_m(k) = \mathbf{h_m}\mathbf{Z}(\mathbf{k}) + \mathbf{w_m}(\mathbf{k}) = \sqrt{\mathbf{E_{s,r}}}\ \mathbf{h_m}\mathbf{R}\mathbf{X}(\mathbf{k}) + \mathbf{w_m}(\mathbf{k}) \tag{4.8}$$

where $\mathbf{h_m}$ is the $1 \times N$ channel vector, $\mathbf{h_m} = [\mathbf{h_{1m}}...\mathbf{h_{Nm}}]$ with h_{im} representing channel gain from i^{th} relay to the m^{th} node, $w_m(k)$ denotes additive white Gaussian noise with variance N_0. $\mathbf{Z}(\mathbf{k})$ and $\mathbf{R}$ can be written as, $\mathbf{Z}(\mathbf{k}) = [\mathbf{z_1}(\mathbf{k})\ \mathbf{z_2}(\mathbf{k})\ \ldots\ \mathbf{z_N}(\mathbf{k})]^{\mathbf{T}}$, $\mathbf{R} = [\mathbf{r_1}\ \mathbf{r_2}\ \ldots\ \mathbf{r_N}]^{\mathbf{T}}$.

Using pilot signals, estimation of the equivalent channel gain $\mathbf{h_m}\mathbf{R}$ can be done similarly to the estimation of channel gain $\mathbf{h_m}$ in conventional STC [19]. Assuming the m^{th} node estimates $\mathbf{h_m}\mathbf{R}$ perfectly and using the orthogonality of the STC, the equivalent received SNR at node m is:

$$\zeta_m(\bar{\zeta}, \mathbf{h_m}, \mathbf{R}) = \frac{\mathbf{E_{s,r}}\|\mathbf{h_m}\mathbf{R}\|^{\mathbf{2}}}{\mathbf{N_0}} = \bar{\zeta}\|\mathbf{h_m}\mathbf{R}\|^{\mathbf{2}} \tag{4.9}$$

We can compute the instantaneous BER by inserting (4.9) in (4.4) and then using (4.6).

4.3.3 Computation of PER

Following the specifications of IEEE 802.11g standard, we employ convolutional codes of rates 1/2, 2/3 and 3/4 with generator polynomials given in [41]. We assume the bit errors in the received stream, which serves as the input to the channel decoder, are independent and identically distributed with the instantaneous BER given as in Section 4.3.1 and Section 4.3.2, and we numerically compute the corresponding PER. For both schemes, we first generate a bit stream and encode it using a chosen convolutional code. The coded bits are flipped randomly according to the BER derived above. The output of the decoder is compared to the bitstream to determine whether a packet is received or not at a particular fading level. Note that due to fading, the received channel strength, and hence the reception of a packet at each node changes over time. For direct transmission, at each node and for a particular fading level, we first determine whether a packet is received or not using the single link BER. Then, using channel simulations, the average PER is computed over all possible fading levels. Hence, the average PER between the two nodes only depends on the modulation and the channel code as well as the distance between the nodes. For cooperative multicast, we compute the average PER from the sender to each node in two steps. We first determine whether a packet is received or not after first hop transmission based on single link BER. The nodes that receive the packets becomes relays. We then compute the BER of the link from relays to each node using the BER computation for R-DSTC. Similar to the single link case, using channel simulations, we compute the average PER over all possible fading levels. For a given node placement ϖ and transmission scheme as in Section 4.3.1 and Section 4.3.2, we find the maximum PER, ϵ_{max}, among all nodes, based on the average PER at each node.

4.4 Multicast using R-DSTC

In this section, we will first we derive a formulation of the video rate for direct transmission and *multicast-RDSTC*, and discuss the optimization of the parameters given the node placement, ϖ. Note that knowing the node placement is equivalent to having the full channel information (such as the sender knows the average channel qualities from each node to the source station as well as among each pair of nodes). In practice, the sender may only have partial channel information (such as the sender only knows the average channel qualities from each node to the sender or the node count). Then, we will consider the system optimization under partial channel information.

4.4.1 Problem Formulation and Optimization under Full Channel Information

In the most general setup, we assume two-hop cooperative multicast where at each hop, we consider the transmission of base and enhancement layer packets. For this setup, we divide a video into segments of duration of T seconds. The time T is shared between the first and second hops. The base layer is transmitted over $t_{1,b}$ and $t_{2,b}$ fractions of each time interval for the first and second hop respectively, where

$$t_b = t_{1,b} + t_{2,b}. \tag{4.10}$$

Similarly, the enhancement layer is transmitted over $t_{1,e}$ and $t_{2,e}$ fractions of each time interval for the first and second hop respectively, where

$$t_e = t_{1,e} + t_{2,e}. \tag{4.11}$$

This leads to

$$t_b + t_e = t_{1,b} + t_{1,e} + t_{2,b} + t_{2,e} = 1. \tag{4.12}$$

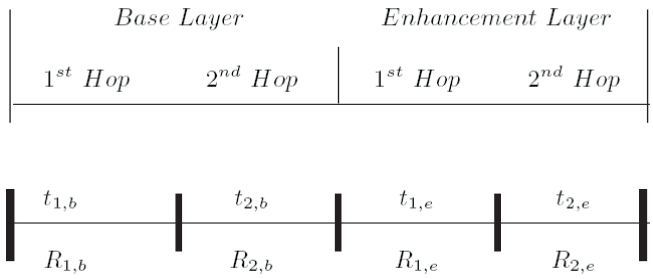

Figure 4.3: Time scheduling and transmission rates for base and enhancement layers at first and second hop.

The time scheduling of the base and enhancement layers along with the transmission rates are illustrated in Figure 4.3.

Following (2.1), the video rates for the base layer at Hop-1 and Hop-2, $R_{v_{1,b}}$ and $R_{v_{2,b}}$, can be expressed as:

$$R_{v_{1,b}} = \gamma_b \beta R_{1,b} t_{1,b} \quad , \quad R_{v_{2,b}} = \gamma_b \beta R_{2,b} t_{2,b} \tag{4.13}$$

where γ_b is the FEC rate for the base layer.

Similarly, the video rates for the enhancement layer at Hop-1 and Hop-2, $R_{v_{1,e}}$ and $R_{v_{2,e}}$, are:

$$R_{v_{1,e}} = \gamma_e \beta R_{1,e} t_{1,e} \quad , \quad R_{v_{2,e}} = \gamma_e \beta R_{2,e} t_{2,e} \tag{4.14}$$

where γ_e is the FEC rate for the enhancement layer.

Below we discuss two different transmission modes: Direct transmission and cooperative multicast, both of which are special cases of the above formulation. For both modes, we further consider single layer and layered cooperation and discuss the benefits of source layering.

Cooperative Multicast

Single layer Cooperation (*multicast-RDSTC*): For single layer cooperation (*multicast-RDSTC*), we set $t_{1,e} = t_{2,e} = 0$ in (4.11), hence, we have $t_e = 0$ and $t_b = t_{1,b} + t_{2,b} = 1$. The first and second hop transmission rates are $R_1 = R_{1,b}$ and $R_2 = R_{2,b}$. The FEC rate $\gamma_c = \gamma_b$ depends on the maximum PER among all nodes after two hop transmission. Since we consider end-to-end packet level FEC, we compute the PER experienced by each node in the multicast group using the formulation in Section 4.3. Note that given the node placement ϖ, the maximum PER, hence γ_c, depends on the transmission rates of both hops, R_1 and R_2 and the corresponding R-DSTC dimension L.

Since we would like Hop-1 and Hop-2 nodes to receive the same video rate, the transmission parameters should be chosen such that $R_{v_1,b} = R_{v_2,b}$. This yields $t_{1,b} = R_2/(R_1+R_2)$, and given ϖ and β, the the corresponding video rate for *multicast-RDSTC* can be expressed as:

$$R_{v_c}(R_1, R_2|\varpi, \beta) = \gamma_c(R_1, R_2|\varpi)\beta\frac{R_1R_2}{R_1+R_2} \tag{4.15}$$

For a given node placement ϖ, for each candidate (R_1, R_2), we first determine the average number of nodes (averaged over different node placements), N_{avg} that can successfully decode the first hop transmission. Among available STC dimensions, L is chosen to be equal or lower than N_{avg} to maximize the diversity gain. Hence in (4.15), we only indicate the dependence of the video rate and the FEC rate on (R_1, R_2). Then for this set of R_1, R_2, L we determine maximum end-to-end average PER (averaged over fading) among all nodes. We determine the suitable FEC of rate γ_c to ensure FEC decoding failure probability is less than ς. We search over all sustainable (R_1, R_2) through an exhaustive search to choose the optimum (R_1, R_2), and the corresponding L, γ_c that maximizes the video rate in (4.15).

Layered Cooperation (*multicast-RDSTC-layered*): In order to provide nodes differentiated quality based on their channel conditions, we consider two layers:

Base and enhancement layer. For layered cooperation (*multicast-RDSTC-layered*), since we want all nodes receive the base layer at the same video rate, we have $R_{v_b} = R_{v_1,b} = R_{v_2,b}$. This yields $t_{1,b} = R_{2,b}t_b/(R_{1,b} + R_{2,b})$. Then, the corresponding video rate for the base layer can be expressed as:

$$R_{v_b}(R_{1,b}, R_{2,b}, t_b|\varpi, \beta) = \gamma_b(R_{1,b}, R_{2,b}|\varpi)\beta\frac{R_{1,b}R_{2,b}}{R_{1,b} + R_{2,b}}t_b \tag{4.16}$$

where γ_b is the FEC rate for the base layer and is determined by the maximum PER after two hop transmission, $\epsilon_{max}(R_{1,b}, R_{2,b}|\varpi)$.

For the enhancement layer, we consider two options: The relays either forward all the enhancement layer packets (with a lower FEC redundancy compared to base layer packets) or not forward any enhancement packets at all. In both options, we require that a certain percentage of nodes μ, receive the enhancement layer. By choosing the enhancement layer FEC rate γ_e, we can adjust the percentage of nodes that receive the enhancement layer with a FEC decoding failure probability below the threshold ς. Therefore, in the first option, γ_e depends on the target μ as well as $(R_{1,e}, R_{2,e}, L_e)$. Furthermore, since all enhancement layer packets are forwarded, we choose the transmission time such that $R_{v_1,e} = R_{v_2,e}$. This yields $t_{1,e} = R_{2,e}t_e/(R_{1,e} + R_{2,e})$. Since $t_e + t_b = 1$, the video rate for the enhancement layer can be expressed as:

$$R_{v_e}(R_{1,e}, R_{2,e}, t_b|\varpi, \beta, \mu) = \gamma_e(R_{1,e}, R_{2,e}|\varpi, \mu)\beta\frac{R_{1,e}R_{2,e}}{R_{1,e} + R_{2,e}}(1 - t_b). \tag{4.17}$$

Alternatively, the enhancement layer packets can go through only one hop transmission, and the sender chooses $R_{1,e}$ and γ_e so that μ percentage of nodes successfully receive the enhancement layer packets in the first hop. Since the enhancement layer packets are not forwarded, the FEC rate only depends on the first hop transmission rate, $R_{1,e}$ as well as μ. In this case, $t_{2,e} = 0$, hence, $t_e = t_{1,e}$. Then the video rate for the enhancement layer is:

$$R_{v_e}(R_{1,e}, t_b|\varpi, \beta, \mu) = \gamma_e(R_{1,e}|\varpi, \mu)\beta R_{1,e}(1 - t_b) \tag{4.18}$$

For the optimization, we set the video rate of the base layer to a target bit rate R_{v_b}. Then, for a given $R_{1,b}, R_{2,b}$, we determine L_b, γ_b to maximize $\gamma_b \frac{R_{1,b}R_{2,b}}{R_{1,b}+R_{2,b}}$ similar to single layer case. Next, we compute t_b using optimized $R_{1,b}, R_{2,b}, \gamma_b, L_b$ such that (4.16) is met for the target base layer video rate R_{v_b}. Note that since we want to maximize R_{v_e}, this results in the lowest t_b, and therefore the largest t_e. For the enhancement layer for the two-hop case, we find all feasible $R_{1,e}, R_{2,e}$ and the corresponding L_e, γ_e that guarantees the reception at μ percent of the nodes. Then, the sender chooses the optimum $R_{1,e}, R_{2,e}$ and the corresponding L_e, γ_e that maximizes, R_{v_e} by exhaustive search. For the one-hop case, after identifying all feasible $R_{1,e}$ and the corresponding γ_e, the optimal parameters are chosen to obtain the maximum R_{v_e} for a target R_{v_b} and μ.

Direct Transmission

Single layer Direct (*Direct-adaptive*): In single layer direct transmission (*Direct-adaptive*), only base layer packets are sent using one hop transmission. This can be achieved by setting $t_{1,e} = t_{2,b} = t_{2,e} = 0$ in (4.12), hence, $t_{1,b} = 1$. We assume the sender transmits at the direct transmission rate R_d, and FEC rate γ_d. By setting $R_d = R_{1,b}$ and $\gamma_d = \gamma_b$ in (4.13), the video rate of direct transmission is

$$R_{v_d}(R_d|\varpi, \beta) = R_{v_{1,b}} = \gamma_d(R_d|\varpi)\beta R_d. \tag{4.19}$$

Given the node placement, for each feasible transmission rate R_d, we first determine the PER at each node. We then choose γ_d based on the maximum PER among all nodes, so that the FEC decoding failure probability is below a preset threshold ς. Among all feasible R_d and corresponding γ_d, we choose the one leading to the highest video rate in (4.19) by exhaustive search. Note that direct transmission does not utilize inter-node channel qualities.

Layered Direct (*Direct-adaptive-layered*): In layered direct transmission (*Direct-adaptive-layered*), base and enhancement layer packets are sent through one-

hop. By setting $t_{2,b} = t_{2,e} = 0$ in (4.10, 4.11), we have $t_b = t_{1,b}$ and $t_e = t_{1,e}$, hence $t_b + t_e = 1$. We assume the sender transmits the base layer and enhancement layers at the direct layered transmission rates, $R_{d,b}$ and $R_{d,e}$ with FEC rates of $\gamma_{d,b}$ and $\gamma_{d,e}$, respectively. The FEC rate $\gamma_{d,e}$ is chosen such that μ percent of nodes successfully receive the enhancement layer packets. By setting $R_{d,b} = R_{1,b}$ and $R_{d,e} = R_{1,e}$ in (4.14), the base and enhancement layer video rates of (*Direct-adaptive-layered*) can be expressed as:

$$R_{v_b}(R_{d,b}|\varpi, \beta) = R_{v_{1,b}} = \gamma_{d,b}(R_{d,b}|\varpi)\beta R_{d,b} t_b, \tag{4.20}$$

$$R_{v_e}(R_{d,e}|\varpi, \beta, \mu) = R_{v_{1,e}} = \gamma_{d,e}(R_{d,e}|\varpi, \mu)\beta R_{d,e}(1 - t_b). \tag{4.21}$$

As with cooperative layered transmission, for a target R_{v_b} and μ, we choose the optimum $R_{d,b}$, $R_{d,e}$ and the corresponding FEC rates that maximize R_{v_e}.

4.4.2 Optimization under Partial Channel Information

In this section, we discuss different options for selection of optimum parameters under partial channel information. We will describe the simulation setup and compare the performance of different schemes in Section 4.6.

Recall that for the full channel information case, the sender needs to know the average channel qualities from each node to itself, as well as among each pair of nodes. In order for the sender to know the average channel quality among the nodes, the nodes could exchange control signals among themselves for measuring the average SNR, and then transmit this information back to the sender. Although having full channel information provides the best results, we recognize that such computation of optimal transmission parameters may be too complex to be done in real time. Therefore, *full-channel* information will be used as a benchmark for more practical schemes with partial channel information. As we will observe in Section 4.6, R-DSTC provides a robust cooperation scheme and suffers minimal performance loss due to partial channel information.

We consider 3 different scenarios for partial channel information: *limited-channel*, *node-count* and *coverage-range*. For the *limited-channel* case, we assume the sender knows the average channel quality between itself and every node in the target coverage area. This requires channel feedback from the nodes; however in this case, inter-node channel qualities are not needed. For the *node-count* case, the only information the sender has is the number of nodes in the multicast coverage range. Finally, the sender only knows the average channel quality at the edge of the coverage range for *coverage-range*. Below, we only discuss the optimization for the single layer; the extension to the layered case can be done similarly.

Cooperative Multicast

For the benchmark R-DSTC with full-channel information (*multicast-RDSTC*), the optimization is carried out as described in Section 4.4.1. Below, we discuss the practical schemes with partial channel information.

R-DSTC with limited-channel information (*multicast-RDSTC-limited***)**: In order to compute the optimal parameters, for a given set of average channel conditions between the sender and the nodes, we generate multiple node placements which have same source-node average channel qualities, but different inter-node average channel qualities. Since some node placements can be very unfavorable to cooperation, we only consider the majority of the node placements for a given set of source-node average channel conditions and optimize the parameters based on 95% of the node placements, by not considering those 5% of node placements with the highest PER. However, when we report the system performance, we evaluate the performance for the worst 5% of the node placements as well. Specifically, for each candidate R_1, R_2 and the corresponding L, among all node placements with the same source-node average channel qualities, we remove the worst 5% of node placements in terms of PER, and find the maximum PER among the remaining 95%, and set γ_c in (4.15) based on this PER. Note that choice of L for a given R_1 can be carried out as

in Section 4.4.1. Then we choose the optimum (R_1, R_2) and the corresponding L, γ_c that maximize the video rate in (4.15). In practice, a table of optimum transmission rates, FEC rate and space time code dimension (R_1, R_2, γ_c and L) for different channel conditions between the sender and the nodes, can be pre-computed and stored at the sender.

R-DSTC with node-count information (*multicast-RDSTC-nodecount*): In order to compute the optimal parameters, for a given node count, we generate different node placements. Different from the *multicast-RDSTC-limited* scheme, here we have different source-node distances as well as different inter-node distances for a given node count. In a manner similar to *multicast-RDSTC-limited* scheme, we only consider the majority of the node placements (i.e. 95% best node placements). We first find the maximum PER among all node placements with the same node count (except for the worst 5% placements) and choose γ_c based on this PER. We then find the optimum (R_1, R_2, L, γ_c)'s to maximize the video rate in (4.15). In practice, a table of optimum transmission rates, space time code dimension and the corresponding FEC rate (R_1, R_2, L and γ_c) for different number of nodes can be pre-computed and stored at the sender.

Note that knowing only the average channel quality at the edge of the coverage range does not provide sufficient information for R-DSTC scheme to work properly, since the worst case scenario there would be having all nodes at the edge of the coverage range, where the improvements from cooperation is minimal. Hence, we did not consider that mode.

Direct Transmission

Direct with limited channel information (*Direct-adaptive*): Since direct transmission only uses channel information from the sender to all the nodes, this mode is the same as the single layer direct as in Section 4.4.1.

Direct with coverage-range information (*Direct*): The sender is as-

(a) RDSTC scheme

(b) Enhanced RDSTC scheme

Figure 4.4: Transmission rates and time scheduling for RDSTC schemes

sumed to know the average PER of the nodes at the edge of the coverage range at the base rate. Then, all packets are transmitted at the base rate of the underlying network (e.g. 6Mbps for IEEE 802.11g) with a packet level FEC at fixed rate γ_d. In our simulations, we choose the symbol energy of the sender such that with direct transmission at the base transmission rate, the nodes at the edge of the coverage range experience a certain average PER. The fixed FEC rate γ_d is chosen based on this average PER such that the FEC decoding failure probability is smaller than ς. This model represents a conventional multicast system.

Note that for direct transmission, node count information results in the same parameters as coverage range information since direct transmission does not use relays.

4.5 Enhanced Multicast using R-DSTC

In this section, we will derive a formulation of the video rate for *enhanced-multicast-RDSTC*, and discuss the optimization of the parameters.

We first illustrate the time scheduling along with their transmission rates for *enhanced-multicast-RDSTC* and compare it with *multicast-RDSTC* in Figure 4.4. Suppose the source packets are transmitted for fractions of time denoted by $t_{1,s}$ and $t_{2,s}$, by the AP and relays for the first and second hop, respectively. Similarly, the

parity packets are transmitted by the AP and the relays for fractions of time $t_{1,p}$ and $t_{2,p}$, respectively. Here, the total time fraction for the first and second hops are $t_1 = t_{1,s} + t_{1,p}$ and $t_2 = t_{2,s} + t_{2,p}$, where $t_1 + t_2 = 1$. Note that, for the *enhanced-multicast-RDSTC*, since we forego the parity packet transmission at the first hop, we have $t_{1,p} = 0$, hence, $t_1 = t_{1,s}$.

Enhanced R-DSTC with full channel information (*enhanced-multicast-RDSTC***):**

For the *enhanced-multicast-RDSTC* scheme, the FEC rate γ_p depends on the maximum PER among all users after two hop transmission, hence, it depends on transmission rates of both hops and the STC dimension, R_1, R_2, L. However, since parity packets are only transmitted at the second hop, the number of parity packets required also depends on the PER of the second hop which is determined by the parity transmission rate R_p as well as the parity transmission STC dimension L_p, therefore, γ_p is a function of $\gamma_p(R_1, R_2, L, R_p, L_p)$.

Assuming that the lost source packets are recovered using packet level FEC, the received rates for the source packets at each hop are $R_{v1} = \beta R_1 t_{1,s}$ and $R_{v2} = \beta R_2 t_{2,s}$, where $t_{1,s} + t_{2,s} + t_{2,p} = 1$. To ensure that all nodes receive video at the same rate, $R_{v1} = R_{v2} = R_v$, we choose $t_{1,s} = R_2(1 - t_{2,p})/(R_1 + R_2)$. Then, we have

$$R_{v_p} = \beta(1 - t_{2,p})\frac{R_1 R_2}{R_1 + R_2} \tag{4.22}$$

Note that (4.22) intrinsically includes γ_p since $t_{2,p}$ depends on the number of parity packets required and the parity packet transmission rate. To recover the lost packets, we need p parity packets resulting in a FEC rate of $\gamma_p = s/(s+p)$. Since the average packet size is $B = R_1 t_{1,s}/s$, the time it takes to transmit p parity packets at a rate R_p can be expressed as:

$$t_{2,p} = pB/R_p = pR_1 t_{1,s}/kR_p = (1 - \gamma_p)R_1 t_{1,s}/\gamma_p R_p \tag{4.23}$$

Combining (4.22) and (4.23), we can derive R_{v_p} for the source packet transmission rates, R_1 and R_2, parity transmission rate R_p, and also for the R-DSTC dimension

for both source and parity packets, L and L_p, as below:

$$R_{v_p}(R_1, R_2, R_p, L, L_p, \beta) = \frac{\gamma_p \beta R_1 R_2 R_p}{(1-\gamma_p) R_1 R_2 + \gamma_p R_p (R_1 + R_2)} \tag{4.24}$$

Among all sustainable R_1, R_2, R_p's, the source chooses the optimum R_1, R_2, R_p and the corresponding γ_p, L, L_p that maximizes the video rate. Similar to the *multicast-RDSTC* case, L and L_p are chosen as close as possible to the average number of relays for given R_1, R_2. For the *enhanced-multicast-RDSTC* case, since the parity relays dynamically change, L_p is adjusted packet by packet while R_p is fixed throughout the transmission. However, considering practical L_p values and the fact that the number of parity relays increases in time, after a few parity packet transmissions, we observe that the system operates at constant L_p.

Enhanced R-DSTC with node count (*enhanced-multicast-RDSTC-nodecount***):** For the *enhanced-multicast-RDSTC-nodecount*), for a given node count, we generate different node placements. Similar to *multicast-RDSTC-nodecount*, we only consider the majority of the node placements (i.e. 95% best node placements). For a given (R_1, R_2, R_p), we first find the maximum p among all node placements with the same node count (except for the worst 5% placements) and choose γ_p based on this p. We then find the optimum $(R_1, R_2, R_p, L, L_p, \gamma_p)$'s to maximize the video rate in (4.24).

4.6 Results

To evaluate and compare the performances of different transmission modes, we study IEEE 802.11g based network whose physical layer transmission rates and their corresponding modulation and convolutional channel coding rates are illustrated in Table 4.2. We consider a coverage radius of $r_d = 100m$, where the access point is at the center of the network and nodes are randomly uniformly distributed in the coverage range. We assume that the fading is independent and constant for

Transmission Rate, R	6Mbps	9Mbps	12Mbps	18Mbps	24Mbps	36Mbps	48Mbps	54Mbps
Modulation	BPSK	BPSK	QPSK	QPSK	QAM-16	QAM-16	QAM-64	QAM-64
Channel Code Rate	1/2	3/4	1/2	3/4	1/2	3/4	2/3	3/4

Table 4.2: Transmission rates for IEEE 802.11g and their corresponding modulation schemes and channel codes

each packet, whose length is typically around 1400 bytes. We use a block size $s = 128$ packets for FEC encoding. For R-DSTC, we choose among orthogonal STC dimensions of $L = 2, 4, 8$. For these STC dimensions, there exist real orthogonal designs which provide full rate for square constellations [43].

In our simulations, we consider different total number of nodes, N_T, corresponding to different density networks and for each node density, we generate 200 different node placements. Then, for each node placement ϖ, we generate 2000 different independent fading levels for all node pairs (including sender to node). We choose the transmission power of the sender such that with direct transmission at the base transmission rate $R_d = 6Mbps$, and the nodes at the edge of the coverage range experience an average PER of 5% (before FEC), which is a typical PER assumption for wireless networks. For the same node count, the optimal transmission parameters and hence achievable video rates for *multicast-RDSTC*, *enhanced-multicast-RDSTC*, *multicast-RDSTC-limited* and *Direct-adaptive* depend on the actual node placements. In the performance curves presented below, for the same node count, we report the average video rates that are averaged over all node placements.

For *multicast-RDSTC* scheme, in order to have comparable energy consumption with direct transmission, we assume that the relay energy per symbol is set to $E_r = E_s/N_{avg}$ where E_s is the symbol energy of the AP and N_{avg} is the average number of nodes that receive the packets correctly at the first hop for a given number of

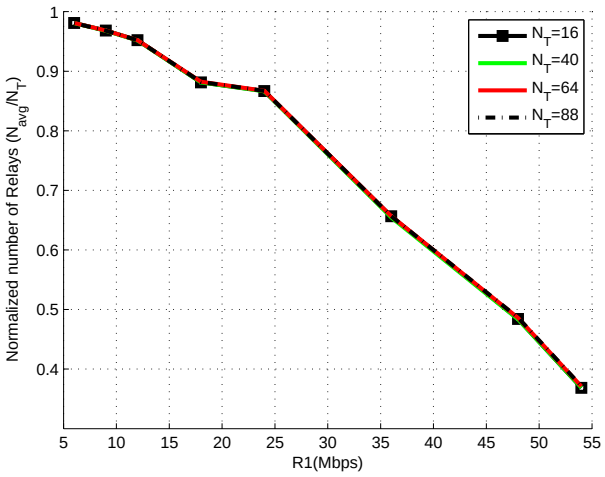

Figure 4.5: N_{avg}/N_T vs R_1

nodes and transmission rate, R_1. N_{avg} is computed based on simulations. Note that N_{avg} depends on the total number of nodes, N_T and first hop transmission rate, R_1. Since the symbol rate is same for all different physical transmission rates, by setting the symbol energy as above, the average power consumed by R-DSTC scheme is on the average equal to direct transmission. In Figure 4.5, we illustrate N_{avg}/N_T versus different first hop transmission rates for different N_T (averaged over node placements and fading levels). We observe that the ratio is almost constant for different number of nodes N_T. Therefore we use this constant ratio (depending on R_1) to normalize each relay's transmission power in all three R-DSTC schemes. Note that even at the highest transmission rate, this ratio is quite large and above 0.3. On the other hand, for the *enhanced-multicast-RDSTC* scheme, the relay energy per symbol is set to $E_r = E_s/N_{relay}$ where N_{relay} is the instantaneous number of parity relays. Note that since the number of parity relays changes from packet to packet, E_r also changes from packet to packet. Through simulations, for a given number of nodes and the number of parity relays after source packet transmissions, we estimate E_r for each

packet numerically.

For the FEC computations, we use $s = 128$ and choose p such that the probability of the residual error after FEC decoding is less than $\varsigma = 0.5\%$. We observe that when using an error-resilient video decoder, there is no observable quality degradation when the loss rate is equal or below this threshold. For the *enhanced-multicast-RDSTC* scheme, for a given node placement, we first run multiple simulations with different fading levels and determine the minimum number of parity packets p that is sufficient to correct the missing packets. This p is used for the performance evaluation.

For direct transmission (*Direct*), we use the base transmission rate $R_d = 6Mbps$ and for an average PER of 5% at the coverage, we apply a FEC rate of $\gamma_d = 0.905$ such that FEC decoding failure probability is below $\varsigma = 0.5\%$. For all the remaining schemes, the optimal parameters for all transmission modes are chosen as described in Sections 4.4.1, 4.4.2 and 4.5.

Next, we will first investigate *multicast-RDSTC* under different channel information. Then, we will present the achievable performance improvements with *enhanced-multicast-RDSTC*.

In Figure 4.6, we illustrate the achievable average video rates for different single layer schemes as a function of the number of nodes. For *Direct*, the video rate does not change with number of nodes as transmission and FEC rates are fixed. For *Direct-adaptive*, since the transmission and FEC rates are chosen based on the node with the worst average channel condition, for a large number of nodes, there is a higher chance that there will be some node at the edge of the coverage range; hence the video rate reduces as the number of nodes increases. For the cooperative multicast systems, as the number of nodes increases, more relays participate in the transmission, resulting in higher video rates. As illustrated in the figure, the proposed schemes outperform both direct transmission and rate-adaptive direct transmission. Our results show that the performance of *multicast-RDSTC-limited* and *multicast-RDSTC-nodecount*

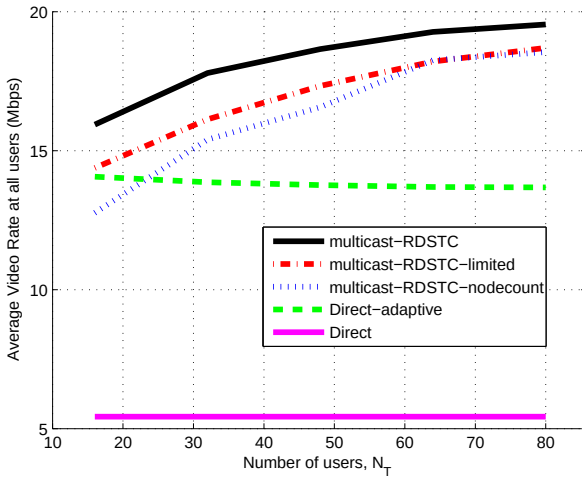

Figure 4.6: Average video rates vs number of nodes for single layer systems ($\beta = 1$).

converge as the number of nodes increases, which suggests that knowing only the node count is almost as good as knowing the average channel conditions between the source station and nodes, when the number of nodes is large. Note that the average video rates reported for *multicast-RDSTC-limited* and *multicast-RDSTC-nodecount* only include the best 95% node placements. We discuss the performance in the remaining 5% node placements below. Furthermore, the achievable video rates by both *multicast-RDSTC-limited* and *multicast-RDSTC-nodecount* are only up to 10% lower than that of the *multicast-RDSTC* requiring full channel information. This demonstrates that cooperation using R-DSTC is indeed very robust and capable of near optimal performance even without full channel information.

In Figure 4.7 and Figure 4.8, for different node counts, we present the optimum transmission rates (R_1, R_2) and the corresponding FEC rates. Note that for all schemes except for *Direct* and *multicast-RDSTC-nodecount*, the optimal transmission rates and corresponding FEC rates depend on the actual node placement for a given node count. The curves in this figure show the average over all node placements.

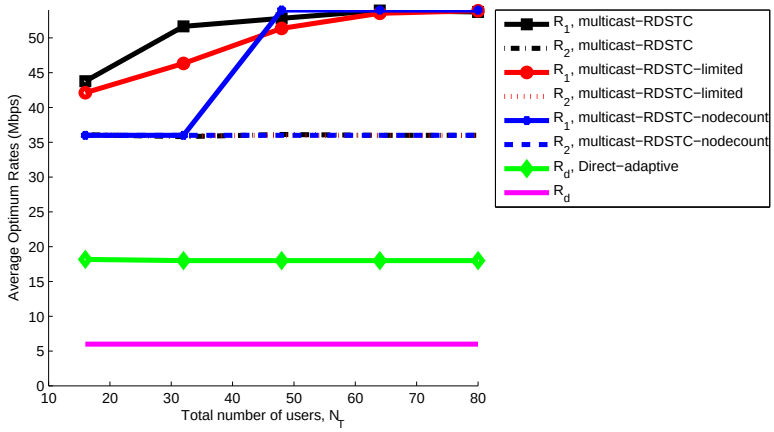

Figure 4.7: Average optimum transmission rates for single layer systems.

We observe that the average first hop transmission rates for the RDSTC schemes are between 48Mbps and 54Mbps. In this transmission rate range, the N_{avg}/N_T ratio is around 0.45 (see Figure 4.5). This means for each packet, almost half of the nodes receive the packet correctly and participate in the second hop transmission. Furthermore, we show that even when the optimum parameters are chosen with partial channel information, they are close to those of R-DSTC with full-channel information.

Recall that in *multicast-RDSTC-limited* and *multicast-RDSTC-nodecount*, the optimum parameters are chosen based on the best 95% of the node placements. All nodes in these placements receive video packets with a FEC decoding failure probability of less than $\varsigma = 0.5\%$. In Figure 4.9, we consider all the node placements (including the worst 5% of node placements) and present the percentage of nodes that receive all the packets with a FEC decoding failure probability of less than $\varsigma = 0.5\%$. We observe that even though the optimum parameters were not particularly chosen for these node placements, for a high density network, almost all the nodes in these node placements receive all the packets.

For layered cooperation, we only evaluate the performance of layered R-

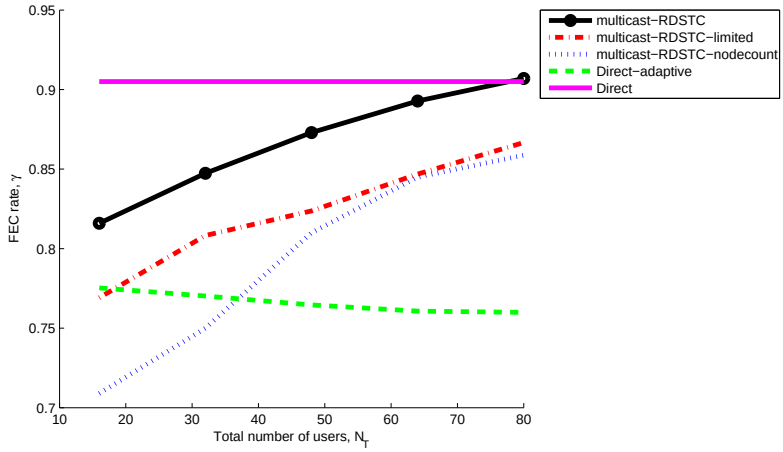

Figure 4.8: Average optimum FEC rates for single layer systems.

DSTC under full channel information (*multicast-RDSTC-layered*), but the results can be extended to other schemes easily. In Figure 4.10, we illustrate the average video rates, for *multicast-RDSTC-layered* and *Direct-Adaptive-layered*, and compare with *multicast-RDSTC* as well as direct transmission schemes for $\mu = 30$ percent. Here we set the base layer rate to $R_{v_b} = 1.5R_{v,d}$ where $R_{v,d}$ is the video rate for direct transmission and evaluate the video rate of the enhancement layer, R_{v_e}. With layered randomized cooperation, $\mu = 30$ percent of the nodes observe significant improvement on the video rate compared to single layered randomized cooperation while the remaining nodes still experience a much better video quality than direct transmission. Furthermore, layered randomized cooperation outperforms layered direct transmission. In Figure 4.11, for a fixed number of nodes, we present the achievable total video rates $(R_{v_b} + R_{v_e})$ as a function of μ for the same base layer rate above. Recall that μ is the percentage of nodes receiving both layers, while $100-\mu$ is the percentage of nodes receiving only base layer, hence as we increase μ, the total achievable video rate reduces, as we provide this rate to more nodes.

In Figure 4.12, we compare the performance of *enhanced-multicast-RDSTC*

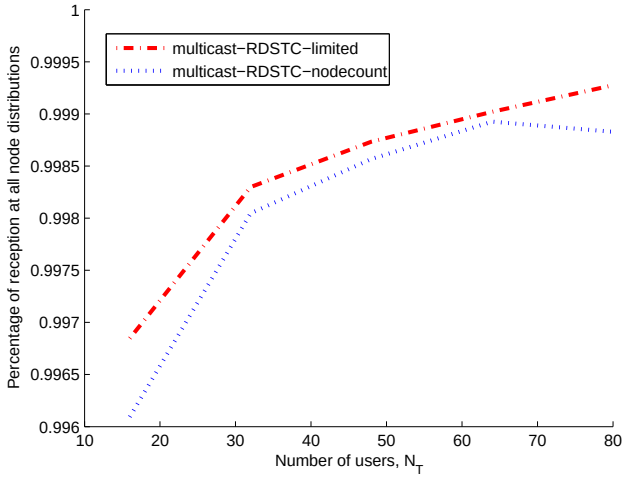

Figure 4.9: Percentage of nodes to receive all packets at all node placements versus number of nodes, N_T

scheme to *Direct*, *Rate Adaptive* and *multicast-RDSTC*. The *enhanced-multicast-RDSTC* scheme provides further improvements in the performance compared to *multicast-RDSTC* by foregoing the first hop transmission of parity packets. Furthermore, we observe that the *enhanced-multicast-RDSTC* is also robust as *multicast-RDSTC* and performs well under the partial channel information (e.g. node count).

In Figure 4.13 and Figure 4.14, we compare the optimum average transmission rates and FEC rates of for *enhanced-multicast-RDSTC* with other schemes. We observe that optimum transmission rates for source packets of *enhanced-multicast-RDSTC*, (R_1, R_2) are similar to the transmission rates of R-DSTC, (R_1, R_2). However, the transmission rate of parity packets is much higher than transmission rate of source packets at the second hop. Therefore, the gains for the *enhanced-multicast-RDSTC* scheme, comes from not only skipped first hop transmission of parity packets but also increased second hop transmission rate.

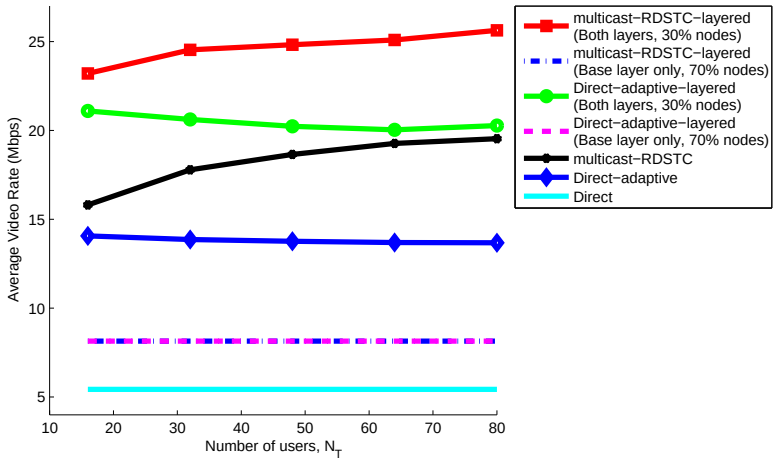

Figure 4.10: Video rates vs number of nodes for $\mu = 30\%$.

4.7 Chapter Summary

In this chapter, we propose a cooperative layered video multicasting scheme using R-DSTC along with packet level FEC to enable error resilient video delivery. We first consider a simple model where the parity packets are only generated at the sender and forwarded by the relays along with the source packets. Three different schemes for single layer cooperation are proposed and optimized based on the availability of the channel information at the sender. Furthermore, a layered scheme is considered where the video rate of the enhancement layer is maximized given a target base layer video rate R_{v_b} and a percentage of nodes μ that receive both base and enhancement layers. Our results show that rate adaptive direct transmission provides more than two times higher video rates as compared to conventional multicast. For single layer cooperation with full channel information, each node experiences the same video rate which is more than three times higher than conventional multicast. For the layered case with full channel information, closer nodes experience more than six times higher video rates, depending on μ, while the distant nodes still experience much better video

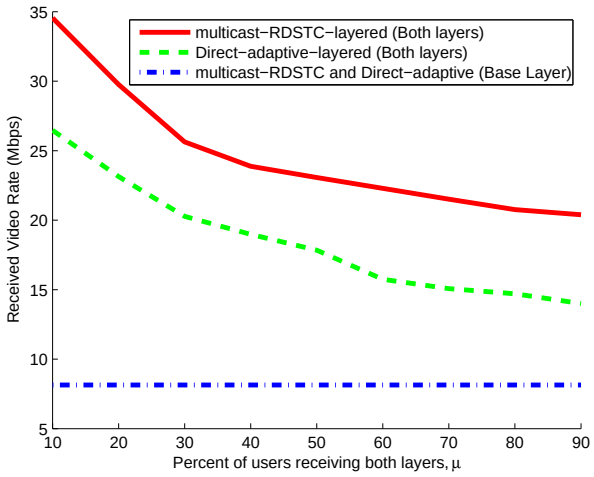

Figure 4.11: Average video rates for layered cooperation for different N_T and μ.

rates compared with the direct transmission. We observe that R-DSTC with limited channel information and R-DSTC with node count perform similarly when there are a large number of nodes in the network. We show that even when the transmission parameters are chosen with partial channel information (for example, only based on node count), the robustness of R-DSTC ensures that the performance loss is negligible compared to R-DSTC with full channel information. We then consider an enhanced model where the parity packet are generated at the relays and transmitted at the second hop using R-DSTC. Two schemes are proposed based on the availability of the channel information at the sender. Our results show that the enhanced R-DSTC scheme provides further performance gains by foregoing the parity packet transmission at the first hop.

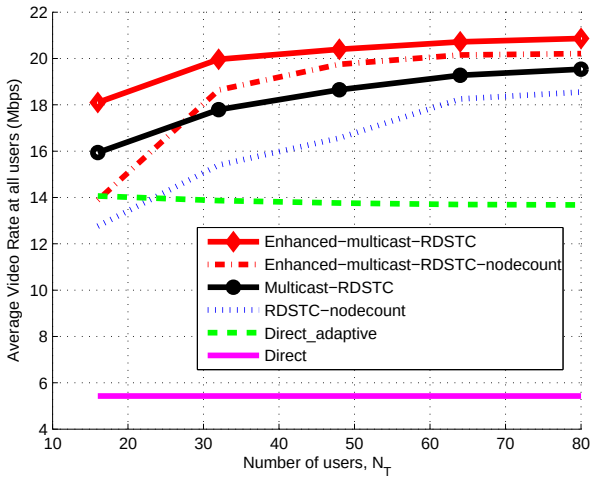

Figure 4.12: Comparison of video rates for *enhanced-multicast-RDSTC* with different systems ($\beta = 1$).

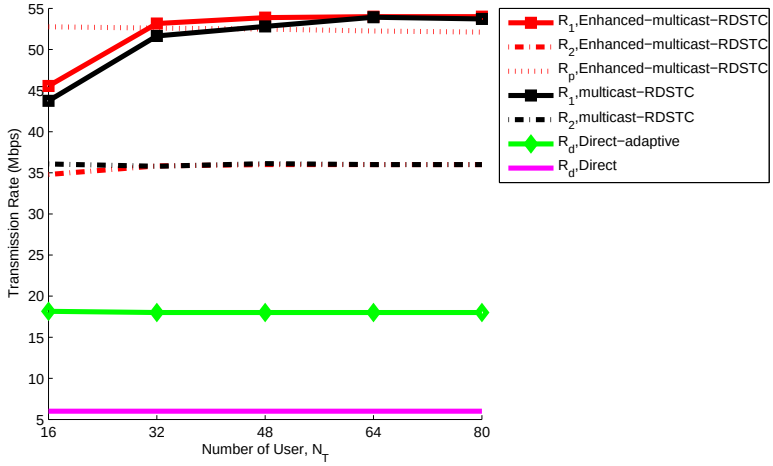

Figure 4.13: Comparison of average optimum transmission rates for *enhanced-multicast-RDSTC* with *multicast-RDSTC*.

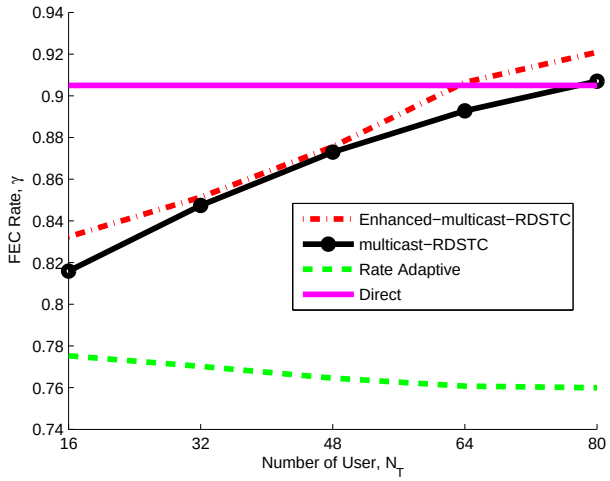

Figure 4.14: Comparison of average optimum FEC rates for *enhanced-multicast-RDSTC* with *multicast-RDSTC*.

Chapter 5

Layered Randomized Cooperative Multicast for Lossy Data in Dense Networks

5.1 Introduction

In the previous chapter, we showed the benefits of cooperative multicast using R-DSTC for a practical wireless network. Specifically, for a IEEE.11g based network, we compute the achievable video rates by considering the associated modulation and channel codes. We study different node placements and present the results averaged over these node placements. In this chapter, we investigate the randomized cooperative multicast system from information theoretic perspective. Rather than considering specific node placements and evaluating video quality as in Chapter 4, we consider lossy data and evaluate end-to-end distortion in a dense network.

We study the multi-stage cooperation scheme of [24] for delivering lossy data such as multimedia signals (audio, image, and video) in a fading environment. As the performance measure, we consider the distortion of the reconstructed signal at the receiver compared with the original source. Multimedia signals also typically have delay constraints, for example, media data has to be delivered and rendered before its scheduled playback time. Therefore, for multimedia multicast, our goal is to minimize the end-to-end distortion of the multicast receivers in a certain coverage

range under a delay constraint. We investigate the effect of decoding SNR threshold, number of hops and the diversity level of the underlying space time code (STC) on the end-to-end distortion of the multicast users at a fixed coverage range.

We also consider source layering to provide receivers signals at different distortion levels commensurate with their channel conditions. We first study the case where different source layers are transmitted sequentially. Unequal error protection (UEP) to different layers is achieved by choosing different SNR thresholds, diversity levels of the STC's and number of hops for different layers.

The transmission of layers can also be done simultaneously by superposition coding. Superposition of source layers has been considered in [44],[45] where the authors show the benefits of superposition in minimizing end-to-end distortion for point-to-point channels over sequential transmission and over single layer transmission. In this chapter, we study layered compression for multicast of lossy data where different source layers are transmitted simultaneously using superposition coding. We compare the two proposed layering schemes and discuss the benefits of layered transmission over single layer transmission. All the analysis is carried out for an i.i.d. Gaussian source where the well-known rate distortion function and the successive refinability [25] are used to determine the encoding-induced distortion at different source rates.

This chapter is organized as follows. We introduce the system model in Section 5.2. We first formulate the expected end-to-end distortion for single layer transmission in Section 5.3. We then study layered transmission for both sequential and superposition transmission of layers in Section 5.4. We summarize the chapter in Section 5.5.

5.2 System Model

We study a network in which node locations are randomly and uniformly distributed over a fixed coverage area. Specifically, we consider a dense network and use the continuum approach following the model [24], where the total relay power density at each hop is fixed. We denote the source power and relay power density as P_s and $\tilde{P}_r$, respectively. We assume independent Rayleigh fading channels between nodes and unit variance additive white complex Gaussian noise. We use a path-loss model, *l(d)*, with

$$l(d) = \begin{cases} 1/d^2 & \text{if} \quad d > d_0 \\ 1/d_0^2 & \text{if} \quad d \leq d_0 \end{cases} \tag{5.1}$$

where d is the distance between the transmitter and the receiver. In general the path loss model $l(d) = 1/d^2$ arises from the free-space attenuation of electromagnetic waves, and it does not hold when d is very small leading to the model in (5.1).

We assume that the broadcast transmission is initiated by the source node by transmitting a channel codeword. Appropriate channel coding is used so that the information is correctly received as long as the received SNR is above the decoding SNR threshold, τ. Every node who receives the transmitted codeword with a signal-to-noise ratio above the threshold, τ, will be able to decode the packet and will forward using randomized cooperation [24]. Each node only transmits at most once. A training preamble in the message helps nodes detect the presence of the packets, estimate the received power, and synchronize the relay transmissions. The relays use a STC of dimension L and the relay transmissions are done simultaneously, even though they may not be symbol synchronized. The first group excites a second group of nodes and they will activate the next group nodes. The subsequent groups of nodes that are activated are referred to as hops. Since the nodes only use the locally available received SNR information to make transmission decisions, the network can operate in a distributed fashion. Note that the transmission rate is R bits per channel

use at each hop where the rate depends on the SNR threshold, τ, as

$$R = \log(1 + \tau) \tag{5.2}$$

In our analysis, we consider two different STC dimensions. In one extreme, we assume a high diversity regime where the relays transmit in orthogonal channels obtained by using a space time code of dimension, $L = \infty$ (orthogonal). In another extreme, we consider a low diversity transmission scheme using a space time code of dimension $L = 1$ (non-orthogonal). Note that the analysis can be extended to arbitrary L using [24].

A channel codeword consists of n channel uses which contains information pertaining to k source samples leading to a bandwidth ratio of $b = n/k$ channel uses per sample. Typically n is large to ensure the Shannon limit in (5.2) is invoked. In general, the bandwidth ratio b is dictated by the application and the channel bandwidth. For example, a channel bandwidth of W Hz suggests that we have W channel uses per second. If the source is sampled at a rate of f_s samples per second and due to the real-time constraints, needs to be sent at the sampling rate, the bandwidth ratio can be expressed as $b = W/f_s$ channel uses per sample. Hence, in this chapter, we use b to characterize the real-time delivery requirement. A bandwidth ratio of b corresponds to transmission of bR bits for each source sample. For a real i.i.d Gaussian source with unit variance, the resulting distortion per source sample becomes:

$$D = 2^{-2bR} \tag{5.3}$$

We assume that each channel codeword sees independent fading. In the case of N hops, we assume n channel uses are equally divided among hops and each hop can use n/N channel uses, leading to a bandwidth ratio of $\frac{n}{kN} = \frac{b}{N}$ per hop. The resulting distortion then becomes

$$D(\tau, b, N) = 2^{-2b\log(1+\tau)/N} \tag{5.4}$$

Equations (5.2) and (5.4) indicate that the distortion depends on the decoding SNR threshold, bandwidth ratio and the number hops.

The end-to-end distortion at a particular location depends not only on the distortion induced by the source code, but also on the error probability due to channel losses at that location. In Section 5.3, we will first formulate the error probability and the end-to-end distortion for single layer transmission and then, in Section 5.4, we will investigate the end-to-end distortion for layered compression where the source layers are transmitted either sequentially or simultaneously using superposition coding.

5.3 Single Layer Transmission

In this section we discuss single layer randomized distributed cooperation. We first revisit the probability of a node at (x, y) receiving the data at the j^{th} hop for a dense network [24]. Then we formulate the expected distortion under a delay constraint which is represented in terms of the bandwidth ratio, b and for a given coverage range, we find the optimum N and τ that minimize the expected distortion.

Let $P_j(x, y)$ denote the probability that the user at location (x,y) receives the information correctly at j^{th} hop. For the first hop (i.e., source transmission), the probability can be expressed as

$$P_1 = Pr\{\|h_1(x, y)\|^2 \geq \tau\} \tag{5.5}$$

where $h_1(x, y)$ is the channel gain at location (x,y) for the first hop transmission and τ is the SNR threshold to be exceeded for the relay node to decode.

For the j^{th} hop ($j > 1$), we only consider users who did not receive the information in the previous hops. All users who receive the information in the previous hop (i.e. $(j-1)^{th}$ hop) will retransmit. The probability of successful reception for

the j^{th} hop can be expressed as,

$$\begin{aligned} P_j &= Pr\{\|h_j(x,y)\|^2 \geq \tau\} \\ &\quad \prod_{i=1}^{i=j-1}[1 - Pr\{\|h_i(x,y)\|^2 \geq \tau\}] \end{aligned}$$

where $h_j(x,y)$ is the equivalent channel gain at location (x,y) given by

$$\|h_j(x,y)\|^2 = \chi^2(2L, \sigma_j^2(x,y)/L), \text{ for L} < \infty \tag{5.6}$$

$$\|h_j(x,y)\|^2 = \sigma_j^2(x,y), \text{ L}=\infty \tag{5.7}$$

where

$$\sigma_j^2(x,y) = \int\int \tilde{P}_r P_{j-1}(x',y') l(x-x', y-y') dx' dy' \tag{5.8}$$

Note that $\sigma_j^2(x,y)$ is the sum of signal powers from all nodes that successfully received the information from the previous hop at location (x,y), $\tilde{P}_r$ is the relay power density and *l(d)* represents the path-loss model in (5.1).

We define $P(x,y;N)$ as the probability of successful reception after N hop transmissions which can be expressed as

$$P(x,y;N) = \sum_{i=1}^{N} P_i(x,y) \tag{5.9}$$

Therefore, the expected distortion at location (x,y), $D_{exp}(x,y)$, is

$$D_{exp}(x,y) = P(x,y;N)D(\tau,b,N) + (1 - P(x,y;N)) \tag{5.10}$$

Note that since we consider a unit variance Gaussian source, when a channel codeword is lost, we observe the maximum distortion, D_{max}=1.

For a five hop system (N=5 and b=8), we compare the end-to-end distortion as a function of distance from the source for different SNR thresholds for nonorthogonal and orthogonal relay transmission in Figure 5.1 and 5.2, respectively. Note that for the orthogonal relay transmission, all nodes within a certain radius r_{th}, (r_{th}=78

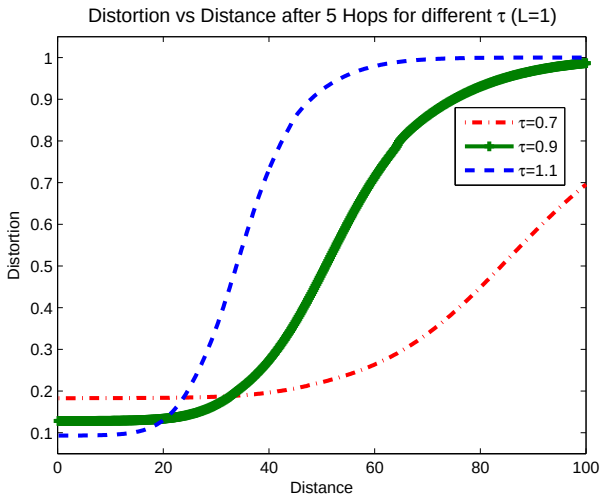

Figure 5.1: Comparison of end-to-end distortion for nonorthogonal relay transmission for different decoding thresholds (τ) ($P_s = 10, \tilde{P}_r = 1, d_0 = 1, N = 5, b = 8$)

for $\tau = 0.7$ in the figure) achieve the same low distortion after five hops. However, beyond this coverage distance, no node is able to receive the packets, leading to maximum distortion. On the other hand, with non-orthogonal relay transmission with the same τ, for $r < r_{th}$ the expected distortion is higher, but the source is able to reach nodes further away than r_{th} with distortion below the maximum value. Another key observation in the figure is that, as we increase τ, since we can send at a higher rate, the distortion at the closer receivers is lower. On the other hand, the corresponding coverage range defined according to some maximum tolerable distortion level also reduces.

For fixed τ, as we increase the number of hops, N, the probability of success also increases. However, as N increases, the time spent for each hop reduces as well increasing the source distortion D in (5.4). Therefore, for a fixed coverage range, there is an optimum τ and N pair that minimize the end-to-end distortion. For a given P_s and $\widetilde{P_r}$, we can express the coverage range after N hop transmissions r_N, as

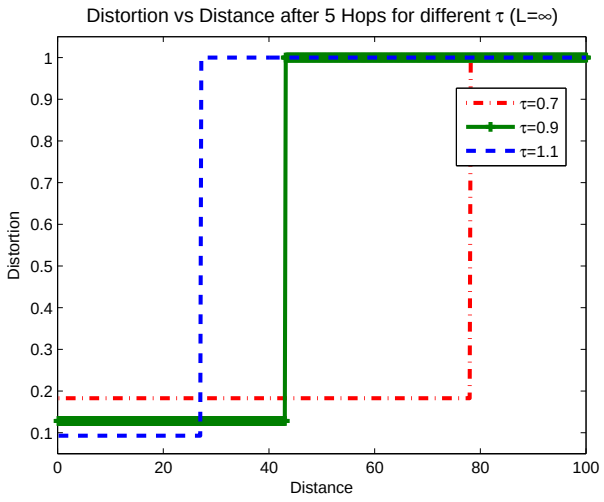

Figure 5.2: Comparison of end-to-end distortion for orthogonal relay transmission for different decoding thresholds (τ) ($P_s = 10, \tilde{P}_r = 1, d_0 = 1, N = 5, b = 8$)

follows:

$$r_N^2 = \frac{P_s}{\tau}\left(\frac{\mu - 1}{\mu - 2}\right)\left(1 - \left(\frac{1}{\mu - 1}\right)^N\right) \tag{5.11}$$

where

$$\mu = e^{\left(\frac{\tau}{\tilde{P}_r \pi}\right)} \tag{5.12}$$

Since the notion of coverage range is more clearly defined for orthogonal transmission, we explore the tradeoff between τ and N for $L = \infty$. Note that for the orthogonal relay transmission, $P(x, y; N)$ is either 0 or 1. We set the coverage range as the furthest point where $P(x, y; N)$ equals to 1. Then, the expected distortion for the nodes in the coverage range can be written as in (5.4).

For the equation above, it is hard to find a simple close form. Thus, for a given coverage range, we exhaustively search through all possible τ's and find the the τ that minimizes D_{exp}. In Figure 5.3, for each coverage range shown in the x-axis, we find the optimum τ and illustrate minimum expected distortion for different number

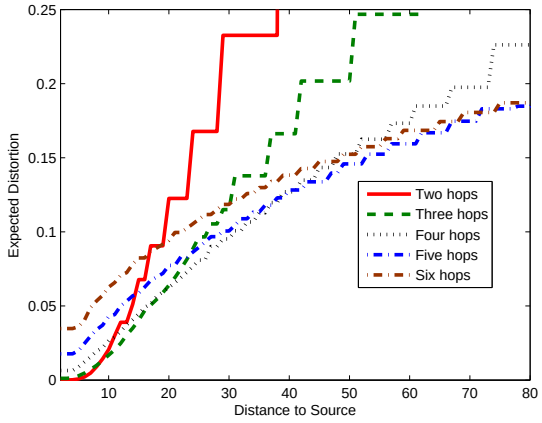

Figure 5.3: Effect of the number of hops on the end-to-end distortion at different coverage ranges with $P_s = 10, \tilde{P}_r = 1, d_0 = 1, b = 8$ (L=∞)

of hops. We observe that, while to reach short distances a small number of hops is optimum, for larger distances, we need more hops. Even with optimized number of hops, the expected distortion increases with the coverage range.

5.4 Layered Transmission

In this section, we discuss layered randomized distributed cooperation in order to provide differentiated quality for the multicast receivers based on their channel conditions. We only consider two layers, base and enhancement layer, to illustrate the main idea. We assume that we have two SNR thresholds: base layer threshold and enhancement layer threshold, τ_b and τ_e, respectively where, $\tau_e > \tau_b$. Next, we will consider two types of layered transmission: sequential layered transmission and superimposed transmission of layers.

5.4.1 Sequential Layered Transmission

In sequential layered transmission, we transmit the base and the enhancement layer sequentially using TDMA (i.e. in different time slots). We assume we use α proportion of the channel frame for the base layer transmission and $1-\alpha$ proportion of the channel frame for the enhancement layer. This suggests that the base and enhancement layer bandwidth ratios are $\alpha b/N_b$ and $(1-\alpha)b/N_e$ where N_b and N_e denote the number of hops for the base and enhancement layer, respectively. We choose $N_b \geq N_e$ since we want the base layer to propagate further. We assume the fading is constant during a channel frame, hence the base and enhancement layer observe the same fading level. At a given node, if the total received signal power is greater than τ_b we assume that base layer is decoded correctly and if the signal power is greater than τ_e we will also receive the enhancement layer.

In the previous section, we showed that the higher the SNR threshold τ, the lower the distortion is, at the expense of reduced coverage range. Hence, the main idea behind choosing different τ's and number of hops for different layers is that we want to guarantee a maximum distortion level to all users (i.e. the base layer distortion) and for users with better channel conditions, we want to reduce the distortion even further. Also recall that as we increase the number of hops, the time spent for each hop reduces, hence the choice of (N_b, N_e) affects the distortion. Note that, for the same number of hops for the base and enhancement layers ($N_b = N_e$), by choosing different (τ_b, τ_e) we can adjust the coverage ranges and the distortion for the base and enhancement layers. For a fixed (τ_b, τ_e), the coverage range depends on how many hops we transmit. Hence, by choosing different number of hops for base and enhancement layers, we have the freedom to adjust the base and enhancement layer coverage ranges. Furthermore, for a fixed (τ_b, τ_e), by changing α, we can adjust the distortion values for the base and enhancement layer.

We next derive a general expected distortion formulation for a given $(\tau_b, \tau_e, N_b, N_e, \alpha)$ and then evaluate the effect of these parameters on the performance.

We define $P_i^b(x,y)$ as the probability of successful reception of base layer at the i^{th} hop. Similarly, the probability of successful reception of enhancement layer is defined as $P_i^e(x,y)$ for the i^{th} hop. The probabilities $P_i^b(x,y)$ and $P_i^e(x,y)$ can be formulated as in Section 5.3. The probability of success after N_b hop transmission for base layer and N_e hop transmission for enhancement layer are denoted as $P_b(x,y;N_b)$ and $P_e(x,y;N_e)$, respectively, and expressed as:

$$P_b(x,y;N_b) = \sum_{i=1}^{N_b} P_i^b(x,y),\ P_e(x,y;N_e) = \sum_{i=1}^{N_e} P_i^e(x,y) \tag{5.13}$$

Choosing $\tau_e > \tau_b$, $N_b > N_e$ and considering that the fading for the base and enhancement layers are the same, reception of the enhancement layer implies the reception of the base layer. Then, we can compute the expected distortion at location (x,y) as follows,

$$\begin{aligned} D_{exp}(x,y) &= P_e(x,y;N_e)D_{b+e}(\tau_b,\tau_e,N_b,N_e,\alpha,b) \\ &\quad +(P_b(x,y;N_b)-P_e(x,y;N_e))D_b(\tau_b,N_b,\alpha,b) \\ &\quad +(1-P_b(x,y;N_b)) \end{aligned} \tag{5.14}$$

where D_{b+e} is the distortion when both base and enhancement layers are received and D_b is the distortion when only base layer received. For Gaussian sources with unit variance, we can compute these distortion values as:

$$D_b = 2^{-2\frac{R_b\alpha b}{N_b}} \tag{5.15}$$

$$D_{b+e} = 2^{-2(\frac{R_b\alpha b}{N_b}+\frac{R_e(1-\alpha)b}{N_e})} \tag{5.16}$$

where

$$R_b = \log(1+\tau_b)\ and\ R_e = \log(1+\tau_e) \tag{5.17}$$

In Figure 5.4 and Figure 5.5, we illustrate the effect of layered cooperation for orthogonal and nonorthogonal relay transmission for a fixed τ_b and τ_e for different

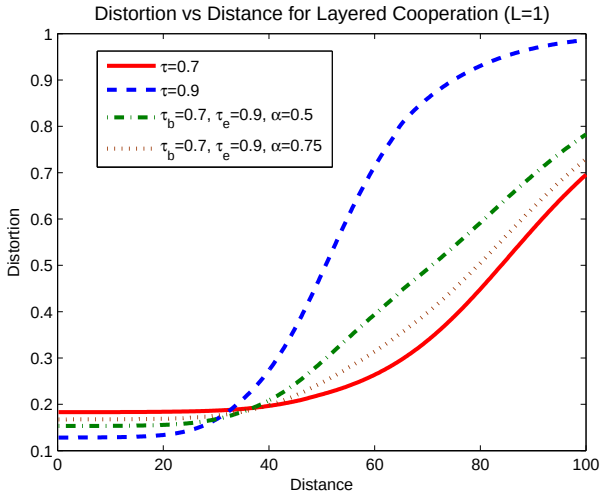

Figure 5.4: Sequential Layered Cooperative Multicast: Comparison of end-to-end distortion for nonorthogonal relay transmissions($P_s = 10, \tilde{P}_r = 1, d_0 = 1, N_b = 5, N_e = 5, b = 8$)

α's. Here we assume both the base and enhancement layers propagate for five hops (N_b=5, N_e=5). We also plot the single layer performance for comparison. Note that, since we use equal number of hops for the base and enhancement layers, the coverage range of the base layer is similar to the single layer case with $\tau = \tau_b$ and the coverage range of the enhancement layer is similar to the single layer case with $\tau = \tau_e$. Moreover with layered transmission, we provide lower end-to-end distortion to closer by nodes than the far away nodes. Alternatively, we can think about the layered transmission as extending the coverage range at the expense of slightly increasing the distortion for the close by nodes. Here, choosing different α, we are able to change the distortion levels at close and far away nodes.

Finally, we consider different number of hops for base and enhancement layer transmission as depicted in Figure 5.6 and Figure 5.7. Here the single layer transmissions has $N = 5$ hops. By choosing different number of hops for base and enhancement layer, we are able to adjust the coverage range of the nodes receiving

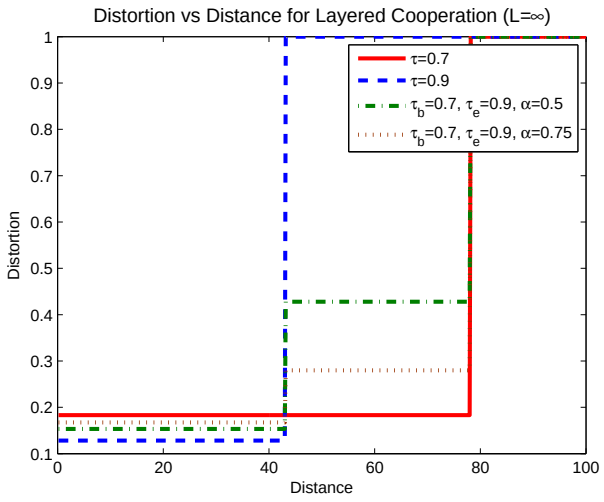

Figure 5.5: Sequential Layered Cooperative Multicast: Comparison of end-to-end distortion for orthogonal relay transmissions($P_s = 10, \tilde{P}_r = 1, d_0 = 1, N_b = 5, N_e = 5, b = 8$)

both the base and enhancement layers. Note that compared to Figure 3.12 where the number of hops for base and enhancement layer are equal, the enhancement layer coverage is smaller but the distortion for the closer receivers is also lower.

5.4.2 Superimposed Transmission of Multiple Layers

In this section, we consider the simultaneous transmission of layers using superposition coding due to its potential benefits over sequential transmission [44],[45]. When we superimpose coded base and the enhancement layers, we use β proportion of the total power for the base layer transmission and $1-\beta$ proportion of the power for the enhancement layer and assume that the same proportionality is applied at the source and at all the relays. At a given node, the base layer is decoded treating the enhancement layer as noise. Then, enhancement layer is extracted by re-encoding and subtracting the base layer from the received signal. Note that, successful decoding of the enhancement layer requires the decoding of the base layer. Also from

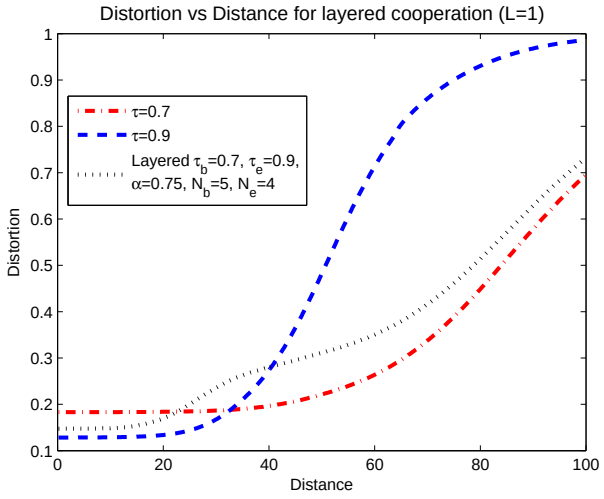

Figure 5.6: Comparison of distortion for layered cooperation with different number of hops at base and enhancement layer for nonorthogonal relay transmissions ($P_s = 10, \tilde{P}_r = 1, d_0 = 1, N_b = 5, N_e = 4, b = 8$)

a source coding perspective, enhancement layer is useless unless base layer is also received. Hence, we need to choose τ_b, τ_e, β such that correct decoding of base layer is guaranteed for decoding of the enhancement layer.

We next derive a general expected distortion formulation considering $(\tau_b, \tau_e, P_s, \tilde{P}_r, \beta)$ for N hop transmission and then evaluate the effect of these parameters on the performance.

The expected distortion at location (x, y) can be expressed as,

$$\begin{aligned} D_{exp}(x,y) &= P_{b+e}(x,y;N)D_{b+e}(\tau_b,\tau_e,N,b) \\ &\quad +(P_b(x,y;N)-P_{b+e}(x,y;N))D_b(\tau_b,N,b) \\ &\quad +(1-P_b(x,y;N)) \end{aligned} \tag{5.18}$$

where D_{b+e} is the distortion when both base and enhancement layers are received and D_b is the distortion when only base layer received. For Gaussian sources with unit

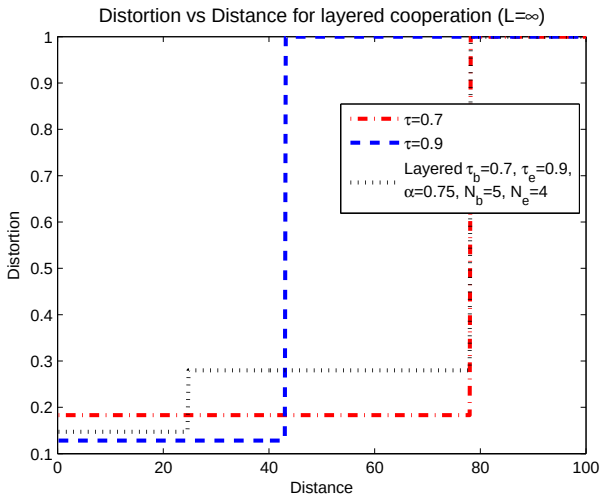

Figure 5.7: Comparison of distortion for layered cooperation with different number of hops at base and enhancement layer for orthogonal relay transmissions ($P_s = 10, \tilde{P}_r = 1, d_0 = 1, N_b = 5, N_e = 4, b = 8$)

variance, using (5.4), we can compute these distortion values as:

$$D_{b+e} = 2^{-2b(R_b+R_e)/N} \text{ and } D_b = 2^{-2bR_b/N} \tag{5.19}$$

where $R_b = \log(1+\tau_b)$ and $R_e = \log(1+\tau_e)$.

Similar to sequential transmission, $P_b(x, y; N)$ and $P_{b+e}(x, y; N)$ denote the probability of success after N hop transmission for base and both base and enhancement layers, respectively, and they are expressed as:

$$P_b(x, y; N) = \sum_{j=1}^{N} P_j^b(x, y) \tag{5.20}$$

$$P_{b+e}(x, y; N) = \sum_{j=1}^{N} P_j^{b+e}(x, y) \tag{5.21}$$

where $P_j^b(x, y)$ denotes the probability that the user at location (x,y) receives either the source's base layer transmission or relay's base layer transmission from the previ-

ous hop correctly at j^{th} hop. Similarly, the probability of successful reception of both base and enhancement layers is defined as $P_j^{b+e}(x,y)$ for the j^{th} hop.

For the first hop (i.e., source transmission), received signal at a node at location (x,y) is given by:

$$\begin{aligned} r(x,y) &= \sqrt{\beta P_s}h(x,y)S_b \\ &\quad + \sqrt{(1-\beta)P_s}h(x,y)S_e + n(x,y) \end{aligned} \tag{5.22}$$

where S_b and S_e represents base and enhancement layer signals and $n(x,y)$ is the additive white Gaussian noise. Then, the probability of receiving the base layer can be expressed as

$$P_1^b(x,y) = Pr\{\frac{\|h_1^b(x,y)\|^2}{1+\|h_1^e(x,y)\|^2} > \tau_b\} \tag{5.23}$$

where $\|h_1^b(x,y)\|^2 = \beta P_s\|h(x,y)\|^2$ is the received SNR at location (x,y) for the base layer and $\|h_1^e(x,y)\|^2 = (1-\beta)P_s\|h(x,y)\|^2$ is the received SNR for the enhancement layer. In (5.23), the base layer is decoded by treating the enhancement layer as noise [47]. We can express (5.23) as,

$$\begin{aligned} P_1^b(x,y) &= Pr\{\frac{\beta P_s\|h(x,y)\|^2}{1+(1-\beta)P_s\|h(x,y)\|^2} > \tau_b\} \\ &= Pr\{\|h(x,y)\|^2 > \frac{\tau_b}{\beta P_s - (1-\beta)P_s\tau_b}\} \end{aligned} \tag{5.24}$$

The probability of correctly decoding the enhancement layer depends on the base layer. Given the base layer is decoded correctly and removed from the received signal, the probability of receiving the enhancement layer can be expressed as

$$P_1^{e|b}(x,y) = Pr\{\|h_1^e(x,y)\|^2 > \tau_e\} \tag{5.25}$$

Note that we can express (5.25) as,

$$P_1^{e|b}(x,y) = Pr\{\|h(x,y)\|^2 > \frac{\tau_e}{(1-\beta)P_s}\} \tag{5.26}$$

Recall that, for (5.25) to be valid, the base layer has to be decoded and subtracted from the received signal. This can be guaranteed under the constraint,

$$\frac{\tau_b}{\beta - (1-\beta)\tau_b} < \frac{\tau_e}{(1-\beta)} \tag{5.27}$$

Under (5.27), $P_1^{e|b}(x,y)$ can be considered as the probability of receiving both the base and enhancement layers leading to

$$P_1^{b+e}(x,y) = P_1^{e|b}(x,y) \tag{5.28}$$

For the j^{th} hop ($j > 1$), we only consider the users who did not receive the information in the previous hops. All users who receive either the base layer or both base and enhancement layers in the previous hop (i.e. $(j-1)^{th}$ hop) will forward. Also, if a node receives the base layer, it will stop listening to subsequent hops even though it does not have the enhancement layer. We assume that if a node only receives base layer, it will use all its power to transmit only the base layer. If it also receives the enhancement layer, it will allocate its total power among the base and enhancement layers according to the proportionality constant, β. For the j^{th} hop, the probability of successful reception for the base layer and the probability of receiving both layers, can be expressed as,

$$\begin{aligned} P_j^b(x,y) &= Pr\{\frac{\|h_j^b(x,y)\|^2}{1+\|h_j^e(x,y)\|^2}) > \tau_b\} \\ &\quad \cdot [1 - \sum_{i=1}^{j-1} P_i^b(x,y)] \end{aligned} \tag{5.29}$$

$$\begin{aligned} P_j^{b+e}(x,y) = Pr \quad \{ \quad & \|h_j^e(x,y)\|^2 > \tau_e, \\ & \frac{\|h_j^b(x,y)\|^2}{1+\|h_j^e(x,y)\|^2}) > \tau_b\} \\ & \cdot [1 - \sum_{i=1}^{j-1} P_i^b(x,y)] \end{aligned} \tag{5.30}$$

where $h_j^b(x,y)$ and $h_j^e(x,y)$ are the equivalent channel gains at location (x,y) for the base and enhancement layers, respectively, given by,

$$\begin{matrix} h_j^b(x,y) \sim N_c(0,\sigma_j^{b2}(x,y)) \\ h_j^e(x,y) \sim N_c(0,\sigma_j^{e2}(x,y)) \end{matrix}, \quad \text{L=1 (non-orthogonal)} \tag{5.31}$$

$$\begin{matrix} \|h_j^b(x,y)\|^2 = \sigma_j^{b2}(x,y) \\ \|h_j^e(x,y)\|^2 = \sigma_j^{e2}(x,y) \end{matrix}, \quad \text{L=}\infty \text{ (orthogonal)} \tag{5.32}$$

where

$$\begin{aligned} \sigma_j^{b2}(x,y) = \int\int \quad [\quad & \tilde{P}_r(P_{j-1}^b(x',y') - P_{j-1}^{b+e}(x',y')) \\ & +\beta\tilde{P}_r P_{j-1}^{b+e}(x',y') \ ] \\ & \cdot l(x-x',y-y')dx'dy' \end{aligned} \tag{5.33}$$

$$\begin{aligned} \sigma_j^{e2}(x,y) = \int\int \quad [\quad & (1-\beta)\tilde{P}_r P_{j-1}^{b+e}(x',y') \ ] \\ & \cdot l(x-x',y-y')dx'dy' \end{aligned} \tag{5.34}$$

In the above formulation which can be derived similar to [24], $\sigma_j^{b2}(x,y)$ represents the sum of signal powers at location (x,y) from all nodes that successfully received the base layer information from the previous hop. Similarly, $\sigma_j^{e2}(x,y)$ represents the sum of signal powers at location (x,y) from all nodes that successfully received the base and enhancement layers from the previous hop. Recall that from (5.27), the nodes that receive the enhancement layer also receive the base layer. So the nodes that receive the enhancement layer are a subset of the nodes who receive the base layer. Hence, $h_j^b(x,y)$ and $h_j^e(x,y)$ are dependent and can be related as $h_j^b(x,y) = \eta h_j^e(x,y) + h_j^n(x,y)$ where $h_j^n(x,y)$ is the equivalent channel gain representing nodes that transmit the base layer when the enhancement layer is not received. Note that $\eta = \sqrt{\beta/(1-\beta)}$. Since $h_j^n(x,y)$ and $h_j^e(x,y)$ are independent, we can show that $h_j^b(x,y)$ and $h_j^e(x,y)$ have the correlation coefficient $\rho = \eta\sigma_j^e/\sigma_j^b$. We can express

$\sigma_j^{b2}(x,y)$ as

$$\sigma_j^{b2}(x,y) = \eta^2 \sigma_j^{e2}(x,y) + \sigma_j^{n2}(x,y) \tag{5.35}$$

where

$$\sigma_j^{n2}(x,y) = \int\int \quad [\quad \tilde{P}_r(P_{j-1}^b(x',y') - P_{j-1}^{b+e}(x',y'))\ ] \cdot l(x-x',y-y')dx'dy' \tag{5.36}$$

For orthogonal relay transmission, we can compute (5.29) and (5.30) by substituting in (5.32). For nonorthogonal relay transmission, note that we can write the former part of (5.29) as

$$Pr\{\frac{\|h_j^b(x,y)\|^2}{1+\|h_j^e(x,y)\|^2}) > \tau_b\} = Pr\{\|h_j^b(x,y)\|^2 - \tau_b\|h_j^e(x,y)\|^2 > \tau_b\} \tag{5.37}$$

In order to compute the above probability, we need to find the probability distribution function of the difference of two correlated chi-square distributed random variables, $\|h_j^b(x,y)\|^2$ and $\|h_j^e(x,y)\|^2$. Let h_1 and h_2 be two dependent zero-mean complex Gaussian variables with correlation coefficient ρ and variances σ_1 and σ_2, respectively. Then, $u = \|h_1\|^2 - \|h_2\|^2$ is a dependent central chi-square difference with a probability distribution function [46], given by,

$$p(u) = \frac{1}{2\pi\sigma_1\sigma_2\sqrt{1-\rho^2}} \exp(-\frac{(\alpha^+ - \gamma^-)u}{4}) K_0(\frac{\gamma^-|u|}{4}) \tag{5.38}$$

where $K_0(u)$ is the modified Bessel function of the second kind and

$$\gamma^- = \frac{[(\sigma_2^2 - \sigma_1^2)^2 + 4\sigma_1^2\sigma_2^2(1-\rho^2)]^{\frac{1}{2}}}{\sigma_1^2\sigma_2^2(1-\rho^2)} \tag{5.39}$$

$$\alpha^{\pm} = \gamma^- \pm \frac{\sigma_2^2 - \sigma_1^2}{\sigma_1^2\sigma_2^2(1-\rho^2)} \tag{5.40}$$

Hence, (5.37) can be computed using (5.38) with $\sigma_1^2 = \sigma_j^{b2}$, $\sigma_2^2 = \tau_b\sigma_j^{e2}$ and $\rho = \eta\sigma_j^e/\sigma_j^b$.

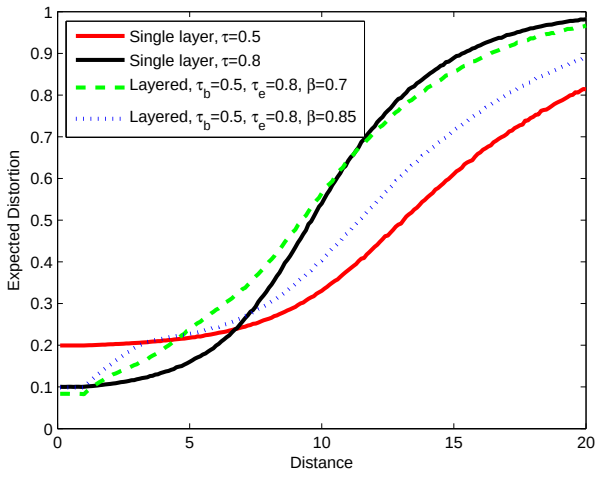

Figure 5.8: The effect of β on the expected distortion for nonorthogonal relay transmissions as a function of distance for $P_s = 10$, $\tilde{P}_r = 2$, $N = 2$, $b = 4$. The 'layered' plot illustrates simultaneous transmission of layers by superposition.

The computation of former part of (5.30) requires the consideration of the above derived joint distribution of $\|h_j^b(x,y)\|^2$ and $\|h_j^e(x,y)\|^2$ and will be evaluated numerically.

We first evaluate the effect of the power allocation, β, on the end-to-end distortion. In Figure 5.8 and Figure 5.9, for a fixed $P_s, \tilde{P}_r, b, N$ we present the expected distortion as a function of distance from the source for two different β's for nonorthogonal and orthogonal relay transmissions, respectively. We also plot the single layer performance for comparison. Note that as we increase β, since we allocate more power to base layer and less power to enhancement layer, base layer propagates more at the expense of enhancement layer propagation. However, base layer can not propagate as far as single layer, since in single layer case all the power is utilized to transmit the same layer. The benefit of layered cooperation is to provide lower distortion to nearby users than single layer transmission at the expense of coverage

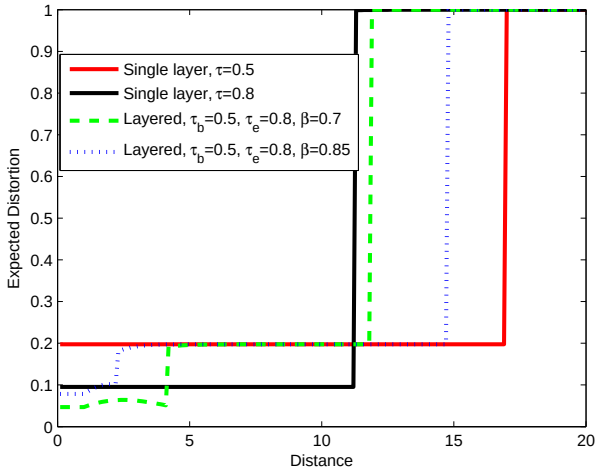

Figure 5.9: The effect of β on the expected distortion for orthogonal relay transmissions as a function of distance for $P_s = 10$, $\tilde{P}_r = 2$, $N = 2$, $b = 4$. The 'layered' plot illustrates simultaneous transmission of layers by superposition.

range. By choosing β, we can adjust the base and enhancement layer coverage ranges. Note that for $\tau_b = \tau$, the base layer quality matches with single layer quality and the nearby users achieve better quality than that of single layer at an expense of reduced coverage range. On the other hand by choosing $\tau_e = \tau$, nearby user quality matches with single layer quality, with reduced enhancement layer coverage range, but base layer reaches farther than that of single layer.

In Figure 5.10 and Figure 5.11, we compare the performance of single layer randomized cooperation, sequential layered randomized cooperation and superimposed layered randomized cooperation. Since the notion of coverage range is more clearly defined for orthogonal transmission, we show the results for $L = \infty$. For the single layer case, we find the optimum τ which minimizes the distortion at a target coverage range, $r_{cov} = 9.3$. For the layered case, we find the optimum parameters such that, all the receivers in a target coverage range observe at least an expected

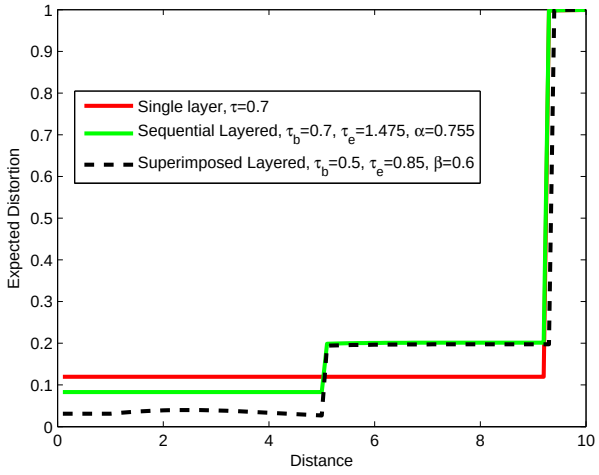

Figure 5.10: Quality improvement at closer receivers: Comparison of expected distortion for single layer randomized cooperation, sequential layered randomized cooperation and superimposed layered randomized cooperation with $P_s = 10$, $\tilde{P}_r = 2$, $N = 2$, $b = 4$ (L=∞)

quality of D_1, while the close-by receivers observe much better quality. We fix the coverage range same as the single layer case that is $r_{cov} = 9.3$ and the maximum distortion in the coverage range to $D_1 = 0.2$. Finally, in order to have a fair comparison between sequential layered transmission and superimposed layered transmission, we also fix the coverage range of the users who will receive both the base and the enhancement layers ($r_{cov}^{b+e} = 5$ in the figure). We find the optimum parameters for each case which minimize the distortion of the close-by receivers, D_{b+e}, in the coverage range of r_{cov}^{b+e}. For the sequential layered transmission α refers to proportion of the base layer transmission time to the all transmission time. As illustrated in Figure 5.10, layered cooperation with superposition improves the quality of the close-by nodes significantly compared to the sequential case.

In a multicast system, the coverage range can also be a design parameter. We also compare sequential and superimposed layered transmission in terms of coverage

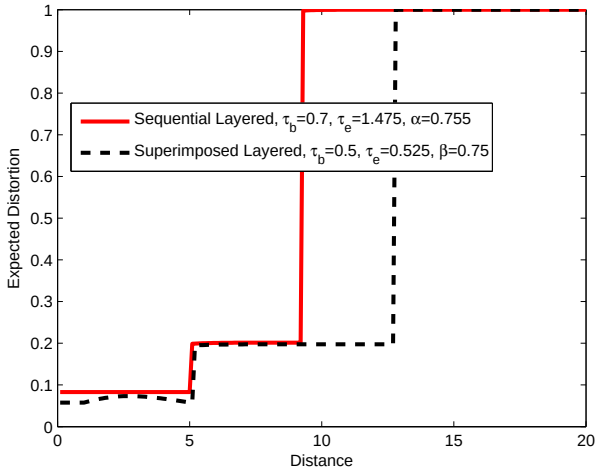

Figure 5.11: Coverage range extension: Comparison of expected distortion for single layer randomized cooperation, sequential layered randomized cooperation and superimposed layered randomized cooperation with $P_s = 10$, $\tilde{P}_r = 2$, $N = 2$, $b = 4$ (L=∞)

range. We fix the maximum distortion in the coverage range to $D_1 = 0.2$ and the coverage range of the users who will receive both the base and the enhancement layers ($r_{cov}^{b+e} = 5$). We then make sure that D_{b+e} of superimposed cooperation is at least as that of sequential transmission and compare the coverage ranges. In Figure 5.11, we show that superimposed layered transmission improves the coverage range of the system from the $r_{cov} = 9.3$ to $r_{cov} = 12.7$ compared to the sequential transmission.

5.5 Chapter Summary

In this chapter, we consider a randomized distributed cooperative multicast to reduce the end-to-end distortion in transmission of lossy sources under delay constraints. We evaluate the system for different decoding SNR thresholds and number of hops within a coverage range. We show that for a given coverage range there is an optimum τ and N which minimize the end-to-end distortion. Furthermore, in order

to provide differentiated quality to users with different channel qualities, we further employ layered cooperation. We study two different layering approaches: sequential layered transmission and superimposed layered transmission. For the sequential layered transmission, we investigate the effect of the time division among different layers and for the superimposed layered transmission we investigate the effect of power allocation of different layers on the distribution of end-to-end quality of nodes under a real-time delivery requirement. We compare these layering schemes and discuss the benefits of layered transmission over single layer transmission.

In this chapter, we considered only specific diversity levels (L=1, L=∞). A future direction is to consider the effect of different diversity levels on the performance of the multicast system. Furthermore, while we assumed both base and enhancement layers use the same underlying STC, it is possible to use different STC's for different layers in order to provide unequal error protection to different layers. This chapter only presented results for 2 hop transmission. Another research direction is to investigate larger number of hops and different real-time delivery requirements. Finally, our model assumes that once a node receives the base layer, it stops listening to subsequent transmissions. By extending the model to enable such nodes to listen until they also receive the enhancement layer, we could further improve the performance of superimposed layered cooperation.

Chapter 6

Conclusion

In this dissertation, we propose the use of cooperative communications for video multicast in infrastructure-based wireless networks. The first part of this dissertation considers user cooperation at MAC layer (two-hop relaying) where the relays transmit the video sequentially in time. Two hop relaying is integrated with packet level FEC and layered coding for both omni-directional and directional relay transmission. In the second part, to improve the spectral efficiency, a joint physical and MAC layer cooperative scheme is considered where the relays transmit the packets simultaneously using R-DSTC. This scheme is also integrated with packet level FEC and layered coding. Two different systems are proposed that differ in the way of parity packet transmission. The final part of the dissertation investigates the randomized cooperative multicast system from information theoretic perspective in a dense network. We further employ layered cooperation where two different layering approaches are considered: sequential layered transmission and superimposed layered transmission.

6.1 Comparison of different systems

Before presenting the contributions of this dissertation, we summarize the similarities and the differences of the above systems in terms of the channel model

used, type of cooperation used, type of network considered and ease of deployment:

- Layered Video Multicast using Relays:

  1. Channel Model: Considers path loss model.
  2. Type of cooperation: Considers cooperation at MAC layer.
  3. Type of network: Considers IEEE 802.11b based network. The optimization depends on the coverage range rather than a specific node placement. Optimum relay placement with this system can be utilized in two ways. First, if the network is dense, the relays can be selected among the intended nodes. Alternatively, optimized relay positions can be used for optimal relay placement in an infrastructure based network where fixed relay nodes are introduced to the system. With fixed relays, the system will work regardless of the distribution of the nodes.
  4. Computational complexity and deployment: Computational complexity to select the optimum parameters is very low. The system can be implemented on the current wireless devices without any hardware modifications.

- Cooperative Layered Video Multicast using R-DSTC:

  1. Channel Model: Considers path loss model with fading.
  2. Type of cooperation: Considers cooperation at physical and MAC layer.
  3. Type of network: Considers IEEE 802.11g based network. The optimization depends on specific node placements.
  4. Computational complexity and deployment: Computation complexity of the optimum parameters is high and depends on the available channel information at the sender. In practice, the optimum parameters can be chosen based on partial channel information at an expense of relatively low

performance loss. Deployment of the system requires some modification at the transmitter and the receiver of the relay nodes due to R-DSTC.

- Layered Randomized Cooperative Multicast for Lossy Data in Dense Networks:

  1. Channel Model: Considers path loss model with fading.
  2. Type of cooperation: Considers cooperation at physical layer.
  3. Type of network: Considers a theoretical dense network.
  4. Deployment: Considers the system from information theoretical perspective. Sheds light on the multicast performance of randomized cooperation by providing theoretical achievable rates.

6.2 Key Contributions

The contributions of this dissertation can be summarized as follows:

- Layered Video Multicast using Relays: Two-hop relaying is integrated with layered video coding and packet level FEC to enable efficient and robust video multicast in infrastructure-based wireless networks. First, transmission with conventional omni-directional antennas is considered where relays have to transmit in non-overlapping time slots in order to avoid collision. In order to improve system efficiency, we next investigate a system in which relays transmit simultaneously using directional antennas. In both systems, we consider a non-layered configuration, where the relays forward all received video packets and all nodes receive the same video quality, as well as a layered set-up, where the relays forward only the base-layer video. For each system setup, we consider optimization of the relay placement, user partition, transmission rates of each hop, and time scheduling between source and relay transmissions. Our optimization considers all possible node locations in the target coverage region, rather than

a particular node distribution. The optimized relay positions can be used for optimal relay placement in an infrastructure based network where fixed relay nodes are introduced to the system. Alternatively, one can select the relays among the intended nodes at optimized relay positions in a dense network. Our analysis shows that the non-layered system can provide better video quality to all nodes than the conventional direct transmission system, and the layered system enables some nodes to enjoy significantly better quality, while guaranteeing other nodes the same or better quality than direct transmission. The directional relay system can provide substantial improvements over the omni-directional relay system. To support our results, a prototype is implemented using open source drivers and socket programming, and the system performance is validated with real-world experiments.

- Cooperative Layered Video Multicast using R-DSTC:

  Two-hop cooperative transmission is considered for video multicast where multiple relays forward the data simultaneously using R-DSTC. This randomized cooperative transmission is further integrated with layered video coding and packet level FEC to enable efficient and robust video multicast in infrastructure-based wireless networks. We first consider a simple model where the parity packets are only generated at the sender and forwarded by the relays along with the source packets. For this case, three different schemes are proposed based on the availability of the channel information at the sender: R-DSTC with full channel information, R-DSTC with limited channel information and R-DSTC with node count. For each of these schemes, we optimize the system operating parameters (transmission rates of both hops and consequently the STC dimension and the FEC rate) based on the channel information, and evaluate the achievable video rate. We then consider an enhanced model where the parity packet are generated at the relays and transmitted at the second

hop using R-DSTC. Two schemes are proposed based on the availability of the channel information at the sender: enhanced R-DSTC with full channel and enhanced R-DSTC with node count. For each of these schemes, we optimize the transmission rates of both source and parity packets, and consequently the STC dimensions and the FEC rate, based on the channel information, and evaluate the achievable video rate. The performance of these schemes are compared with rate adaptive direct transmission and conventional multicast that does not use rate adaptation. Our results show that while rate-adaptive direct transmission provides better video quality than conventional multicast, all proposed randomized cooperative schemes outperform both strategies significantly as long as the network has enough nodes. Furthermore, we show that the performance gap between R-DSTC with full channel information and R-DSTC with limited channel information or node count is relatively small, indicating that even when the transmission parameters are chosen with partial channel information (for example only based on node count), the robustness of R-DSTC ensures that the performance loss is negligible compared to R-DSTC with full channel information. The enhanced R-DSTC provides further performance gains by foregoing the parity packet transmission at the first hop. We further consider a layered cooperative multicast system, which provides better video quality to the nodes with better channel conditions.

- Layered Randomized Cooperative Multicast for Lossy Data in Dense Networks: Randomized distributed cooperation is studied from information theoretical perspective. Using end-to-end distortion as a performance metric and assuming a delay constraint, we investigate the relation among the decoding SNR threshold, number of hops, diversity level of underlying Space Time Code (STC), coverage range and the distribution of end-to-end quality over nodes in the coverage range. In order to provide differentiated quality to nodes with different channel strengths, we further employ layered cooperation. We study two different

layering approaches: sequential layered transmission and superimposed layered transmission. For the sequential layered transmission, we investigate the effect of the time division among different layers and for the superimposed layered transmission we investigate the effect of power allocation of different layers on the distribution of end-to-end quality of nodes under a real-time delivery requirement.

Bibliography

[1] S.-H.G. Chan, X. Zheng, Q. Zhang; W.-W. Zhu, Y.-Q. Zhang, "Video loss recovery with FEC and stream replication," *IEEE Transactions on Multimedia*, Volume: 8 , Issue: 2 , 2006 , Page(s): 370 - 381

[2] I. V. Bajic, "Efficient cross-layer error control for wireless video multicast," *IEEE Transactions on Broadcasting*, Volume: 53, Issue: 1, 2007, Page(s): 276 - 285

[3] H. Yousefi'zadeh, H. Jafarkhani, A. Habibi, 'Layered media multicast control (LMMC): real-time error control," *IEEE Transactions on Multimedia*, Volume: 8, Issue: 6, 2006, Page(s): 1219 - 1227

[4] T. A. Lee, S. G. Chan, Q. Zhang, W. Zhu, and Y. Zhang, "Allocation of layer bandwidths and FECs for video multicast over wired and wireless networks," *IEEE Transactions on Circuits and Systems for Video Technology*, vol. 12, no. 12, December 2002. pp 1059-1070.

[5] T. Kim and M. Ammar. "A comparison of heterogeneous video multicast schemes layered encoding or stream replication," *IEEE Transactions on Multimedia*, 7(6):11231130, December 2005.

[6] W.Wei and A. Zakhor, "Multiple tree video multicast over wireless Ad-Hoc networks," *IEEE Transactions on Circuits and Systems for Video Technology*, 17(1):215, January 2007.

[7] C. Chou, A. Misra, and J. Qadir, "Low latency broadcast in multi- rate wireless

mesh networks," *IEEE JSAC Special Issue on Multi-hop Wireless Mesh Networks*, 2006.

[8] X. Zhu, T. Schierl, T. Wiegand, B. Girod, " Video multicast over wireless mesh networks with scalable video coding (SVC)," in *Proceedings of VCIP*, 2008.

[9] A. Sendonaris, E. Erkip, and B. Aazhang, "User cooperation diversity-Part I: System Description ," *IEEE Transactions on Commununications*, vol. 51, pp. 1927-38, November 2003.

[10] A. Sendonaris, E. Erkip, and B. Aazhang, "User cooperation diversity-Part II: Implementation Aspects and Performance Analysis ," *IEEE Transactions on Commununications*, vol. 51, pp. 1939-48, November 2003.

[11] J. N. Laneman, D. N. C. Tse, and G. W. Wornell, "Cooperative diversity in wireless networks: Efficient protocols and outage behavior," *IEEE IT*, vol. 50, no. 12, p. 3062, December 2004.

[12] P. Liu, Z. Tao, Z. Lin, E. Erkip, and S. Panwar, " Cooperative wireless communications: A cross-layer approach," *IEEE Wireless Communications*, 13(4):8492, August 2006.

[13] P. Liu, Z. Tao, S. Narayanan, T. Korakis, and S. Panwar, "CoopMAC: A cooperative MAC for wireless LANs," *IEEE Journal of Selected Topics In Communications*, Volume 25, Issue 2,p.340, February 2007

[14] H. Y. Shutoy, D. Gunduz, E. Erkip and Y Wang, "Cooperative source and channel coding for wireless multimedia communications," *IEEE Journal of Selected Topics In Signal Processing*, Vol. 1, Issue 2, p.295, Aug. 2007

[15] H. Shutoy, Y. Wang and E. Erkip, "Cooperative source and channel coding for wireless video transmission", in *Proceedings of IEEE ICIP*, 2006.

[16] J. N. Laneman, D. N. C. Tse, and G. W. Wornell, "Cooperative diversity in wireless networks: Efficient protocols and outage behavior," *IEEE Transactions on Information Theory*, vol. 50, no. 12, pp. 3062, December 2004.

[17] V. Tarokh, H. Jafarkhani, and A. Calderbank, " Space-time block codes from orthogonal designs," *IEEE Transactions on Information Theory*, vol. 45, no. 5, pp. 1456-1467, July 1999.

[18] S. Alamouti, "A simple transmit diversity technique for wireless communications," *IEEE Journal on Selected Areas in Communications*, vol. 16, no. 8, pp. 1451-1458, October 1998.

[19] B. S. Mergen and A. Scaglione, "Randomized space-time coding for distributed cooperative communication," *IEEE Transactions on Signal Processing*, pp. 5003-5017, October 2007.

[20] F. Verde, T. Korakis, E. Erkip, and A. Scaglione, "On avoiding collisions and promoting cooperation: Catching two birds with one stone," in *Proceedings of IEEE SPAWC*, July 2008.

[21] P. Liu, Y. Liu, T. Korakis, A. Scaglione, E. Erkip, S. Panwar, " Cooperative MAC for rate adaptive randomized distributed space-time coding, in *Proceedings of IEEE GLOBECOM*, November 2008.

[22] P. Liu, C. Nie, E. Erkip and S. Panwar, "Robust cooperative relaying in a wireless LAN: Cross-layer design and performance analysis, in *Proceedings of IEEE GLOBECOM*, December 2009.

[23] O. Alay, T. Korakis, Y. Wang, S. Panwar, "Dynamic rate and FEC adaptation for video multicast in multi-rate wireless networks", to appear, *ACM/Springer Mobile Networks and Applications (MONET), Special Issue on Advances In Wireless Testbeds and Research Infrastructures.*

[24] B. Sirkeci-Mergen, A. Scaglione, and G. Mergen, "Asymptotic analysis of multi-stage cooperative broadcast in wireless networks", *Joint special issue of IEEE Trans. on Information Theory and IEEE/ACM Trans. On Networking*, June 2006.

[25] W. Equitz and T. Cover, "Successive refinement of information", *IEEE Trans. Inform. Theory*, vol. 37, no. 2, pp. 269275, March 1991.

[26] I. S. Reed and G. Solomon, "Polynomial codes over certain finite fields", J.Soc. Industrial Appl. Math., vol. 8, pp. 300-3004, 1960

[27] B. Lin, P. Ho, L. Xie, X. Shen, "Optimal relay station placement in IEEE 802.16j networks", in *ACM IWCMC*, 2007.

[28] J. Cannons, L. Milstein, K. Zeger, "Wireless Relay Placement", in *IEEE RWS*, 2009.

[29] B. Lin, P. Ho, L. Xie, X. Shen, "Optimal Relay Station Placement in Broadband Wireless Access Networks", *IEEE Transactions on Mobile Computing*, June 2009.

[30] O. Alay, K. Guan, Y. Wang, E. Erkip, S. Panwar and R. Ghanadan, "Wireless Video Multicast in Tactical Environments", in *IEEE MILCOM*, November 2008.

[31] R.R. Choudhury, X. Yang, R. Ramanathan, N. H. Vaidya Using Directional Antennas for Medium Access Control in Ad Hoc Networks, in *ACM MobiCom*, September 2002.

[32] T. Korakis , G. Jakllari , L. Tassiulas, A MAC protocol for full exploitation of directional antennas in ad-hoc wireless networks, *ACM MobiHoc*, June, 2003.

[33] "Iperf: The TCP/UDP Bandwidth Measurement Tool," http://dast.nlanr.net/Projects/Iperf/.

[34] O. Alay, T. Korakis, Y. Wang, S. Panwar, "An Experimental Study of Packet Loss and Forward Error Correction in Video Multicast over IEEE 802.11b Network", in *IEEE CCNC*, 2009

[35] "Wireless Implementation Testbed Laboratory," http://witestlab.poly.edu/wiki/

[36] T. Korakis, Z. Tao, S. Makda, B. Gitelman, S. Panwar, "To Serve is to Receive Implications of Cooperation in a Real Environment", in *Networking 2007*, May 2007.

[37] "MadWifi: Linux kernel drivers for Wireless LAN devices," http://madwifi.org/

[38] ITU-T Recommendation H.264, "Advanced video coding for generic audiovisual services," 2003.

[39] Joint Scalable Video Model (JSVM), " JSVM Software, Joint Video Team, Doc. JVT-X203, Geneva, Switzerland, June 2007.

[40] A. Kamerman, G. Aben Personal, "Throughput performance of wireless LANs operating at 2.4 and 5 GHz," in *IEEE PIMRC*, 2000.

[41] LAN MAN Standards Committee of the IEEE Computer Society, ANSI/IEEE Std 802.11, "Part 11: Wireless LAN medium access control (MAC) and physical layer (PHY) specifications: high-speed physical layer extension in the 2.4 GHz Band," IEEE 802.11 Standard, 1999.

[42] H. Jafarkhani, "Space-time coding: theory and practice", Cambridge University Press, 2005

[43] J. G. Proakis, "Digital communications", New York, McGraw-Hill, 2001.

[44] D. Gunduz and E. Erkip, " Source and channel coding for cooperative relaying," *IEEE IT*, vol. 53, no. 10, pp. 3453-3475, October 2007

[45] D. Gunduz and E. Erkip, "Joint source channel codes for MIMO block fading channels," *IEEE IT*, vol. 54, no. 1, pp. 116-134, January 2008.

[46] "Probability Distributions Involving Gaussian Random Variables: A Handbook for Engineers and Scientists ", pages 25-34, http://www.springerlink.com/content/p330m4596057h316/

[47] T. M. Cover and J. A. Thomas, "Elements of Information Theory", Wiley-Interscience, 1991.

List of Publications

Journal Papers

1. O. Alay, T. Korakis, Y. Wang, E. Erkip, S. Panwar, "Layered Wireless Video Multicast using Relays", *IEEE Transactions on Circuits and Systems for Video Technology.* (*in press*)

2. O. Alay, T. Korakis, Y. Wang, S. Panwar, "Dynamic Rate and FEC Adaptation for Video Multicast in Multi-rate Wireless Networks", *ACM/Springer Mobile Networks and Applications (MONET), Special Issue on Advances in Wireless Testbeds and Research Infrastructures.* (*in press*)

3. O. Alay, P. Liu, Y. Wang, E. Erkip, S. Panwar, "Layered Wireless Video Multicast using Randomized Distributed Space Time Codes", under review, *IEEE Transactions on Multimedia.*

4. O. Alay, E. Erkip and Y. Wang, "Asymptotic Analysis of Layered Randomized Cooperative Multicast for Lossy Data", to be submitted to *IEEE Transactions on Wireless Communications.*

Conference Papers

1. O. Alay, Z. Guo, Y. Wang, E. Erkip, S. Panwar, "Enhanced Parity Packet Transmission for Video Multicast using R-DSTC", to appear, IEEE PIMRC.

2. T. Q. Duong, O. Alay, E. Erkip, H. J. Zepernick, "End-to-End Performance of Randomized Distributed Space-Time Codes", to appear, IEEE PIMRC.

3. O. Alay, P. Liu, Y. Wang, E. Erkip, S. Panwar, "Error Resilient Video Multicast using Randomized Distributed Space-time Codes", *in Proceedings of IEEE ICASSP,* Dallas, TX, March, 2010.

4. O. Alay, P. Liu, Z. Guo, L. Wang, Y. Wang, E. Erkip, S. Panwar, "Cooperative Layered Video Multicast using Randomized Distributed Space-time Codes", *in Proceedings of IEEE Infocom MOVID Workshop,* Rio De Janeiro, Brazil, April, 2009.

5. O. Alay , C. Li, A. Rai, T. Korakis, Y. Wang and S. Panwar, "Dynamic Rate and FEC Adaptation for Video Multicast in Multi-rate Wireless Networks", *in Proceedings of IEEE Tridentcom,* Washington D.C., April 2009.

6. O. Alay , Z. Xu, T. Korakis, Y. Wang and S. Panwar, "Implementing a Cooperative MAC Protocol for Wireless Video Multicast", *in Proceedings of IEEE WCNC,* Budapest, Hungary, April 2009.

7. O. Alay, X. Pan, E. Erkip and Y. Wang, "Layered Randomized Cooperative Multicast for Lossy Data: A Superposition Approach", *in Proceedings of IEEE CISS,* Baltimore, MD, March 2009.

8. O. Alay, T. Korakis, Y. Wang and S. Panwar, "Is Physical Layer Error Correction sufficient for Video Multicast over IEEE 802.11g Networks?", *in Proceedings of IEEE CCNC,* Las Vegas, NV, January 2009.

9. O. Alay, T. Korakis, Y. Wang and S. Panwar , "An Experimental Study of Packet Loss and Forward Error Correction in Video Multicast over IEEE 802.11b Network", *in Proceedings of IEEE CCNC,* Las Vegas, NV, January 2009.

10. O. Alay, K. Guan, Y. Wang, E. Erkip, S. Panwar and R. Ghanadan, "Wireless Video Multicast in Tactical Environments", *in Proceedings of IEEE MILCOM,* San Diego, CA, November 2008.

11. O. Alay, R. Ding, E. Erkip, Y. Wang and A. Scaglione, "Layered randomized cooperation for multicast", *in Proceedings of IEEE 42nd Annual Asilomar Conference on Signals, Systems and Computers,* Pacific Grove, CA, October 2008 (invited).

12. O. Alay, T. Korakis, Y. Wang and S. Panwar, "Layered Wireless Video Multicast using Directional Relays", *in Proceedings of IEEE ICIP,* San Diego, CA, October 2008.

13. O. Alay, T. Korakis, Y. Wang, E. Erkip, S. Panwar, "Layered Wireless Video Multicast using Omni-directional Relays", *in Proceedings of IEEE ICASSP,* Las Vegas, NV, April 2008.

14. O. Alay, E. Erkip and Y. Wang, "Cooperative Transmission of Correlated Gaussian Sources", *in Proceedings of IEEE 41st Annual Asilomar Conference on Signals, Systems and Computers,* Pacific Grove, California, November 2007.

15. O. Alay, H. Shutoy, D. Gunduz, E. Erkip, Y. Wang, "Cooperative Source and Channel Coding for Wireless Multimedia Communications", *in Proceedings of 16th Annual Wireless and Optical Communications Conference,* NJ, April 2007

16. O. Alay, G. B. Akar, "Fast Mode Decision for Intra Prediction in H.264", *in Proceedings of IEEE 14th Signal Processing and Communications Applications Conference,* Antalya, April 2006

Patents

1. O. Alay, T. Korakis, Y. Wang, S. Panwar, "Dynamic Rate and FEC Adaptation for Video Multicast in Multi-rate Wireless Networks", filed, April 2010.

2. O. Alay, T. Korakis, Y. Wang, E. Erkip, S. Panwar, "Layered Video Multicast using Relays", filed, December 2008.